DESIGN AND SYNTHESIS OF MODIFIED NUCLEOSIDE ANALOGS AGAINST EMERGING VIRUSES

by

RANSOM A. JONES

(Under the Direction of Uma S. Singh)

ABSTRACT

Many nucleoside and nucleotide analogs have been approved as efficacious and selective clinical antiviral drugs. However, emerging infectious viruses and ongoing viral mutations are a challenging problem for the scientific community. To tackle viral infections and viral drug resistance, continuous drug discovery and development is essential. In this effort, the synthesis of a 4′-*α*-fluoromethyl carbocyclic adenosine analog, and dioxolane derived 7-deazapurine nucleosides have been reported and evaluated as antiviral agents. The invented synthetic route for the synthesis of the 4'-fluoro-methyl carbocyclic ring is novel and was utilized for the construction of the carbocyclic adenosine nucleoside (**15**). 7-Deazapurine dioxolane nucleoside analogs have been synthesized and evaluated for antiviral activity, and one analog has demonstrated potent Anti-Epstein-Barr virus (EBV) activity. On-going in-vitro testing on the synthesized nucleosides may lead to potent antiviral preclinical candidates and will open a new path of full structural-activity relationship evaluation.

INDEX WORDS: Antivirals, Carbocyclic Nucleosides, Dioxolane Nucleosides, SARS-CoV-2, Epstein Barr Virus, Drug Discovery, DNA/RNA Polymerase

DESIGN AND SYNTHESIS OF MODIFIED NUCLEOSIDE ANALOGS AGAINST EMERGING VIRUSES

by

RANSOM A. JONES

B.S., University of Georgia, 2022

A Thesis Submitted to the Graduate Faculty of The University of Georgia in Partial Fulfillment of the Requirements for the Degree

MASTER OF SCIENCE

ATHENS, GEORGIA

2023

DESIGN AND SYNTHESIS OF MODIFIED NUCLEOSIDE ANALOGS AGAINST EMERGING VIRUSES

by

RANSOM A. JONES

Major Professor:	Uma S. Singh
Committee:	Gurvinder S. Rekhi
	Eugene Douglass

Electronic Version Approved:

Ron Walcott
Vice Provost for Graduate Education and Dean of the Graduate School
The University of Georgia
May 2023

ACKNOWLEDGEMENTS

I would like to begin by expressing my deepest graduate to my mentor Dr. Uma Singh, who provided unwavering encouragement and relentless support throughout my time at the Chu Drug Discovery Group. His tireless work and in-depth knowledgebase have been instrumental in my growth as a scientist. I'm also extremely grateful to my colleague, Dr. Yugandhar Kothapalli, whose friendship, and helpful advice have been crucial to my success. Outside of the college, I would like to extend my extreme appreciation to my mentor, Dr. Conrad Santini, whose wealth of knowledge and experience changed my insights not only in the world of chemistry, but in life as well. I would like to extend my sincere thanks to my committee members, Dr. Gurvinder Rekhi and Dr. Eugene Douglass, who have offered specific insight into improving my thesis and research. Dr. Rekhi has also acted as a mentor to me during my time in both my graduate and undergraduate degrees, and his experience and wisdom has been invaluable. In addition, I would like to thank Dr. Wided Missaoui, who has extended past the role of professor, and has become a dear friend and colleague of mine.

I would like to extend sincere gratitude to Dr. David Chu, whose support and funding made this thesis and research possible. I also had the pleasure to work with Dr. Varughese Mulamoottil, whose initial training and instruction was essential to my success. I gratefully acknowledge the assistance of Alaina Lombardo, for her aid in the physical synthesis of many compounds, and Carl (Bill)

Trieshmann, for his crucial instruction in molecular modeling. I’m deeply indebted to my family, who have supported me mentally, emotionally, and often financially throughout my studies. To my mother, Rhonda Jones-Thomas, your profound belief in me, unparalleled support, and character have given me the confidence and work ethic which propelled this work. Finally, to my best friend and fiancé, Lindsey Grace Hall, your love, companionship, personality, and smile have been my driving force every day, and without them this would not be possible.

TABLE OF CONTENTS

Page

LIST OF FIGURES

Page

CHAPTER 1

Introduction and Literature Review

1.1 EMERGING INFECTIOUS VIRUSES

Viruses are ubiquitous throughout nature, and historically have wreaked havoc when spread to the human population. Influenza pandemics, such as the Russian flu in the late 1800's and the Spanish flu in the early 1900's, along with the ongoing SARS-CoV-2 pandemic have caused mass casualties and global economic turmoil.[1] The effects of viruses on society are not solely limited to pandemic conditions. Human Immunodeficiency Virus (HIV), the causative virus for Acquired Immunodeficiency Syndrome (AIDS), has been estimated to have killed over 36 million people globally.[2] Polio, a now functionally eradicated disease in the western hemisphere, has disabled and killed millions worldwide.[3] Herpes viruses range from producing genital sores to mononucleosis and are associated with multiple sclerosis (MS), cognitive impairment, and several lymphomas.[4, 5] Poxviruses, such as smallpox, cause painful lesions and have resulted in over 300 million deaths worldwide.[6] Additionally, the recent outbreak of the monkeypox virus has been declared a national emergency. [7] This list of infectious RNA and DNA viruses is far from exhaustive, and the true toll viruses have taken on humanity cannot be understated.

Viruses are deceptively simplistic; their small and often simple genome encodes for few proteins, often less than 10, and relies heavily on the host cell to

multiply.[8] Often, these genes (RNA or DNA) are protected by a protein capsid.[9] Some viruses have an additional envelope, a lipid bilayer surrounding the nucleocapsid, which may contain glycoproteins, or other specific markers.[10] The small genome of viruses often includes only a few essential non-structural proteins (nsp). These can include viral proteases, which cut proteins into smaller polypeptides, DNA/RNA polymerases (which catalyze nucleotide polymerization), and other enzymes to assist in replication.[11] The small genome combined with the reliance on host cell machinery, results in difficulty designing selective, potent, and safe antiviral drugs.

Viruses can be split into two groups based on their genetic material, either RNA (ribonucleic acid) or DNA (deoxyribonucleic acid). Common RNA viruses include orthomyxoviruses (influenza), flaviviridae viruses (hepatitis C, zika, dengue, and West Nile virus), coronaviruses (severe acute respiratory syndrome coronavirus 1 & 2 (SARS-CoV-1&2), middle east respiratory syndrome coronavirus (MERS-CoV)), and the retrovirus (HIV).[12] Common DNA viruses include Herpesviruses (herpes simplex virus 1 & 2 (HSV-1 & 2), varicella zoster virus (VZV), Epstein-Barr virus (EBV), cytomegalovirus (CMV), and Kaposi's sarcoma-associated herpesvirus (KSHV)), Poxviruses (Smallpox, Vaccinia, Cowpox, and Monkeypox (MPX)), and hepatitis-B virus (HBV).[4, 13] Within these two groups, further division can be drawn based on DNA/RNA strand and sense, either double/singled stranded and positive/negative sense.[9] The diversity of viral genomes and significant rate of mutations (roughly 10^{-3} substitutions/site/year in RNA viruses) adds neglection and inefficacy to approved antiviral drugs and

demonstrates the need for continued efforts in antiviral discovery and development.[14]

In the 21st century, SARS-CoV-2, commonly known as COVID-19, brought antiviral research efforts to the forefront of the public eye. So far, the World Health Organization (WHO) has reported over 6.89 million deaths globally and 760 million confirmed cases.[15] In addition to the deadly initial spread, multiple variants of SARS-CoV-2 have emerged worldwide, such as Alpha (B.1.1.7), Delta (B.1.617.2), and Omicron (B.1.1.529), which adds challenges to current approved treatment.[16] Each variant introduces genetic differences, which may result in increased virulence, transmissibility, and antiviral/vaccine resistance, continuing the cycle of infection and prolonging pandemic conditions. Though numerous antiviral drugs have emerged to treat SARS-CoV-2, including remdesivir, molnupiravir, the combination therapy nirmatrelvir/ritonavir (Paxlovid™) **(Figure 1.1)**, and monoclonal antibody therapy, the ongoing mutations of SARS-CoV-2 requires continuous efforts for new antiviral agents.[17]

The recent outbreak of Monkeypox (MPX) throughout Europe and the United States, outside its endemic regions in central and western Africa, has exceeded 70,000 infected.[18] Monkeypox is associated with painful/ulcerative lesions across the body, with a traditional fatality rate of up to 15%, though notably the recent outbreak shows a fatality rate of only 0.025%.[18] Smallpox medications such as cidofovir, may show potential efficacy in treating monkeypox, though clinical data is scarce, and there is no current approved cure.[19]

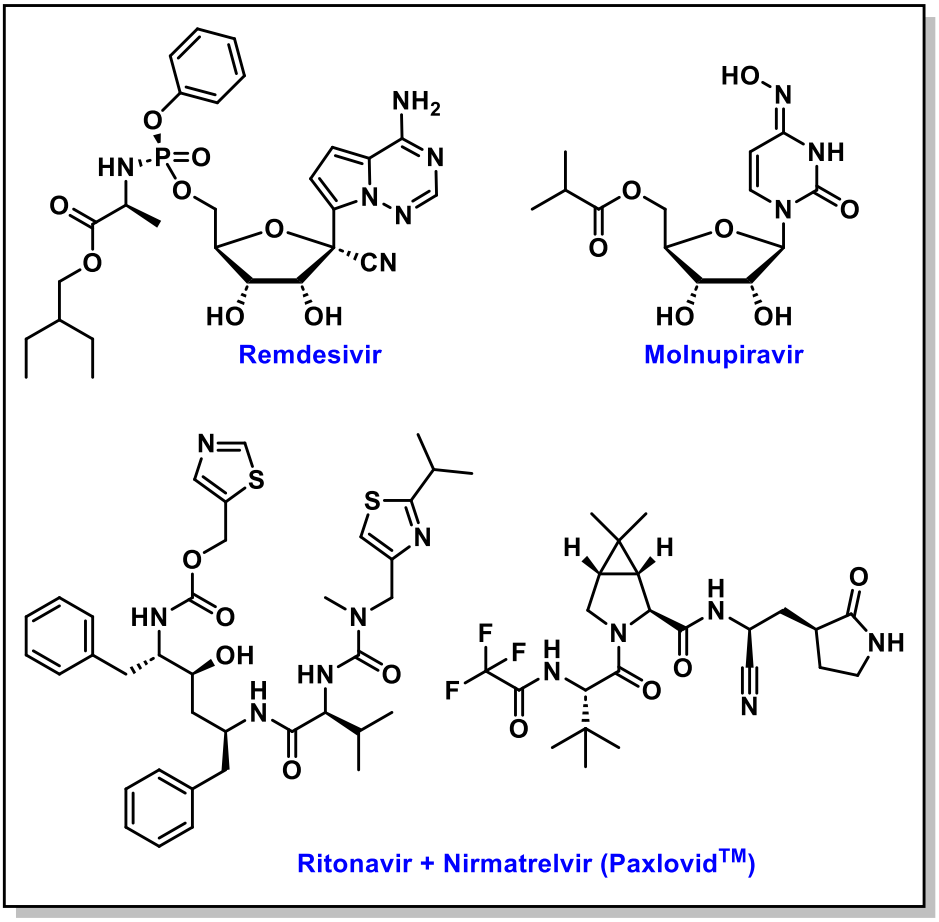

Figure 1.1 Structure of FDA approved small molecule drugs against SARS-CoV-2.

Epstein-Barr Virus (EBV) is ubiquitous, with over 90% of the worldwide population infected.[20] While often asymptomatic, EBV is known to cause lymphatic and epithelial cancers.[21] In addition, mononucleosis, a disease characterized by extreme fatigue and sore throat, commonly referred to as mono, is caused by EBV.[22] Recent studies reveal that EBV is also associated with multiple sclerosis (MS).[5, 23] Globally, approximately 2.8 million people have MS, and recent studies of longitudinal analysis on the US troops (active adults on duty) have revealed a high prevalence of EBV associated with MS. Rather than infectious

mononucleosis, the risk of MS increases 32-fold after EBV infections.[5] Treatment is often based on symptoms, and there is no currently approved specific antiviral drug to treat EBV.

Another herpesvirus, Cytomegalovirus (CMV), is also ubiquitous, infecting around 65% of the population in industrialized countries, and nearly 100% in other countries.[24] Similar to EBV, CMV is often asymptomatic, and presents as mononucleosis in immune-comprised individuals.[24] Fetal abnormalities can be caused by congenital CMV, include cerebral palsy due to brain calcifications, microcephaly, and even fetal death.[25] EBV and CMV also create complications in organ transplant patients, along with immunocompromised individuals such as chemotherapy recipients and HIV patients.[26] It is evident that EBV is constantly detected in numerous cancers, including nasopharyngeal carcinoma, Hodgkin's and non-Hodgkin's lymphoma subtypes, EBV-associated gastric carcinoma, leiomyosarcoma, and natural killer (NK)/T cell carcinomas.[27] In immunosuppressive conditions, it causes fatal lymphoproliferative disorder. Broad spectrum antivirals are available, though again there is no specific cure for these viruses.

HIV, commonly known to develop into acquired immunodeficiency syndrome (AIDS), is unique in terms of its life cycle and utilizes a reverse transcriptase to transcribe RNA into DNA.[28] This virus is often referred to as a "slow virus" because it may take years after infection to show symptoms and leads to a weak immune system, which may result in secondary infections. The WHO estimates over 38 million individuals are living with HIV, including 1.7 million

children.[29] Although currently, many antivirals are available to treat HIV infections, this pervasive disease has been shown to have a high rate of mutation, and viral resistance has resulted in non-treatable HIV cases.[30]

The infection of Hepatitis B Virus (HBV) leads to chronic Hepatitis B (CHB) and causes liver cirrhosis. Hepatitis B is characterized by inflammation of the liver, cirrhosis, and liver failure, with the possibility of progression to death.[31] The severe infection of HBV results in hepatocellular carcinoma (HCC).[32] HBV is an enveloped DNA virus, with its genome encoded in a relaxed circular DNA.[32] HBV is spread through direct contact with bodily fluids, including blood, semen, and vaginal fluids. Reported symptoms include jaundice, fatigue, and loss of appetite that may not appear until nearly 6 months after infection.[31] Drugs such as entecavir, adefovir, and tenofovir are FDA approved for HBV treatment.[33] However, due to the multifaced life cycle of HBV, to date a complete cure for HBV has not been invented. Additionally, in account of ongoing viral resistance, continuous drug discovery is required for the complete cure of HBV.

Name	Genome Material	Virus Family
SARS-CoV-2	RNA	Coronaviridae[34]
MPX	DNA	Poxviridae[35]
EBV	DNA	Herpesviridae[36]
CMV	DNA	Herpesviridae[36]
HIV	RNA[a]	Retroviridae[37]
HBV	DNA	Hepadnaviridae[38]

Table 1.1 Summary of Emerging Infectious Viruses. [a]Utilizes reverse transcriptase to incorporate into human DNA.

1.2 NUCLEOSIDE DRUGS

Antiviral drugs act upon various mechanism of actions with varying structures all in the common goal to inhibit viral growth and infections. Common antiviral targets include entry inhibitors, capsid inhibitors, protease inhibitors, and DNA/RNA polymerase inhibitors.[39] Under the category of polymerase inhibition, this can further be broken down specifically into RNA or DNA polymerase inhibitors, dependent on the viral genome. Polymerase inhibitors also can be divided into two groups based on structure, nucleotide and non-nucleotide antivirals. Nucleosides consist of a ribose sugar, coupled with a nucleobase, which on phosphorylation leads to the active nucleotides (triphosphate form). Nucleotide triphosphates are the building blocks of DNA/RNA, they are incorporated into the growing chain and lead to chain propagation **(Fig 1.2)**. Several, nucleoside molecules are being used as antiviral drugs, that on phosphorylation are converted into their active nucleotides.

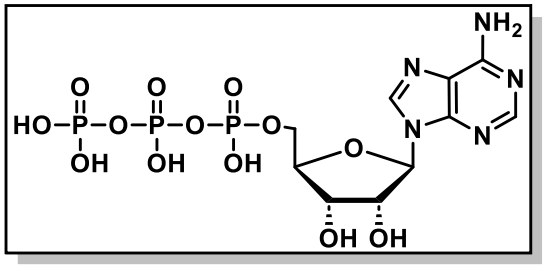

Figure 1.2 Structure of adenosine triphosphate. A naturally occurring nucleotide used in RNA polymerization.

To date, there are various altered nucleos(t)ide drugs that have been approved as antivirals.[33] Acyclovir, famciclovir, and vidarabine for VZV/HSV, ganciclovir and cidofovir for CMV, entecavir, lamivudine, adefovir, and tenofovir for HBV, abacavir and zidovudine for HIV, and sofosbuvir for HCV are nucleos(t)ide drugs currently used in practice (**Fig 1.3**).[33, 40] Common synthetic modifications often are either on the sugar ring or the coupled nucleobase. Furthermore, altered strategic approaches include opening the sugar ring, inserting a carbocyclic ring, replacing the ribose with a heterocyclic ring, and modifications on the nucleobase.

The two central mechanisms for a nucleotide polymerase inhibitor are to either incorporate into the actively growing RNA/DNA chain of the virus and act as a chain terminator, or through direct inhibition of the polymerase. Through various potential differing mechanisms of nucleosides, such as chain termination, delayed chain termination, or conformational changes, a failure in viral replication occurs.[41] Nucleos(t)ide drugs selectively target the viral genome without causing toxicity to humans. It has been observed that modifications and introduced complexities in nucleos(t)ide structures increase their viral specificity.[40] In the effort towards continuous antiviral drug discovery to combat emerging viruses, further approaches to introduce various modifications and substitutions that affect potency and efficacy hold immense value.

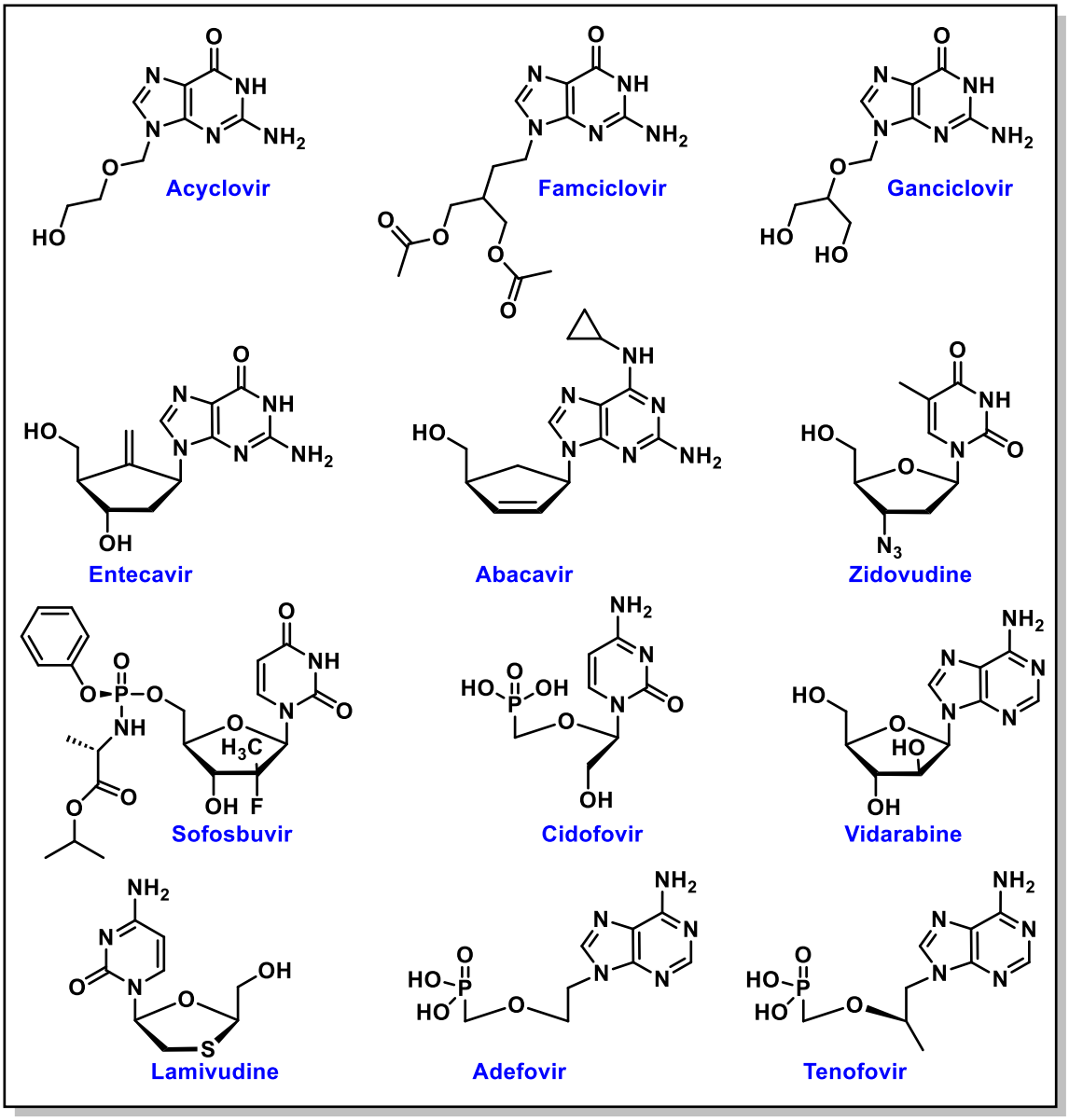

Figure 1.3 Structures of FDA approved antiviral nucleos(t)ide analogs.

CHAPTER 2

Synthesis of the 4′-α-fluoromethyl Carbocyclic Nucleoside as an Antiviral Agent

2.1 INTRODUCTION

In late 2019, the SARS-CoV-2 virus emerged and led to pandemic conditions worldwide. The outbreak of this virus again fueled the development of small molecules as well as monoclonal antibodies as antivirals against coronaviruses. Small molecules offer an advantage in improved stability and out-patient administration as compared to biologics. In this regard, nucleotide polymerase inhibitors offered a necessary and promising start for both the wild type as well as mutated viral strains. In these efforts, remdesivir, which had previously been developed for Ebola, expressed clinical efficacy against SARS-CoV-2 in early antiviral evaluations.[42]

The structure of remdesivir is composed of a traditional ribose ring, with an additional 1′-CN group and altered purine base, which enhances its selectivity towards SARS-CoV-2 RNA-dependent RNA-polymerase (RdRp). Remdesivir acts as both an RdRp inhibitor and a delayed chain terminator, potentially due to the 1′-CN group.[43] Furthermore Cryo-EM structural determination of the SARS-CoV-2 RdRp complex, reveals remdesivir bound to nsp-12 (PDB 7BV2).[44] On the basis of this published Cryo-EM structure, medicinal chemists are applying in-silico docking approaches to find a better molecule against this virus.

Carbocyclics are a special class of nucleos(t)ide molecules where the oxygen of the ribose ring is replaced by carbon. These carbocyclic nucleos(t)ides demonstrate increased physical, enzymatic, and metabolic stability towards the glycosidic bond.[40] We previously have observed this benefit to also come with less cellular toxicity and improved selectivity towards viral DNA/RNA polymerases.[45] In this regard, carbocyclic nucleos(t)ides offer a promising underexplored pharmacophore for antiviral drug discovery by medicinal chemists. Based on these alterations, multiple carbocyclic nucleos(t)ide analogs have been FDA-approved as antiviral drugs, such as abacavir for HIV and entecavir for HBV (**Fig 1.3**). With the cyclopentyl ring structure, there is additional opportunities for modifications which may produce more potent antivirals.

Lumicitabine, a cytidine analogue with a 2′-fluoro replacing the 2′-hydroxy and a 4′-methylchloro addition, showed promising activity against respiratory syncytial virus (RSV).[46] This finding reveals that the addition of a halomethyl group on the cyclopentyl ring may express a better antiviral profile against various viruses. Additionally, another recent compound, 4′-fluorouridine, a uridine analog with a 4′-*α*-fluoro addition, showed both RSV and SARS-CoV-2 inhibition.[47] Fluorine offers specific benefits over other halogens, as it is isosteric to hydrogen in size, though highly electronegative, allowing for an additional hydrogen bond to form within the binding pocket. It is also evident that fluorine may induce specific conformational locking, which may offer a delayed chain termination.[48] In these efforts our group has invented FMCA and its prodrug FMCAP as promising candidates against wild type and drug resistant HBV.[49, 50] FMCA is a 2′-*β*-fluoro-

6′-methylene carbocyclic adenine nucleoside analog where fluorine has demonstrated additional hydrogen bonding in the viral polymerase pocket.[50]

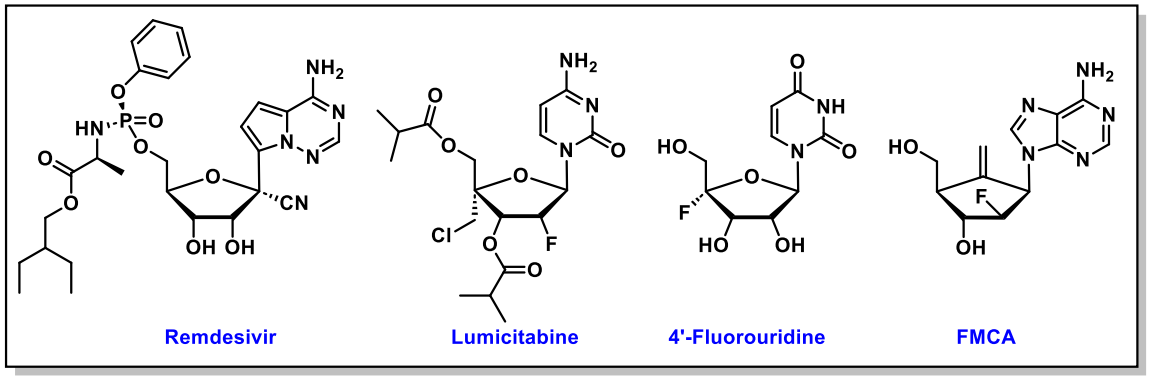

Figure 2.1 Structures of remdesivir, lumicitabine, 4′-fluorouridine, and FMCA

While halogen insertions on a traditional ribose ring have been thoroughly explored, due to the tedious and tough synthesis, halogenation on a carbocyclic ring has not been significantly explored and offers an open area for structure-activity relationships (SAR). Taking the lead from the above points, it was a keen interest of this project to explore the challenging synthesis and antiviral evaluation of 4′-*α*-fluoromethyl carbocyclic nucleoside analogs. Previously 4′-halomethyl ribose nucleosides have been reported in literature, while there are no synthetic reports for carbocyclic analogs. To insert the 4′-*α*-fluoromethyl on the carbocyclic ring, a previously synthesized carbocyclic ketone was selected as a starting material.[51] The synthesis of the key carbocyclic ketone was accomplished via D-ribose, utilizing our previously reported method.[51]

2.2 RESULTS AND DISCUSSION

Chemistry

To afford the target 4′-*α*-fluoromethyl carbocyclic nucleoside **15**, commercially available ketone **1** was utilized to initiate the planned synthetic route.[52] Ketone **1** was reduced through the well-known Luche Reduction.[53] **1** was treated with $CeCl_3 \cdot 7H_2O$ and $NaBH_4$ in MeOH to exclusively afford the *α*-hydroxy **2** in 96% yield. Benzylation of the hydroxy on **2** was performed with Benzyl Bromide and NaH in DMF to give compound **3** in 76% yield. To oxidize the 5th position hydroxy selectively, specific protection of the 2nd and 3rd hydroxy groups of **4** was necessary. This was achieved through treating **3** with a TFA/H_2O mixture to afford deprotected compound **4** in 67% yield. Subsequently, the 2nd and 3rd position hydroxyls were selectively protected with an acetonide group by treating compound **4** with 2,2-dimethoxypropane (DMP) and catalytic p-TSA in acetone to afford compound **5** in 72% yield.

To oxidize the 5th position hydroxy, compound **5** was treated with Dess Martin Periodinane in DCM to afford **6**. In the attempt of purification of **6** via silica gel chromatography, degradation of **6** was observed. Therefore, it was concluded that the aldehyde is unstable on the strained carbocyclic ring. Thus intermediate **6** was moved forward to next step without further purification. To construct diol **7**, an aldol type condensation was performed on **6**. Compound **6** was condensed with 37% formaldehyde in the presence of a 1M NaOH solution in THF and reduced in-situ with $NaBH_4$ to give diol **7** in 34% yield. To furnish the desired *α* (down) fluoromethyl key intermediate **12**, selective protection of the *β* hydroxy was required.

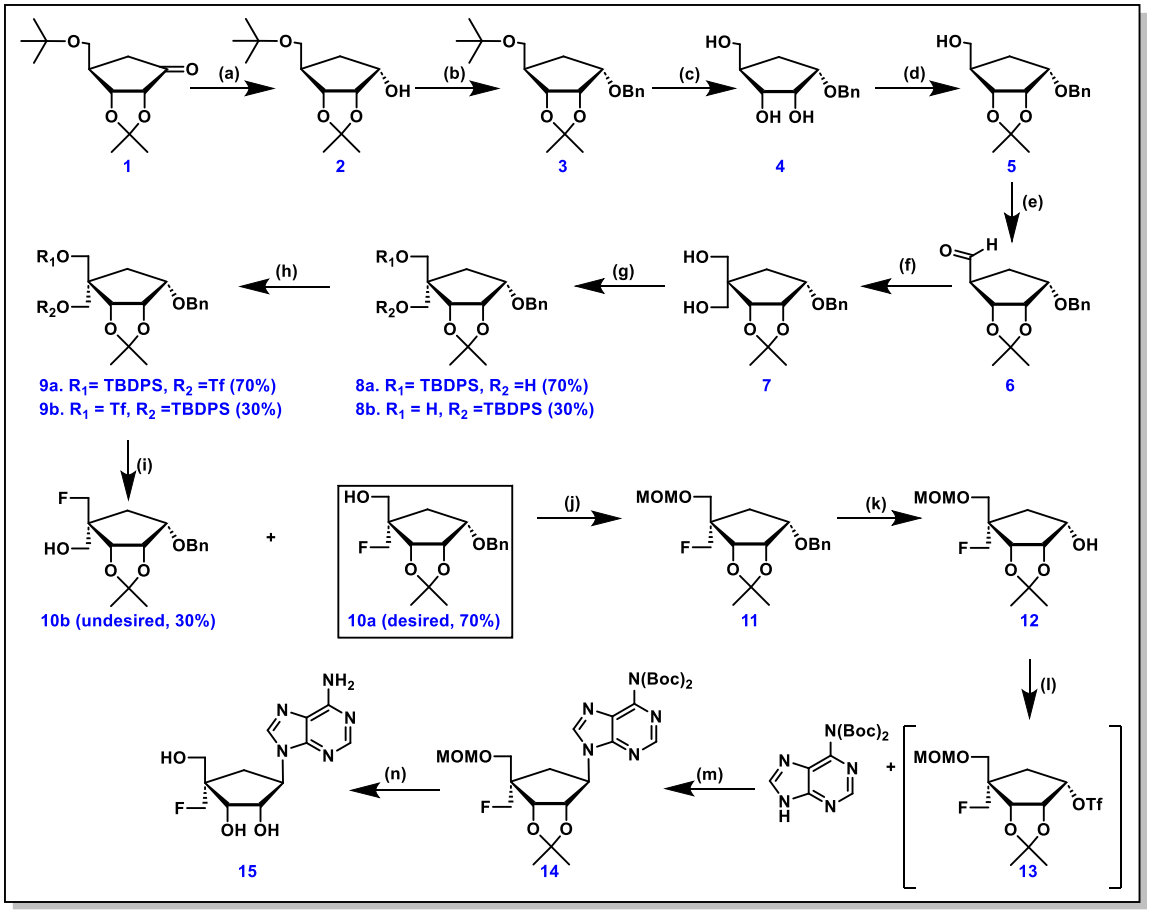

Scheme 2.1 Synthetic route for targeted compound 15 via ketone 1.

Reagents and Conditions: (a) $NaBH_4$, $CeCl_3 \cdot 7H_2O$, Methanol; (b) NaH, BnBr, DMF; (c) TFA/water (2:1); (d) 2,2-dimethoxypropane, p-TSA, acetone; (e) Dess-Martin periodinane, DCM; (f) 37% aqueous CH_2O/wt, 1M NaOH, $NaBH_4$, THF; (g) TBDPSCl, imidazole, DCM; (h) Tf_2O, pyridine, DCM; (i) TBAF (1M solution in THF), THF; (j) MOM-Cl, DIPEA, DCM; (k) Pd-C, H_2, MeOH; (l) Tf_2O, pyridine, DCM; (m) NaH, 18-crown-6-ether, DMF; (n) TFA, DCM.

Selective protection of the 4-*β*-hydroxymethyl of compound **7** was challenging, and various protecting groups were tried, but in each case a mixture of *α* and *β* protected intermediates **8a** and **8b** were obtained in a ratio of 1:1 which

were not separable via column chromatography. Therefore, it was thought that by inserting a bulkier protecting group, selective protection of the *β*-hydroxymethyl of **7** would be favored. In these efforts, compound **7** was treated with tert-butyl(chloro)diphenylsilane (TBDPSCl), a bulky molecule, and imidazole in DCM to afford a selective protected intermediate **8a (desired, 70%)** and **8b (undesired 30%)** in 66% yield. Separation of **8a** and **8b** was tried via silica gel chromatography, but in every attempt a diastereomeric mixture of **8a**/**8b** was collected in ratio of 7:3.

Thus, to construct compound **10a**, a direct fluorination was accomplished with the mixture of **8a**/**8b** (ratio 7:3). First, fluorination was attempted with the traditional diethylaminosulfur trifluoride (DAST) reagent, but in this effort minimal formation of the fluorinated product was produced, and major degradation was observed on the thin layer chromatography (TLC) plate. Therefore, a nucleophilic substitution strategy was adopted, for which a triflate leaving group was prepared from a mixture of **8a** and **8b**. Compounds **8a** and **8b** were treated with triflic anhydride (Tf_2O) and pyridine in DCM to afford **9a** and **9b** in 80% yield. With the triflate isomeric mixture **9a** and **9b**, fluorination was carried out in-situ with tetrabutylammonium fluoride (TBAF). However, during the fluorination of the isomeric mixture **9a** and **9b**, full deprotection of TBDPS was also observed and gave compounds **10a** (desired, *α*-fluoro) and **10b** (undesired *β*-fluoro) in 16% and 2% yield respectively. Intermediates **10a** and **10b** revealed a good separation on TLC, which was encouraging and indicated the application of column

chromatography for the separation of diastereomers **10a** and **10b**. Furthermore, compounds **10a** and **10b** were purified by silica gel column chromatography.

Compound **10a** was selected for the next step reaction. To protect the *β*-hydroxy of **10a,** it was treated with MOM-Cl (chloromethyl methyl ether) and DIPEA (diisopropylethylamine) in DCM to give the MOM protected compound **11** in 66% yield. The next goal was the benzyl deprotection of compound **11** which was achieved via hydrogenation. Compound **11** was dissolved in MeOH and treated with Pd-C (10% on carbon) in the presence of hydrogen at 4-5 parr pressure at rt to give key intermediate **12** in 70% yield. To construct the target compound **15,** it was important to confirm the stereo conformation of the *β*-MOM-protected hydroxy methyl and α-fluoro-methyl of compound **12**.

To confirm the stereo conformation of the 4-*β*-MOM-protected hydroxy methyl and 4-*α*-fluoro-methyl of **12**, ^{1}H-NMR and ^{1}H-^{1}H ROESY (Rotating-frame nuclear Overhauser effect spectroscopy) experiments were performed (**Figure 2.2**). In the ROESY spectra, the down acetonide $(CH_3)_2$ protons δ 1.50 & 1.35 ppm showed correlation with the down 4-*α*-fluoromethyl (CH_2) protons δ 4.63-4.33. In addition, the up *β*-MOM (CH_2) protons δ 3.43 & 3.40 ppm showed correlation with the H-6 (CH_2) protons δ 1.98 ppm. The ^{1}H-^{1}H ROESY analysis confirms the correct conformation of the 4-*β*-MOM-protected hydroxy methyl and 4-*α*-fluoromethyl of key intermediate **12**.

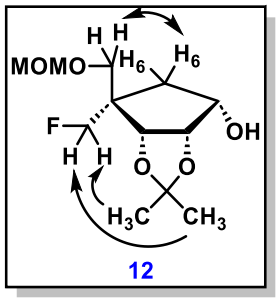

Figure 2.2 ^{1}H-^{1}H ROESY correlations for compound 12

To couple the adenine base to **12** in the stereo-specific *β* conformation, initially a Mitsunobu coupling reaction was carried out. However, it was observed that the 1-hydroxy on the carbocyclic ring of **12** was almost inactive for the Mitsunobu coupling reaction and no coupled product was detected and reactants were as such on TLC. To overcome this problem, leaving group S_N2 reactions were performed (**Scheme 2.1**). Compound **12** was converted to triflate **13** by treating **12** with Tf_2O in the presence of pyridine in DCM to give **13** which was used immediately in situ. In a separate flask, Boc protected adenine was treated with NaH in DMF with 18-crown-6-ether as a phase-transfer catalyst. To this mixture, compound **13** was added dropwise, to afford **14** in 20% yield. Finally, deprotection of **14** was performed with a 20% solution of TFA/DCM to give the desired compound **15** in 85% yield.

Molecular Modeling

*Molecular modeling of compound **15** was performed by using Schrödinger Suite modules.* Cryo-EM crystallized remdesivir monophosphate in the SARS-CoV-2 RdRp protein structure (PDB 7BV2)[44] was taken for modeling studies to

gain insight into how compound **15** binds inside the bonding pocket of SARS-CoV-2 RdRp. Protein preparation and subsequent docking of the native remdesivir monophosphate yielded an RMSD (root mean square deviation) (when compared to the prepped crystal structure) of 0.406, and a docking score of -9.814. The nucleobase ring of remdesivir showed pi-cation interactions with arginine 555, along with pi-pi stacking with uridine P:20 (**Figure 2.3**). The 1-N on the nucleobase ring a showed hydrogen bonding interaction with uridine T: 10, while the 6-amino expressed hydrogen bonding with uridine P:20 and T:10. The 3′-hydroxy revealed hydrogen bonding with an endogenous phosphate group A: 1003, while finally the attached phosphate group showed salt bride formation with both magnesium ions, A: 1005 and A: 1004, along with hydrogen bonding with uridine P: 20.

In the above-described grid for remdesivir monophosphate, the 4′-*α*-fluoromethyl carbocyclic adenosine (**15**) monophosphate analog was docked and demonstrated a comparable docking score of -8.705. In a similar fashion, the 6-amino of the adenine base showed hydrogen bonding with uridine T:10. Additionally the adenine ring showed pi-cation interactions with arginine 555 and pi-pi stacking with uridine P:20. The 3′-hydroxy retained hydrogen bonding with uridine P:20, and finally the attached phosphate group formed salt bridges with the magnesium ions A: 1004 and A: 1005. Notably, the fluorine atom did not appear to interact with either the protein or RNA fragment, but instead seemed to position in an empty pocket.

Pi-cation interactions between both ligands with arginine 555 as well as 6-amino hydrogen bonding to uridine T: 10 was conserved among both structures.

The attached phosphate of compound **15** also expressed similar salt bridge formation with the magnesium ions. However, no additional fluorine hydrogen bonding was apparent, but overall, the docking pose of **15** seems indicative of potential similar binding as compared to remdesivir.

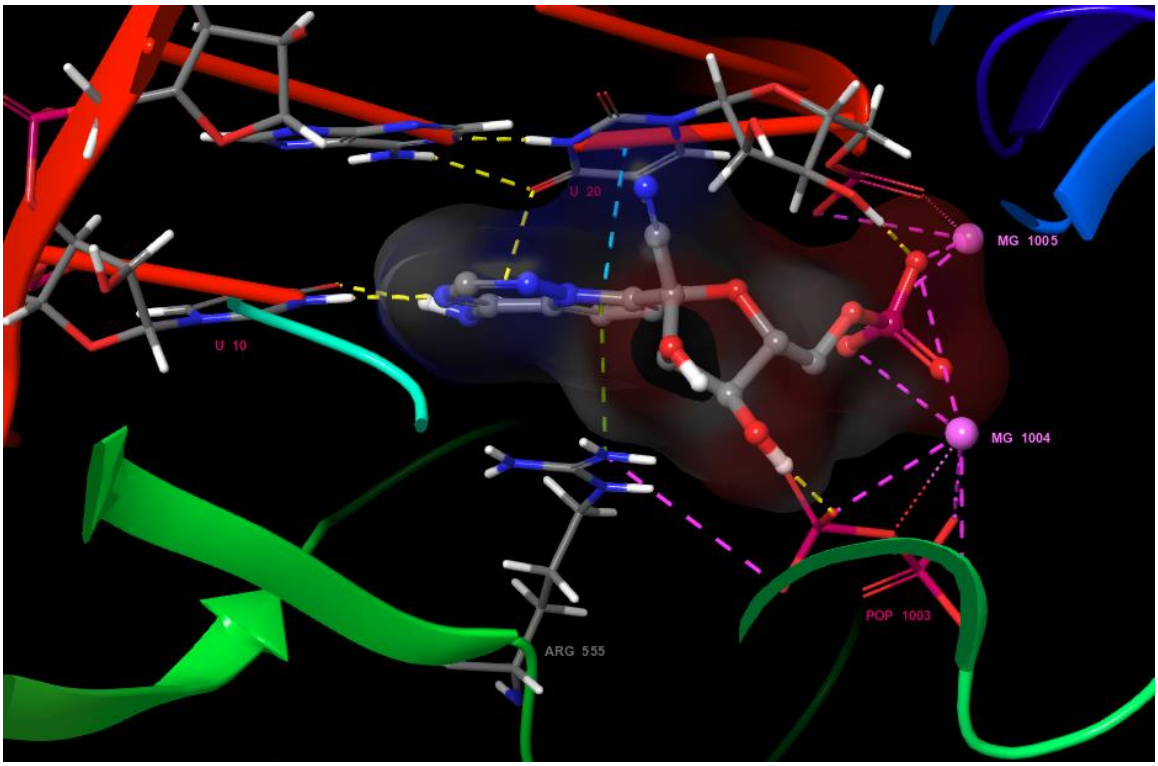

Figure 2.3 Remdesivir 3d binding interactions.

Hydrogen bonding interactions are depicted in a dashed yellow line. Pi-cation interactions are represented as a dashed green line. Salt-bridges are shown as dashed pink lines. Pi-Pi stacking is represented as a dashed cyan line.

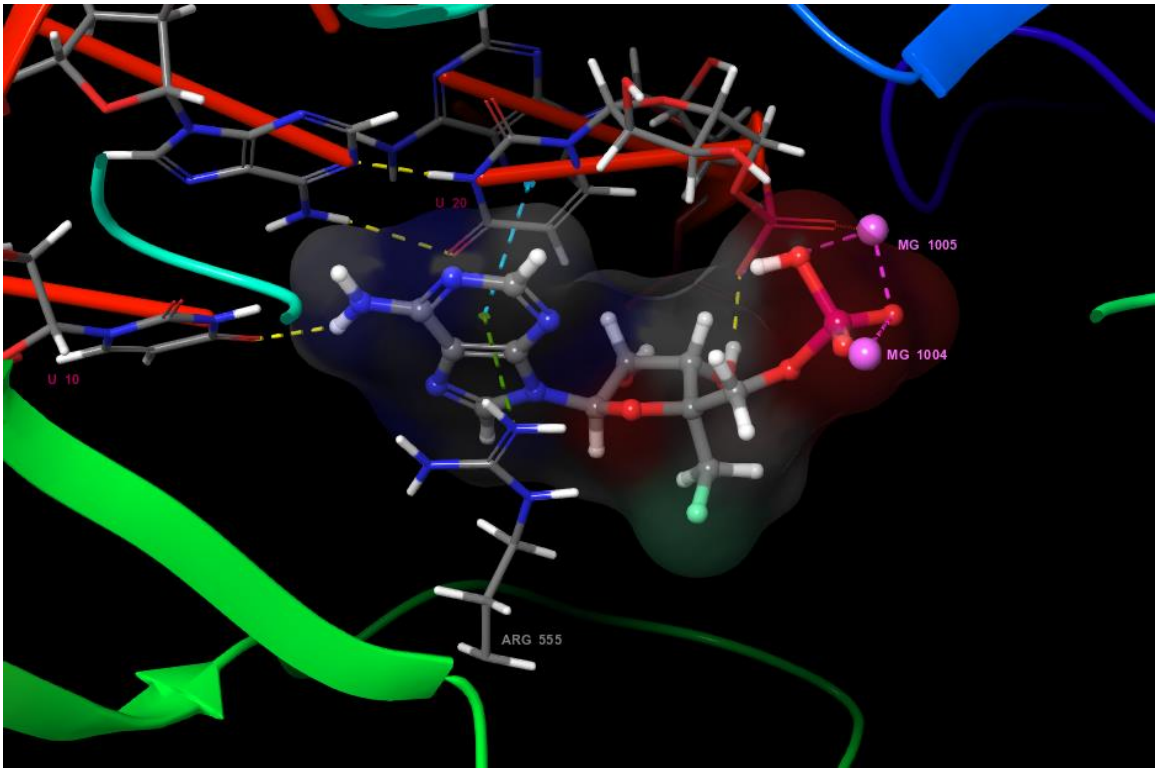

Figure 2.4 4′-*α*-fluoromethyl carbocyclic adenosine 3d binding interactions.

Hydrogen bonding interactions are depicted in a dashed yellow line. Pi-cation interactions are represented as a dashed green line. Salt-bridges are shown as dashed pink lines. Pi-Pi stacking is represented as a dashed cyan line.

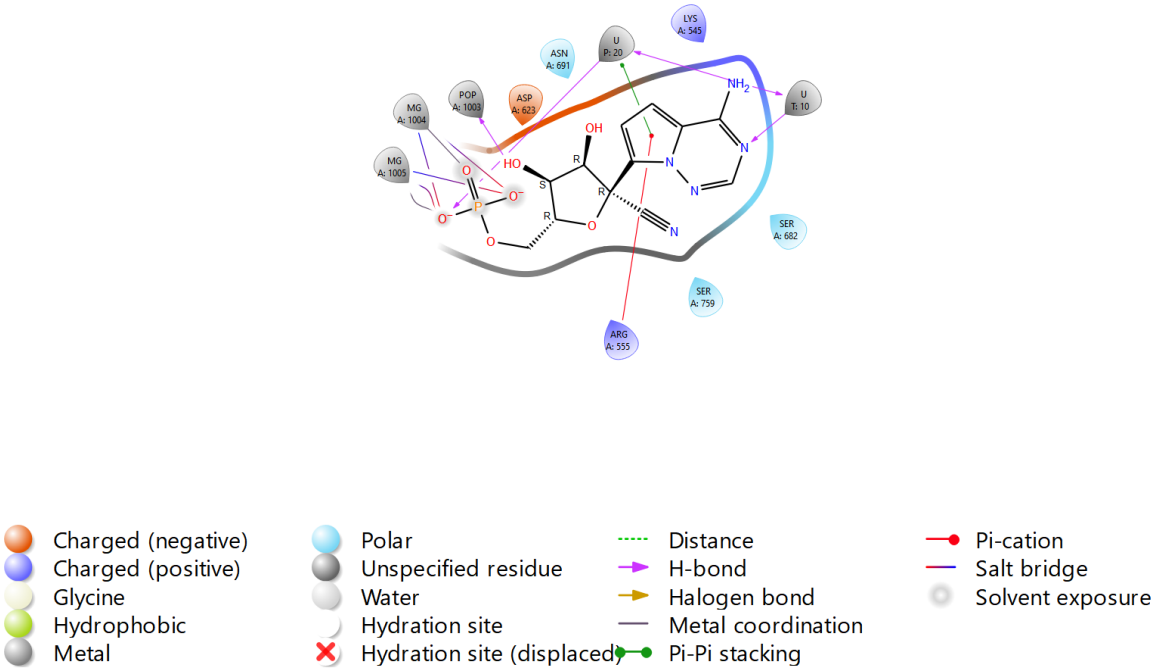

Figure 2.5 Remdesivir 2d binding interactions.

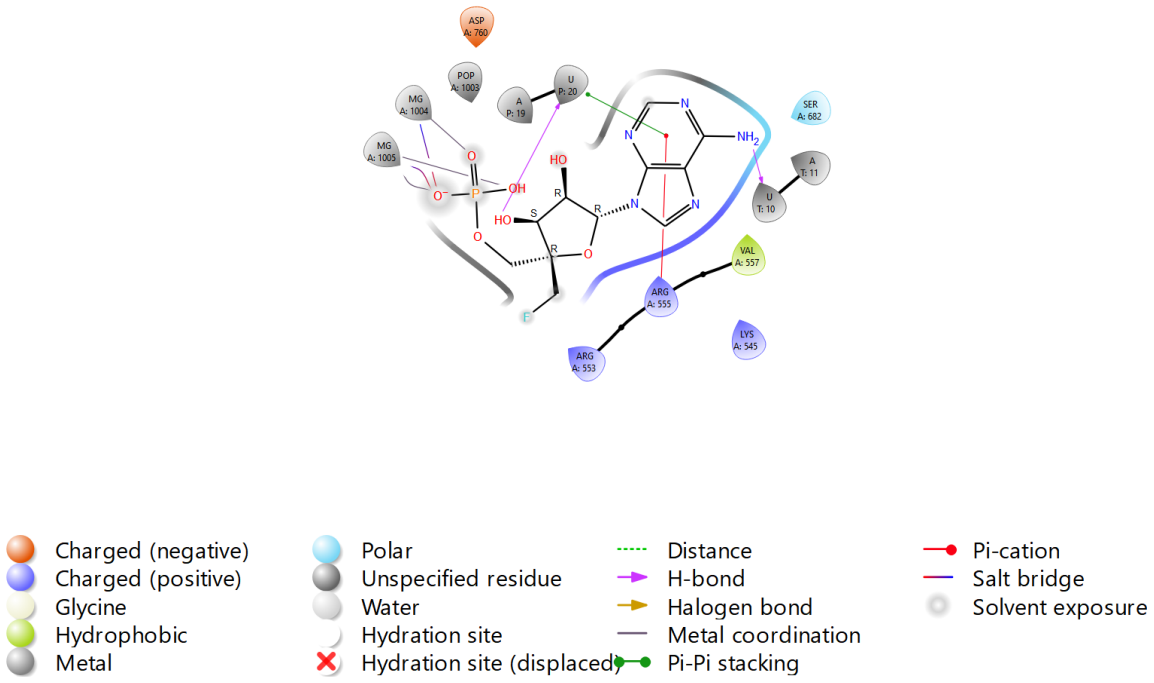

Figure 2.6 4′-*α*-fluoro-methyl carbocyclic adenosine 2d binding interactions.

Antiviral Activity

To evaluate the antiviral potency of compound **15**, it was screened against SARS-CoV-2 in Vero E6 and Huh 7.0 cell lines with standard reference drugs remdesivir and molnupiravir.[43] In these cell lines, target nucleoside **15** did not demonstrate significant antiviral activity against SARS-CoV-2. Additional screenings of **15** are in progress against coronaviruses and flaviviruses (zika and dengue) and any findings will be reported in future communications.

2.3 EXPERIMENTAL PROTOCOL

Materials

All solvents and reagents were purchased from Sigma-Aldrich and Fisher Scientific and were used without any further purification. Reactions were monitored *via* thin-layer chromatography (TLC) plates (silica gel GF 250 microns) and were visualized with a UV lamp at 254nm or developed with either a solution of 15% sulfuric acid in methanol or iodine. Melting point data were recorded *via* a Laboratory Devices Mel-Temp II apparatus and are uncorrected. High resolution mass spectra were recorded on a Bruker Impact II. Nuclear Magnetic Resonance spectra were recorded on a Varian Inova 500 spectrometer at 500, 125, and 470 MHz for ^{1}H, ^{13}C, ^{19}F NMR respectively with tetramethyl silane as the internal standard for ^{1}H and ^{13}C NMR. $CFCl_3$ (trichloro-fluoro methane) was used as the internal standard reference for ^{19}F NMR. Chemical shifts (δ) are represented as s (singlet), bs (broad singlet), d (doublet), dd (double doublet), t (triplet), q (quartet), and m (multiplet). Optical Rotations were recorded on a JASCO DIP-370 digital

polarimeter. U.V spectra were recorded on a Beckman DU-650 spectrophotometer.

Synthetic Protocol and Analytical Data

(3aS,4S,6R,6aR)-6-(tert-butoxymethyl)-2,2-dimethyltetrahydro-4H-cyclopenta[d][1,3]dioxol-4-olol (2). To a stirred solution of **1** (3.0 g, 12.38 mmol) in dry MeOH (50 mL) cooled to -78°C was added $CeCl_3 \cdot 7H_2O$ (6.9 g, 18.57 mmol). The mixture was stirred for 30 minutes, after which $NaBH_4$ (515 mg, 13.62 mmol) was added portion wise. The mixture was stirred for an additional 15 minutes and warmed to 0°C. The mixture was quenched with aqueous NH_4Cl (25 mL) and was concentrated under reduced pressure. The remaining material was dissolved in EtOAc, titrated to a slightly acidic pH with a 10% aqueous acetic acid solution (<1.0 mL), washed with water (50mL x 2), and dried over Na_2SO_4. The organic layer was concentrated under reduced pressure, and the obtained crude residue was purified via column chromatography (5% EtOAc/Hexanes) to afford **2** as a white solid. Yield: (2.90g, 96%); MP 61-65 °C; $[\alpha]^{24}_D$ = -16.48 (c 0.5, $CHCl_3$); ^{1}H NMR (500 MHz, $CDCl_3$) δ 4.45-4.40 (m, 2H), 4.23-4.19 (m, 1H), 3.31-3.28 (m, 1H), 3.20-3.17 (m, 1H), 2.20-2.15 (m, 1H), 1.85-1.77 (m, 2H), 1.47 (s, 3H), 1.33 (s, 3H), 1.11 (s, 9H); ^{13}C NMR (125 MHz, $CDCl_3$) δ 110.8, 83.6, 79.7, 72.7, 72.1, 63.1, 42.2, 36.1, 27.5, 26.3, 24.4; HRMS (ESI-TOF) m/z: [M +H]+ Calcd for $C_{13}H_{25}O_4$ 245.1753; Found 245.1747.

(3aS,4S,6R,6aR)-4-(benzyloxy)-6-(tert-butoxymethyl)-2,2-dimethyltetrahydro-4H-cyclopenta[d][1,3]dioxole (3). To a stirred solution of **2** (2.9 g, 11.87 mmol) in anhydrous DMF (30 mL) under N_2 cooled to 0°C, was added 60% NaH (712 mg, 17.81 mmol). The mixture stirred for 30 minutes at 0°C, after which benzyl bromide (2.1 mL, 17.81 mmol) was added dropwise. The mixture was stirred for an additional 10 minutes and warmed to room temperature (rt). The mixture was quenched with ice-cold water (25 mL), extracted with EtOAc (25mL x 3), washed with water (50 mL x 2), and dried over Na_2SO_4. The organic layer was concentrated under reduced pressure and the derived crude oil was purified via column chromatography (6% EtOAc/Hexanes) to afford **3** as an oil. Yield: (3.0 g, 76%); $[\alpha]^{24}_D$ -47.76 (c 0.1, $CHCl_3$); ^{1}H NMR (500 MHz, $CDCl_3$) δ 7.37-7.23 (m, 5H), 4.65 (d, *J* = 12.0 Hz, 1H), 4.57 (d, *J* = 12.5 Hz, 1H), 4.50 (t, *J* = 5.5 & 10.5 Hz, 1H), 4.35 (d, *J* = 5.5 Hz, 1H), 4.01-3.92 (m, 1H), 3.20 (q, *J* = 5.0 & 8.5 Hz, 1H), 3.12 (q, *J* = 5.0 & 8.5 Hz, 1H), 2.12-2.03 (m, 2H), 1.72-1.68 (m, 1H), 1.50 (s, 3H), 1.31 (s, 3H), 1.03 (s, 9H); ^{13}C NMR (125 MHz, $CDCl_3$) δ 138.7, 128.4, 128.0, 127.6, 110.7, 83.0, 79.3, 78.4, 71.7, 63.5, 42.6, 31.8, 27.4, 26.7, 24.7; HRMS (ESI-TOF) m/z: [M +Na]+ Calcd for $C_{20}H_{30}O_4Na$ 357.2042; Found 357.2042.

(1R,2R,3S,5R)-3-(benzyloxy)-5-(hydroxymethyl)cyclopentane-1,2-diol (4). In a round bottom flask containing **3** (3.0 g, 8.96 mmoL) was added ice-cold TFA/water (9 mL, 2:1). The mixture was stirred for 10 minutes, after that it was heated at 60°C, and stirred for an additional 4 h. The mixture was co-evaporated three times with MeOH (20mL x 3), neutralized with a 28% aqueous NH_4OH

solution, and again co-evaporated with MeOH. The derived residue was purified via column chromatography (5% MeOH/DCM) to afford **4** as a white solid. Yield: (1.46g, 67%); MP (112-115°C); $[\alpha]^{23}_{D}$ +7.23 (c 0.6, MeOH); ^{1}H NMR (500 MHz, CD_3OD) δ 7.36-7.22 (m, 5H), 4.55 (dd, *J* = 10.0 & 40.0 Hz, 2H), 3.98 (t, *J* = 5.0 & 10.0 Hz, 1H), 3.85-3.82 (m, 1H), 3.72-3.69 (m, 1H), 3.58 (dd, *J* = 5.0 & 10.0 Hz, 1H), 3.49 (dd, *J* = 5.0 & 10.0 Hz, 1H), 2.25-2.18 (m, 1H), 2.02-1.96 (m, 1H), 1.73-1.67 (m, 1H); ^{13}C NMR (125 MHz, $CDCl_3$) δ 138.5, 128.0, 127.6, 127.3, 78.4, 73.4, 72.7, 71.1, 63.1, 44.9, 29.9; HRMS (ESI-TOF) m/z: [M+H]+ Calcd for $C_{13}H_{19}O_4$ 239.1283; Found 239.1278.

((3aR,4R,6S,6aS)-6-(benzyloxy)-2,2-dimethyltetrahydro-4H-cyclopenta[d][1,3]dioxol-4-yl)methanol (5). To a stirred solution of **4** (9.0 g, 37.8 mmol) in anhydrous acetone (150 mL) under N_2 was added 7.0 mL dimethoxy-propane (56.7 mmol). The mixture was cooled to 0°C, and 300 mg catalytic p-TSA was added. The mixture stirred for 2 hours, after which it was quenched with solid $NaHCO_3$ until slightly basic, filtered through a celite bed, and concentrated under reduced pressure. The residue was diluted in EtOAc (50 mL), washed with water (50mL x 2), brine (50mL x 2), dried over Na_2SO_4, and concentrated under reduced pressure. The crude residue was purified via column chromatography (2.5% MeOH/DCM) to give **5** as a colorless oil. Yield: (7.6g, 72%); $[\alpha]^{26}_{D}$ = -36.14 (c 0.5, $CHCl_3$); ^{1}H NMR (500 MHz, $CDCl_3$) δ 7.36-7.24 (m, 5H), 4.66 (d, *J* = 15.0 Hz, 1H), 4.57-4.53 (m, 2H), 4.41 (d, *J* = 5.0 Hz, 1H), 3.86-3.82 (m, 1H), 3.46 (dd, *J* = 5.0 & 10.0 Hz, 1H), 3.36 (dd, *J* = 10.0 & 15.0 Hz, 1H), 2.17-2.04 (m, 2H), 1.97 (bs, 1H),

1.72-1.68 (m, 1H), 1.50 (s, 3H), 1.31 (s, 3H); ^{13}C NMR (125 MHz, $CDCl_3$) δ 138.5, 128.4, 127.9, 127.7, 111.3, 82.0, 79.1, 78.4, 71.9, 64.1, 44.6, 30.9, 26.5, 24.7; HR-MS (ESI-TOF) m/z: $[M + H]^+$ Calcd for $C_{16}H_{23}O_4$ 279.1596; found 279.1594.

((3aR,6S,6aS)-6-(benzyloxy)-2,2-dimethyltetrahydro-4H-cyclopenta[d][1,3]dioxole-4,4-diyl)dimethanol (7). To a stirred solution of **5** (3.0 g, 10.79 mmol) in anhydrous DCM (25 mL) under N_2, cooled to 0°C, were added 6.85 g Dess Martine Periodinane (16.2 mmol). The mixture was stirred for one hour at room temperature, after which it was diluted with additional DCM (25 mL). The mixture was washed with aqueous $Na_2S_2O_3$ (50 mL), aqueous $NaHCO_3$ (50 mL), and water (50 mL). The organic layer was concentrated under reduced pressure, dissolved in EtOAc (50 mL), and again washed in the above manner. The organic layer was concentrated under reduced pressure to give crude intermediate **6** (2.1 g), which was immediately used as such without further purification. Compound **6** was dissolved in THF (20 mL), and to the stirred solution under N_2 was added 37% formaldehyde (8.75 mL, 108.0 mmol). To this mixture, NaOH (1M aqueous, 15.2 mL) was added dropwise slowly over 5 minutes. The mixture was stirred for 70 minutes at room temperature, after which it was cooled to 0°C, and $NaBH_4$ (1.47g, 38.8mmol) was added portion wise. The mixture was stirred for two hours at room temperature, after which it was quenched with aqueous NH_4Cl (30 mL), and 10% aqueous acetic acid (<1.0mL) until slightly acidic. The mixture was extracted with EtOAc (30mL x 2), washed with water (50 mL x 2), dried over Na_2SO_4, and concentrated under reduced pressure to afford the crude residue. The residue was

purified by column chromatography (15% EtOAc/Hexanes) to afford **11** as an oil. Yield: (1.13g, 34%); $[\alpha]^{25}_{D}$ = +5.645 (c 0.5, $CHCl_3$; ^{1}H NMR (500 MHz, $CDCl_3$) δ 7.36-7.27 (m, 5H), 4.65-4.62 (m, 2H), 4.57 (d, *J* = 12.0 Hz, 1H), 4.47 (d, *J* = 5.5 Hz, 1H), 3.88-3.84 (m, 2H), 3.65 (d, *J* = 11.5 Hz, 1H), 3.52 (d, *J* = 11.0 Hz, 1H), 3.41 (d, *J* = 11.0 Hz, 1H), 1.64 (d, *J* = 9.0 Hz, 2H), 1.54 (s, 3H), 1.33 (s, 3H); ^{13}C NMR (125 MHz, $CDCl_3$) δ 138.2, 128.5, 128.0, 127.9, 111.4, 81.4, 79.4, 72.0, 68.1, 67.6, 47.9, 33.3, 26.1, 24.3; HR-MS (ESI-TOF) m/z: $[M + H]^+$ Calcd for $C_{17}H_{25}O_5$ 309.1702; found 309.1698.

((3aR,4S,6S,6aS)-6-(benzyloxy)-4-(((tert-butyldiphenylsilyl)oxy)methyl)-2,2-dimethyltetrahydro-4H-cyclopenta[d][1,3]dioxol-4-yl)methanol (8a and 8b mix of diastereomers). To a dry mixture of **7** (1.1 g, 3.57 mmol) and imidazole (0.97 g, 14.28 mmol) were added 2.0 mL anhydrous DCM under N_2. The stirred solution was cooled to 0°C, at which TBDPSCl (0.84 mL, 3.21 mmol) were added, and the mixture was stirred for 2 hours at 0°C. The mixture was then quenched with water (50 mL) and extracted with DCM (50 mL). The organic layer was dried over Na_2SO_4 and concentrated under reduced pressure to afford a crude residue, which upon purification gave diastereomers **8a** and **8b** as an inseparable oil. Yield: (1.29 g, 66%); ^{1}H NMR (500 MHz, $CDCl_3$) (mix of diastereomers) δ 7.73-7.71 (m, 1H), 7.61-7.56 (m, 2H), 7.43-7.25 (m, 12H), 4.68-4.62 (m, 1H), 4.56-4.41 (m, 2H), 4.17 (d, *J* = 5.0 Hz, 1H), 3.96-3.86 (m, 1H), 3.70-3.65 (m, 2H), 3.55-3.53 (m, 1H), 3.33-3.31 (m, 1H), 1.97-1.79 (m, 2H), 1.56 (s, 3H), 1.30 (s, 3H), 1.02 (s, 9H); ^{13}C NMR (125 MHz, $CDCl_3$) (mix of diastereomers) δ 138.5, 135.8, 135.7, 135.6,

133.0, 129.9, 128.5, 128.0, 127.9, 127.8, 127.7, 111.1, 110.9, 82.7, 81.01, 79.4, 78.6, 71.9, 66.3, 65.0, 48.9, 47.5, 33.1, 27.0, 26.1, 24.4, 24.1, 19.3; HR-MS (ESI-TOF) m/z: [M + H]+ Calcd for $C_{33}H_{43}O_5Si$ 547.2880; found 547.2877.

((3aR,4S,6S,6aS)-6-(benzyloxy)-4-(fluoromethyl)-2,2-dimethyltetrahydro-4H-cyclopenta[d][1,3]dioxol-4-yl)methanol (10a). To a stirred solution of diastereomers **8a** and **8b** (1.29 g, 2.36 mmol) in anhydrous DCM (20 mL) and anhydrous pyridine (0.86 mL, 10.62 mmol) cooled to -78°C were added 0.6 mL trifluoromethanesulfonic anhydride (3.54 mmoL). The mixture was allowed to stir for 1 hour at room temperature. After that the reaction mixture was quenched with ice-cold water (50 mL), extracted with DCM (30 mL), and washed twice with water (50 mL x 2). The organic layer was dried over Na_2SO_4 and concentrated under reduced pressure to yield 1.18 g of inseparable crude diastereomers **9a** and **9b**, which were immediately dissolved in 18 mL anhydrous THF under N_2. The stirred solution was cooled to 0°C, after which tetrabutylammonium fluoride (6.1 mL, 1M solution in THF) was added dropwise. The mixture stirred for 24 hours, and was then quenched with 20 mL aqueous NH_4Cl, diluted with water (30mL), and extracted with EtOAc (50mL). The organic layer was dried over Na_2SO_4 and concentrated under reduced pressure to afford a crude separable residue. Diastereomeric purification was obtained with column chromatography (8-12% EtOAc/Hexanes) to afford pure **10a** (235 mg, 16%) and **10b** (32 mg, 2.1%) as a yellow foam. $[\alpha]^{25}_D$ = -17.04 (c 0.5, $CHCl_3$); ^{1}H NMR (500 MHz, $CDCl_3$) δ 7.37-7.26 (m, 5H), 4.70-4.55 (m, 4H), 4.41 (dd, *J* = 9.0 & 47.5 Hz, 1H), 4.33 (d, *J* = 5.5 Hz,

1H), 3.95-3.90 (m, 1H), 3.48 (dd, *J* = 11.0 & 29.0 Hz, 2H), 1.88-1.84 (m, 1H), 1.72-1.68 (m, 1H), 1.53 (s, 3H), 1.32 (s, 3H); ^{13}C NMR (125 MHz, $CDCl_3$) δ 138.2, 128.5, 128.0, 127.8 111.4, 86.0, 84.7, 81.2, 79.0, 71.9, 64.1, 47.7, 32.7, 26.0, 24.3; ^{19}F NMR (470 MHz, $CDCl_3$) δ -227.7 (t, *J* = 47.0 & 94.0 Hz, 1F); HR-MS (ESI-TOF) m/z: $[M + Na]^+$ Calcd for $C_{17}H_{23}FO_4Na$ 333.1478; found 333.1474.

((3a*R*,4*R*,6*S*,6a*S*)-6-(benzyloxy)-4-(fluoromethyl)-2,2-dimethyltetrahydro-4*H*-cyclopenta[*d*][1,3]dioxol-4-yl)methanol (**10b)**: $[\alpha]^{25}_D$ = -5.27 (c 0.25, $CHCl_3$); ^{1}H NMR (500 MHz, CDCl3) δ 7.36-7.25 (m, 5H), 4.78 (d, *J* = 5.0 Hz, 1H), 4.66-4.62 (m, 2H), 4.58-4.50 (m, 3H), 4.33 (d, *J* = 5.0 Hz, 1H), 4.27 (d, *J* = 5.0 Hz, 1H), 3.38-3.34 (m, 1H), 2.19 (q, *J* = 5.0 & 10.0 Hz, 1H), 2.03 (t, *J* = 15.0 & 25.0 Hz, 1H), 1.44 (s, 3H), 1.33 (s, 3H); ^{13}C NMR (125 MHz, CDCl3) δ 138.1, 128.5, 127.9, 111.1, 83.9, 81.3, 77.9, 76.3, 75.9, 71.8, 44.6, 36.4, 26.0, 24.2; ^{19}F NMR (470 MHz, $CDCl_3$) δ -227.21 (t, *J* = 47.0 & 94.0 Hz, 1F); HR-MS (ESI-TOF) m/z: $[M + Na]^+$ Calcd for $C_{17}H_{23}FO_4Na$ 333.1478; found 333.1473.

(3aR,4S,6S,6aS)-6-(benzyloxy)-4-(fluoromethyl)-4-((methoxymethoxy) methyl)-2,2-dimethyltetrahydro-4H-cyclopenta[d][1,3]dioxole (11). To a stirred solution of **10a** (600 mg, 1.93 mmol) in anhydrous DCM (12 mL) cooled to 0°C and under N_2 were added 0.85 mL DIPEA (4.83 mmol). The mixture was stirred for 15 minutes, after which 0.3 mL MOM-Cl (3.86 mmol) were added dropwise. The solution was allowed to stir overnight at room temperature, after which it was cooled to 0°C and an additional aliquot of DIPEA (0.25 mL) and MOM-Cl (0.10mL) were added sequentially. The mixture was allowed to stir at room

temperature for 8 hours, after which it was concentrated under reduced pressure, diluted with EtOAc (50mL), washed with aqueous NH_4Cl (50 mL x 2), dried over Na_2SO_4, and concentrated under reduced pressure. The obtained crude was purified via column chromatography (6% EtOAc/Hexanes) to afford **11** as a colorless oil. Yield: (450 mg, 66%); $[\alpha]^{25}_D$ = -15.40 (c 0.6, $CHCl_3$); ^{1}H NMR (500 MHz, $CDCl_3$) δ 7.37-7.25 (m, 5H), 4.67-4.62 (m, 2H), 4.58-4.52 (m, 4H), 4.38 (dd, *J* = 8.5 & 47.5 Hz, 1H), 4.29 (d, *J* = 5.5 Hz, 1H), 3.99-3.94 (m, 1H), 3.38-3.30 (m, 2H), 3.24 (s, 3H), 1.89-1.85 (m, 1H), 1.75-1.71 (m, 1H), 1.54 (s, 3H), 1.33 (s, 3H); ^{13}C NMR (125 MHz, $CDCl_3$) δ 138.3, 128.5, 128.0, 127.8, 111.3, 96.6, 84.9, 83.5, 81.7, 79.2, 71.8, 68.5, 55.3, 47.0, 33.3, 26.1, 24.3; ^{19}F NMR (470 MHz, CDCl3) δ -228.11 (t, *J* = 47.0 & 94.0 Hz, 1F); HRMS (ESI-TOF) m/z: $[M + H]^+$ Calcd for $C_{19}H_{28}FO_5$ 355.1921; found 355.1915.

(3aS,4S,6S,6aR)-6-(fluoromethyl)-6-((methoxymethoxy)methyl)-2,2-dimethyl tetrahydro-4H-cyclopenta[d][1,3]dioxol-4-ol (12). In a parr hydrogenator, compound **11** (480 mg, 1.35 mmol) was dissolved in 25 mL MeOH, followed by 240 mg palladium activated charcoal (10% Pd/C) and treated with H_2 at 5 PSI for 6 hours. Afterwards, the solution was passed through a celite bed and the obtained filtrate was concentrated under reduced pressure, and purified via column chromatography (13% EtOAc/Hexanes) to afford **12** as a viscous colorless solid. Yield: (250 mg, 70%); $[\alpha]^{25}_D$ = +12.53 (c 0.3, $CHCl_3$); ^{1}H NMR(500 MHz, $CDCl_3$) δ 4.63-4.52 (m, 2H), 4.60 (s, 2H), 4.37 (dd, *J* = 9.0 & 47.5 Hz, 1H), 4.38 (d, *J* = 6.0 Hz, 1H), 4.28-4.22 (m, 1H), 3.44 (d, *J* = 9.5 Hz, 1H), 3.40 (d, *J* = 9.5 Hz, 1H), 3.35

(s, 3H), 2.44 (d, *J* = 10.0 Hz, 1H), 1.98 (q, *J* = 7.0 & 13.0 Hz, 1H), 1.50 (s, 3H), 1.49-1.47 (m, 1H), 1.35 (s, 3H); ^{13}C NMR (125 MHz, $CDCl_3$) δ 111.3, 96.7, 84.7, 83.3, 82.2, 79.6, 71.1, 68.7, 55.5, 47.5, 37.1, 25.9, 24.2; ^{19}F NMR (470 MHz, $CDCl_3$) δ -227.82 (t, *J* = 47.0 & 94.0 Hz, 1F); HRMS (ESI-TOF) m/z: $[M + Na]^+$ Calcd for $C_{12}H_{21}FO_5Na$ 287.1265; found 287.1268.

di-tert-butyl(9-((3aS,4R,6S,6aR)-6-(fluoromethyl)-6-((methoxymethoxy) methyl)-2,2-dimethyltetrahydro-4H-cyclopenta[d][1,3]dioxol-4-yl)-9H-purin-6-yl)iminodicarbonate (14). To a stirred solution of **12** (100.0 mg, 0.379 mmol) in anhydrous DCM (5 mL) was added 0.14 mL pyridine (1.70 mmol). The mixture was cooled to -78°C, and 0.1 mL of triflic anhydride (0.57 mmol) were added dropwise. The mixture was allowed to warm to 0°C and continue stirring for 50 minutes, after that the reaction mixture was diluted with DCM (50 mL), washed with water (50 mL x 2), and dried over Na_2SO_4 to afford intermediate **13**, which was used as such in the next step without further purification. In a separate round bottom flask, 253 mg of N,N-6-diboc-adenine (0.76 mmol) were dissolved in DMF (3.0 mL) under N_2. To this, 37.0 mg NaH (0.83 mmol) and 220 mg 18-Crown-6 ether (0.83 mmol) were added, and the mixture was allowed to stir at 70 °C for 4 hours. The mixture was cooled to 0°C, at which **13** was added by dissolving in DMF (1.0 mL), and the mixture was allowed to stir at room temperature for 72 hours. The mixture was concentrated *in vacuo*, diluted with EtOAc (50 mL), washed with water (50 mL x 2), brine (50 mL), and dried over Na_2SO_4. The organic layer was concentrated under reduced pressure and the derived crude residue was purified via column

chromatography (22% EtOAc/Hexanes) to afford **14** as a viscous solid. Yield: (30 mg, 20%); ^{1}H NMR (500 MHz, $CDCl_3$) δ 8.84 (s, 1H), 8.14 (s, 1H), 5.19 (t, *J* = 5.5 & 12.0 Hz, 1H), 4.99-4.94 (m, 1H), 4.76-4.70 (m, 1H), 4.69 (s, 2H), 4.66-4.63 (m, 1H), 4.57 (dd, *J* = 9.5 & 40.5 Hz, 1H), 3.67 (d, *J* = 9.5 Hz, 1H), 3.58 (d, *J* = 11.0 Hz, 1H), 3.37 (s, 3H), 2.52-2.49 (m, 2H), 1.56 (s, 3H), 1.46 (s, 18H), 1.31 (s, 3H); ^{13}C NMR (125 MHz, $CDCl_3$) δ 153.3, 152.0, 150.7, 144.1, 129.7, 114.0, 96.8, 84.5, 83.9, 83.0, 82.9, 69.8, 61.5, 55.6, 48.0, 35.3, 27.9, 26.8, 24.7; ^{19}F NMR (470 MHz, CDCl3) δ -230.35 (t, *J* = 47.0 & 94.0 Hz, 1F); HRMS (ESI-TOF) m/z: $[M+H]^+$ Calcd for $C_{27}H_{41}FN_5O_8$ 582.2939; found 582.2938.

(1S,2R,3S,5R)-5-(6-amino-9H-purin-9-yl)-3-(fluoromethyl)-3-(hydroxymethyl) cyclopentane-1,2-diol (15). To a stirred solution of **14** (30mg, 0.051mmol) in anhydrous DCM (2.0mL) under N_2 was added a solution of TFA in DCM (1:1, 2mL). The mixture was allowed to stir for 48 hours at room temperature, after which it was concentrated under reduced pressure, co-evaporated with methanol, and neutralized with 28% aqueous ammonium hydroxide solution. The derived crude residue was purified via column chromatography (9% MeOH/DCM) to afford **15** as a white powder. Yield: (13mg, 85%); UV(Water) λmax 260.0 nm (pH 7.4), λmax 260.0 nm (pH 11.0); $[\alpha]^{25}_{D}$ = -32.98 (c 0.50, CH_3OH); ^{1}H NMR (500 MHz, CD_3OD) δ 8.17 (s, 1H), 8.16 (s, 1H), 4.88 (q, *J* = 10.0 & 19.5 Hz, 1H), 4.76-4.64 (m, 2H), 4.47 (dd, *J* = 9.0 & 47.5 Hz, 1H), 4.02 (d, *J* = 4.5 Hz, 1H), 3.68 (s, 2H), 2.18-2.13 (m, 1H), 2.01-1.96 (m, 1H); ^{13}C NMR (125 MHz, CD_3OD) δ 155.9, 152.0, 149.6, 140.7, 83.9, 82.6, 75.0, 73.2, 64.0, 59.7, 31.3, 22.5; ^{19}F NMR (470 MHz, CD_3OD)

δ -232.40 (t, *J* = 47.0 & 94.0 Hz, 1F); HRMS (ESI-TOF) m/z: $[M + H]^+$ Calcd for $C_{12}H_{17}FN_5O_3$ 298.1315; found 298.1311.

Molecular Modeling Methodology

Protein structures were downloaded from protein data bank (PDB, 7BV2), and chains B and C were removed.[44] Chain A, the bound RNA, and the metal ions were then prepared using Schrodinger Maestro. Water molecules were removed from the surrounding areas and were not present in the binding site. The covalently bound remdesivir monophosphate (RDV-MP) was separated from the RNA chain. A docking grid was generated using glide with the centroid surrounding RDV-MP acting as the binding pocket. Compared Docking score, utilizing Glide, was performed on both remdesivir monophosphate, and monophosphorylated 4′-*α*-fluoromethyl carbocyclic adenosine (**15**). RMSD analysis was performed with a superposition subroutine via Schrodinger Maestro to compare the docked remdesivir monophosphate to the cryoEM structure.

Protocol and Method for Antiviral Efficacy and Cytotoxicity Assays

The antiviral activity of synthesized compound **15** was evaluated by Prof. Robert Jeff. Hogan in the Dept. of Infectious Diseases & Dept. of Biomedical Sciences College of Veterinary Medicine and Dr. Steven P. Maher in the Center for Tropical and Emerging Global Diseases at the University of Georgia. Compound **15** was tested for antiviral activity against SARS-CoV-2 strains USA-WA1/2020 and Hong Kong/VM20001061/2020, both viruses were obtained

through BEI Resources (Manassas, VA) and have been sequenced. The *in-vitro* activity assay is based on a 384-well microtiter plate format with remdesivir as positive controls.[54] Vero E6 (ATCC, C1008) or Human Huh 7.5 cells are added to 384 well plates at 2 x 10^3 cells per well. Stock compound powders are dissolved to be 50mM in DMSO and serially diluted in DMSO using automation (Beckman Coulter). After incubation at 37°C in 5% CO_2 for 24 hours, a pin tool is used to transfer 40nL from the 1000x dilution plate to the assay plate holding 40 µL media per well, generating a 1x final compound concentration and 1:1000 DMSO concentration per well (DMSO alone is used as the negative control). Each assay plate is copied such that one is infected with SARS-CoV-2 while the other is uninfected to assess cytotoxicity. Two hours after addition of compounds, virus is added to the plate designated for infection to achieve 0.01 and 0.1 plaque forming units (PFU) per cell and 100% cell death in negative control wells. After incubation for 72 hours at 37°C in 5% CO_2, cytopathic effect is measured by adding 4 µL of 10x Prestoblue cell viability reagent (Thermo Fisher) to each well, incubating for 1hr at 37°C, and then reading at 540/580 nm with a Bio-Tek Synergy H1 plate reader. Raw fluorescence values are normalized to positive and negative controls and then EC_{50}'s is calculated using algorithms built into CDD Vault. The geometric mean of historical runs of remdesivir is used to validate each assay run; the EC_{50} of remdesivir must be 3-fold higher or lower than the historical geometric mean for the run to be valid.

2.4 CONCLUSION

Overall, a novel procedure for the synthesis of 4′-α-fluoromethyl carbocyclic adenosine analog **15** has been developed in 14-steps with 0.1% total yield. The synthesis commenced with carbocyclic ketone (**1**), and through reduction and protection intermediate 5-hydroxy (**5**) was constructed. Subsequent oxidation and condensation of (**5**) gave diol (**7**) which on selective bulky protection followed by fluorination yielded 4-*α*-fluoromethyl carbocyclic intermediate (**10a**). Key intermediate **15** was synthesized from **10a** via sequential protection and deprotection. Finally coupling of adenine via an S_N2 mechanism furnished the target nucleoside (**15**). This is the first report of the synthesis of 4'-*α*-fluoromethyl derived carbocyclic nucleosides. The reported protocols are beneficial for the medicinal chemist and open a new avenue for the synthesis of new analogs 4'-derivatized nucleoside and nucleotides against various emerging viruses. However, so far, compound **15** has not demonstrated significant antiviral activity against SARS-CoV-2. Furthermore, antiviral evaluation against Flaviviruses is in progress. However, the novel synthesis of 4^{th} position methyl halogens on a carbocyclic ring may offer medicinal and synthetic chemists to elaborate complete structural-activity relationships (SAR) of this class of nucleoside against various emerging viruses.

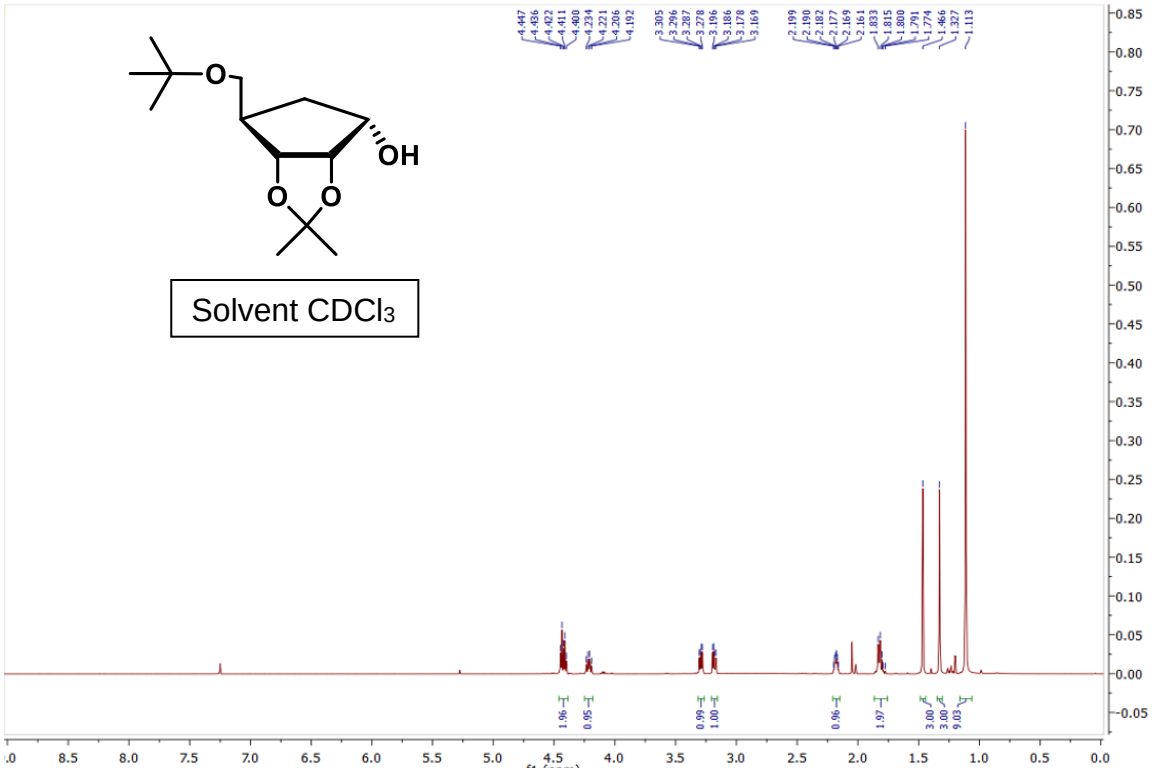

Figure 2.7 ^{1}H NMR of Compound 2.

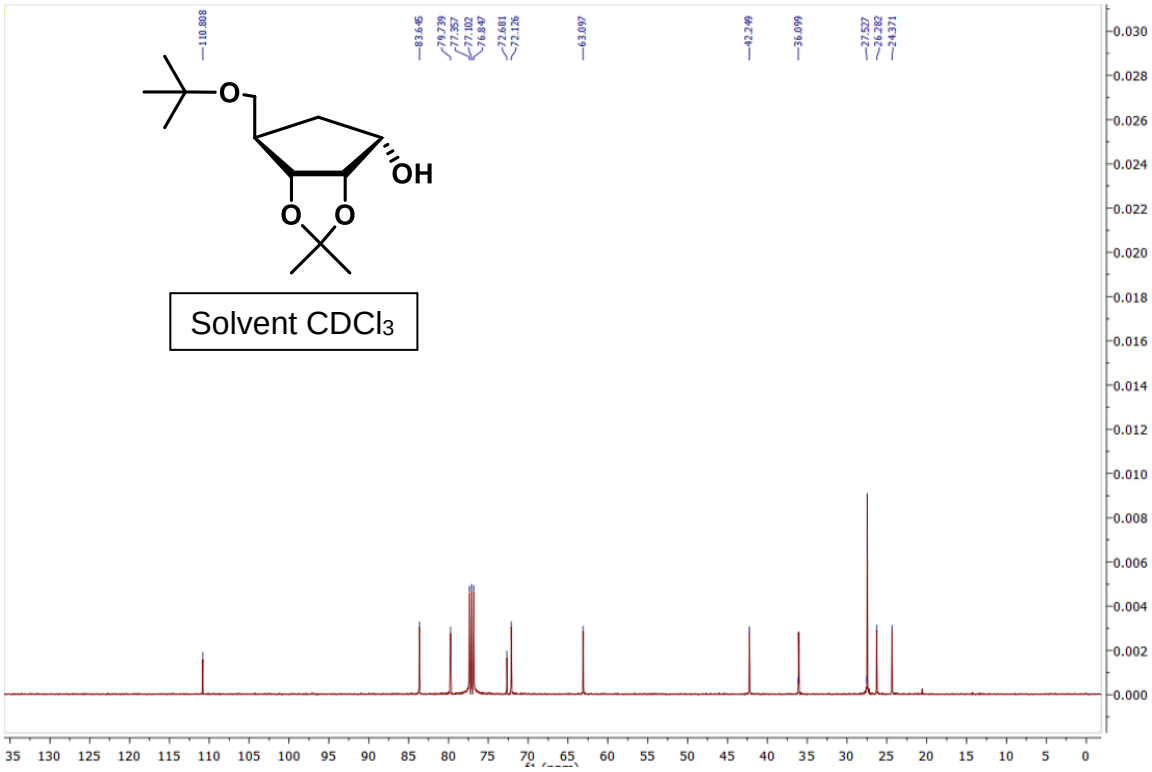

Figure 2.8 ^{13}C NMR of compound 2.

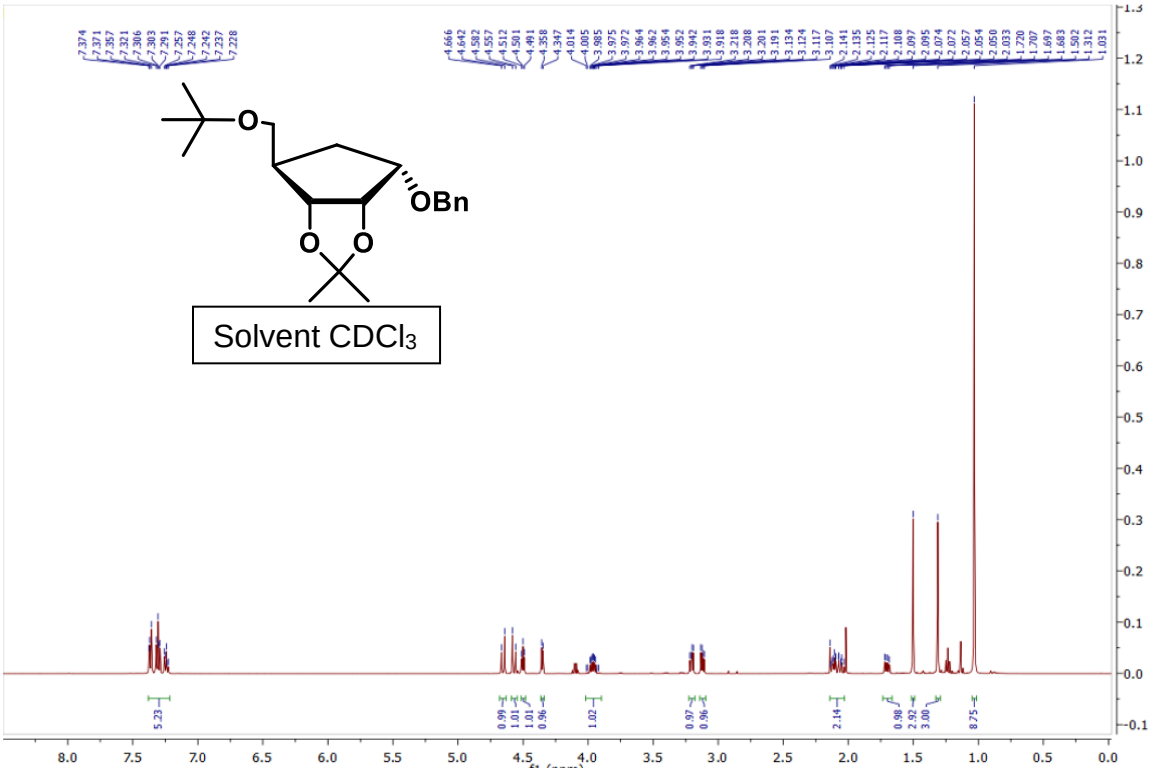

Figure 2.9 ^{1}H NMR of compound 3.

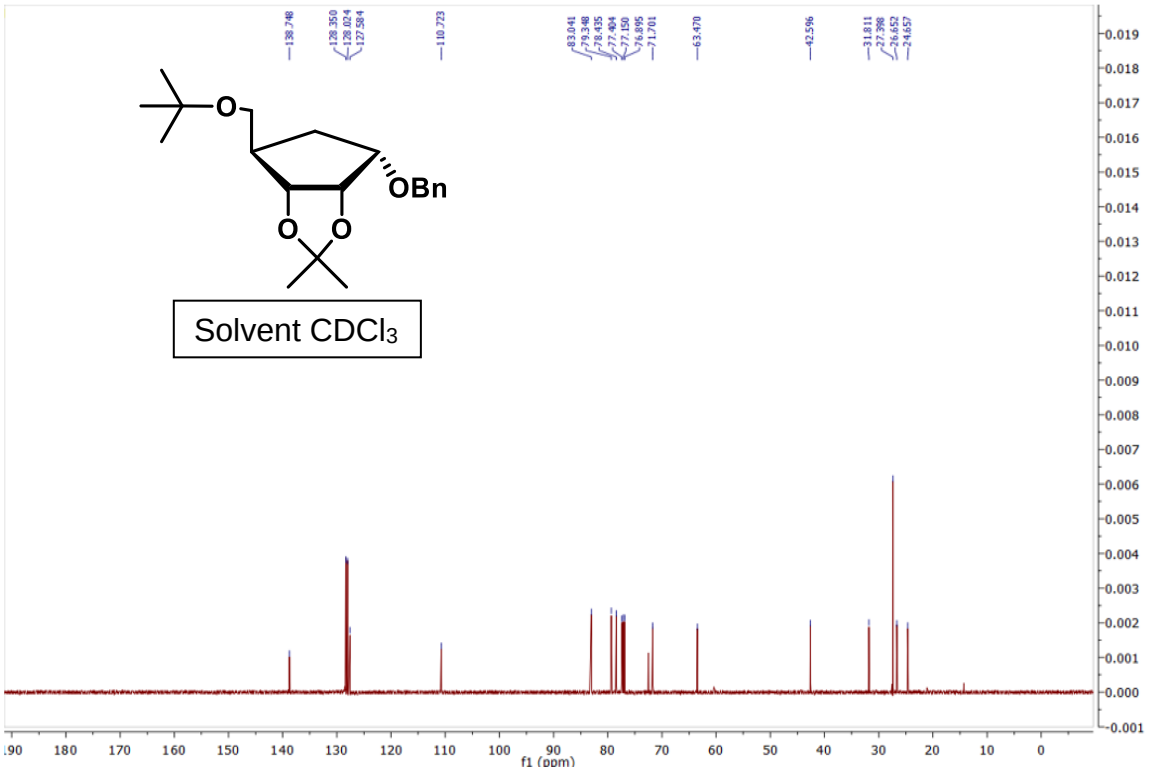

Figure 2.10 ^{13}C NMR of compound 3.

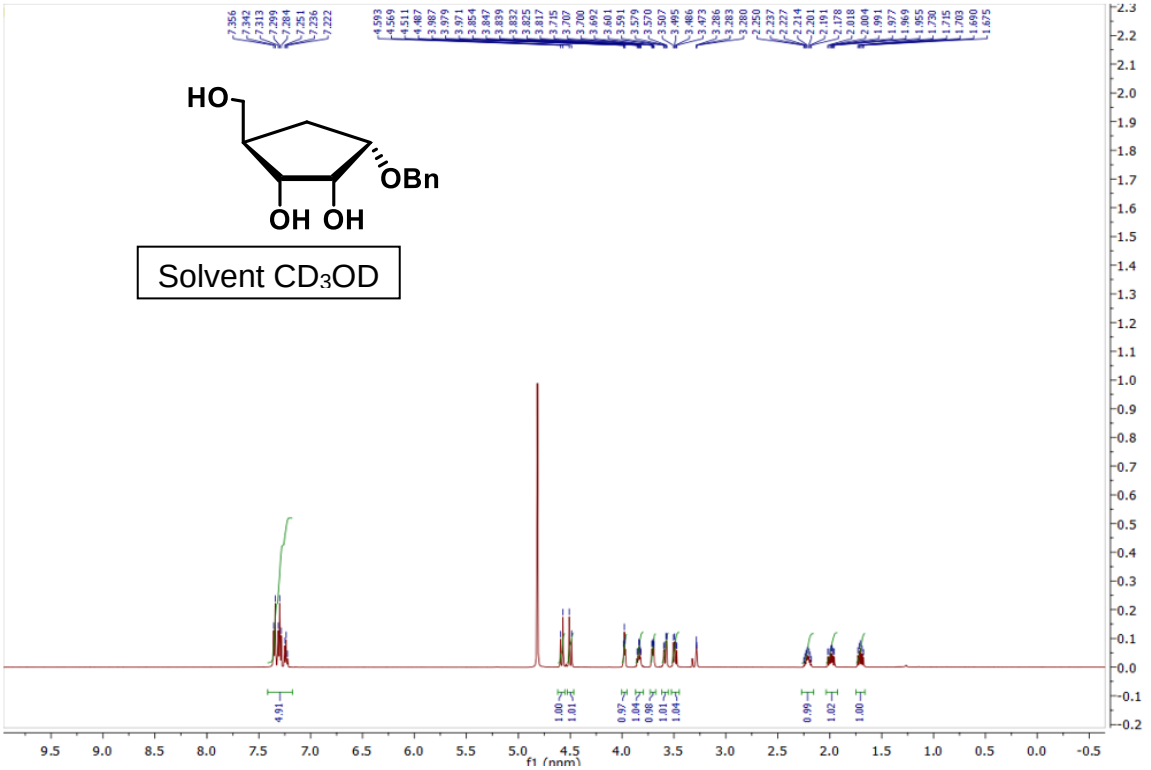

Figure 2.11 ^{1}H NMR of compound 4.

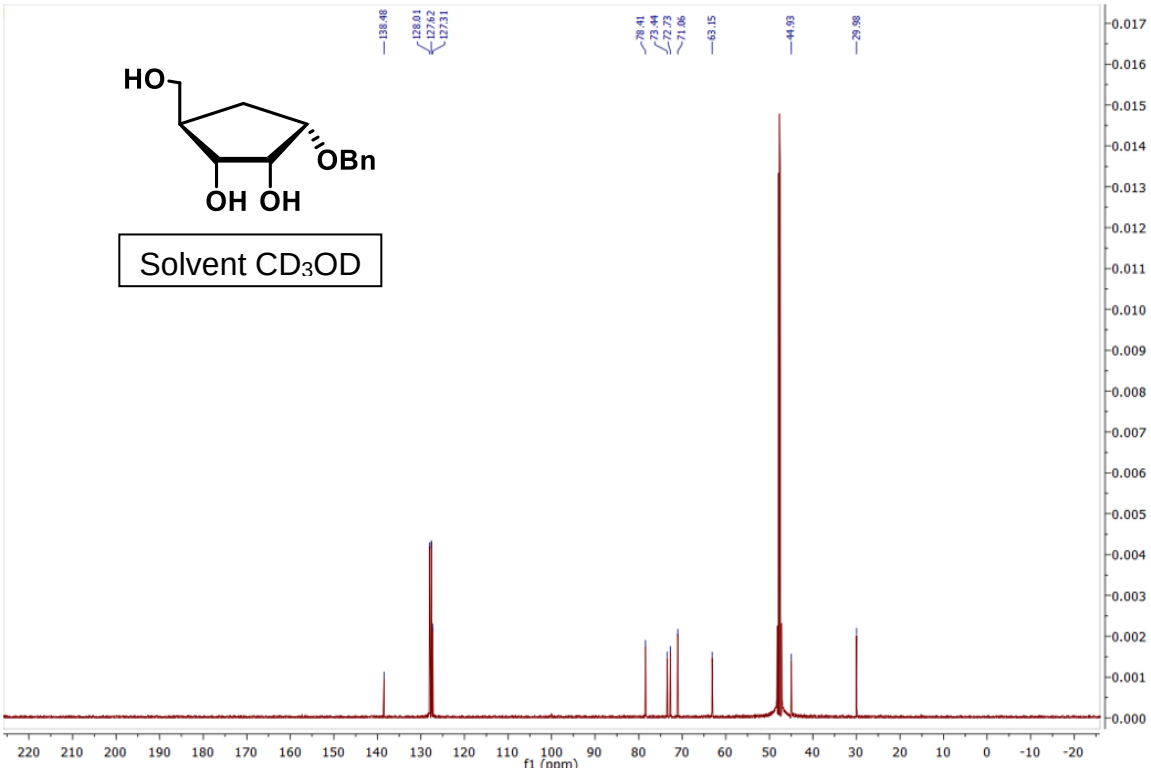

Figure 2.12 ^{13}C NMR of compound 4.

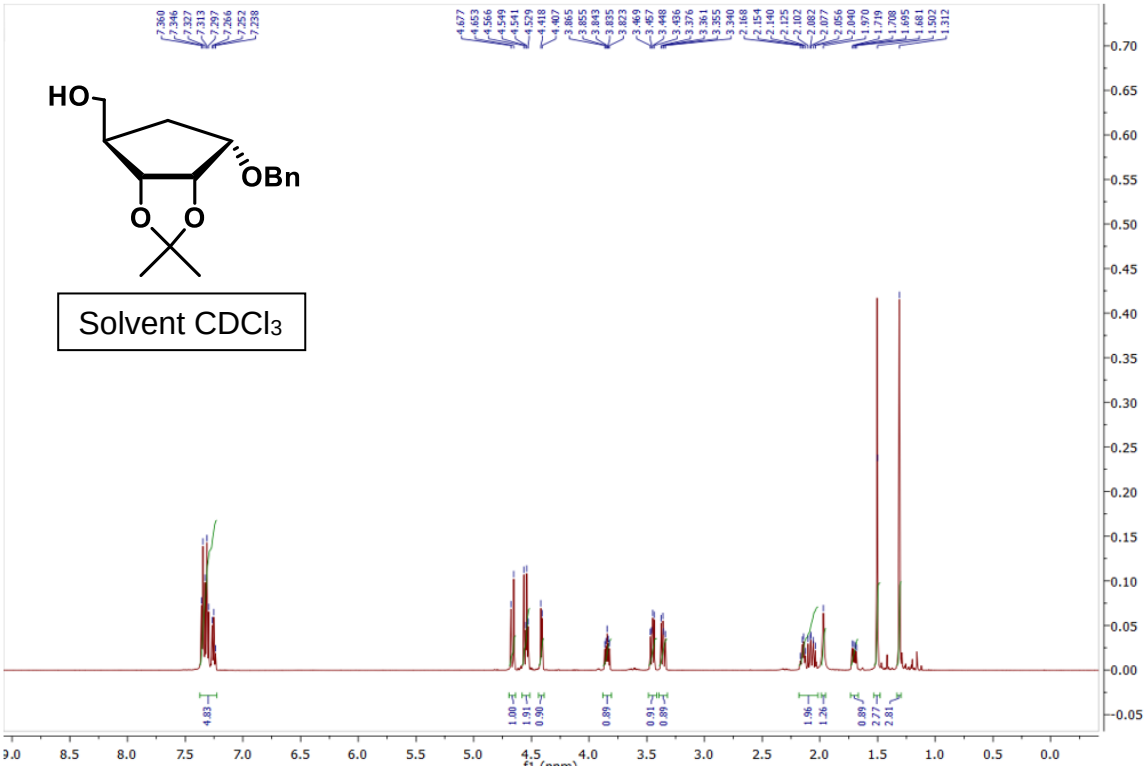

Figure 2.13 ^{1}H NMR of compound 5.

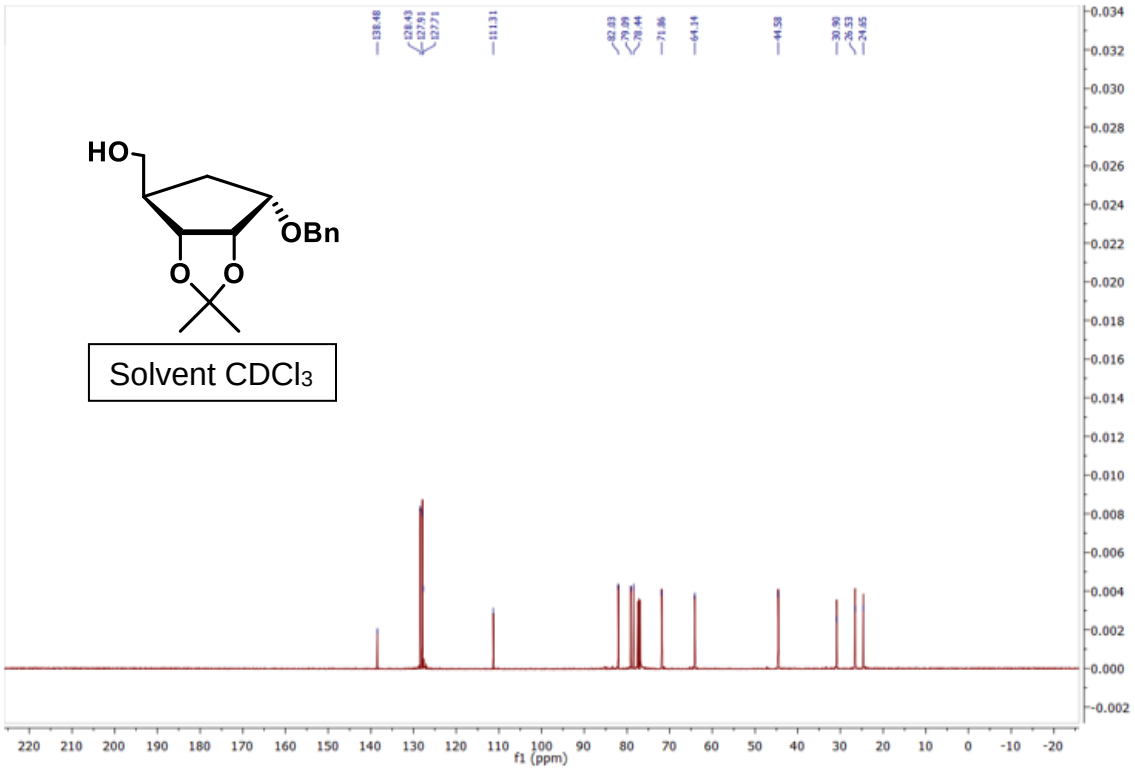

Figure 2.14 ^{13}C NMR of compound 5.

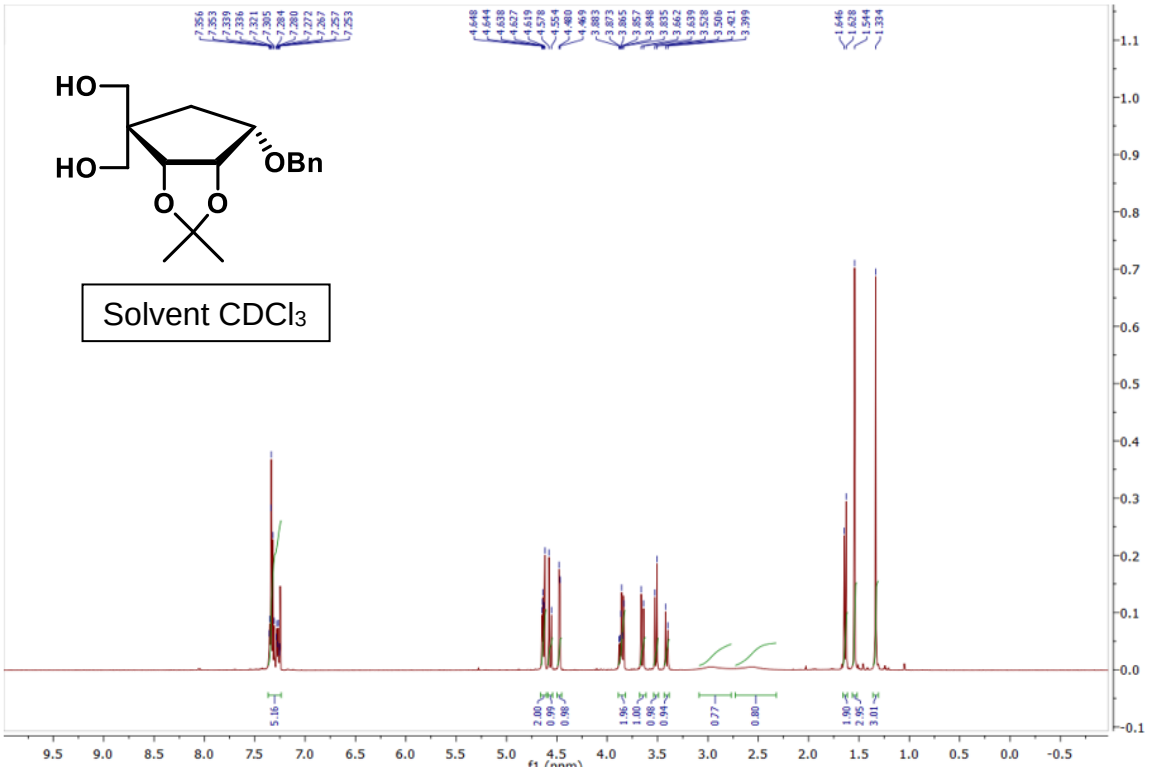

Figure 2.15 ^{1}H NMR of compound 7.

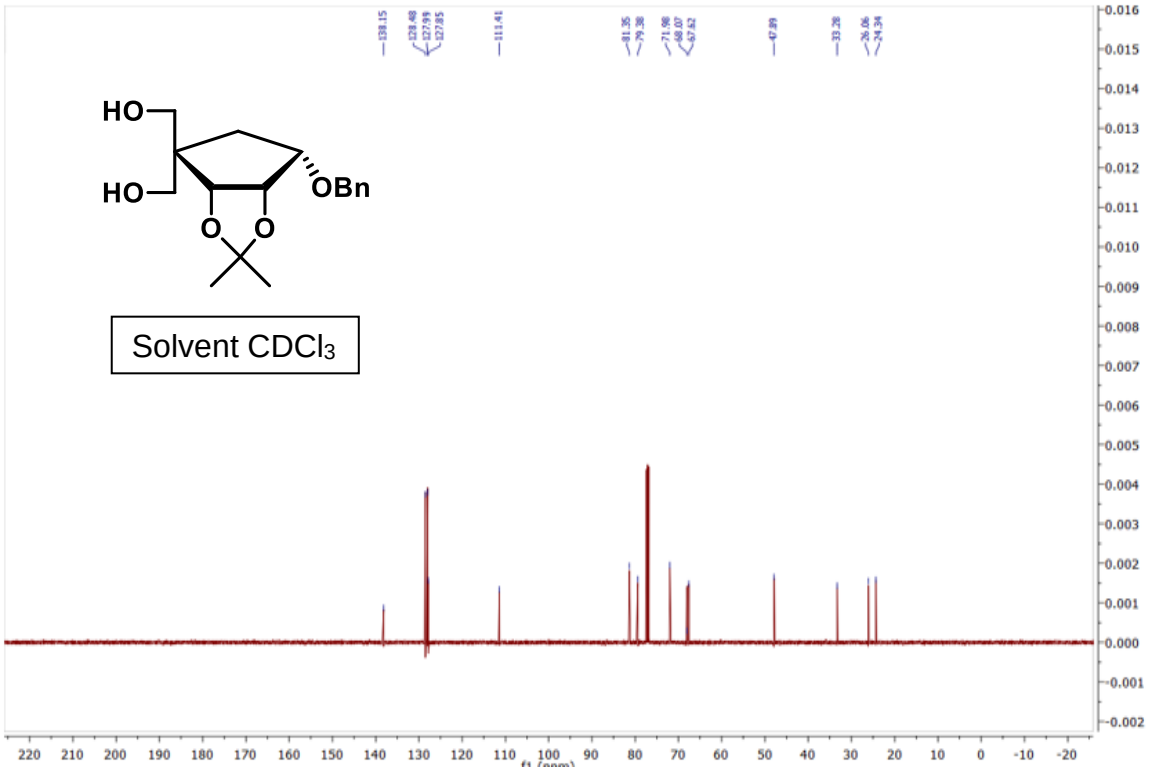

Figure 2.16 ^{13}C NMR of compound 7.

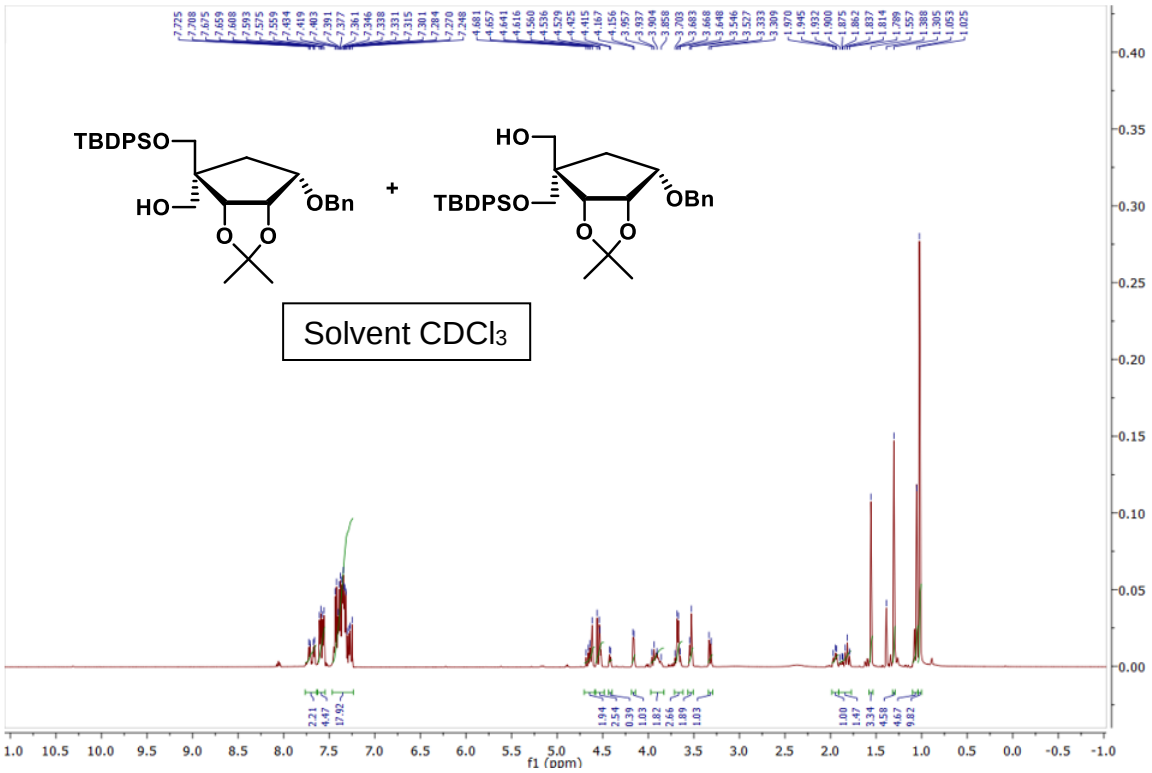

Figure 2.17 ^{1}H NMR of compounds 8a and 8b.

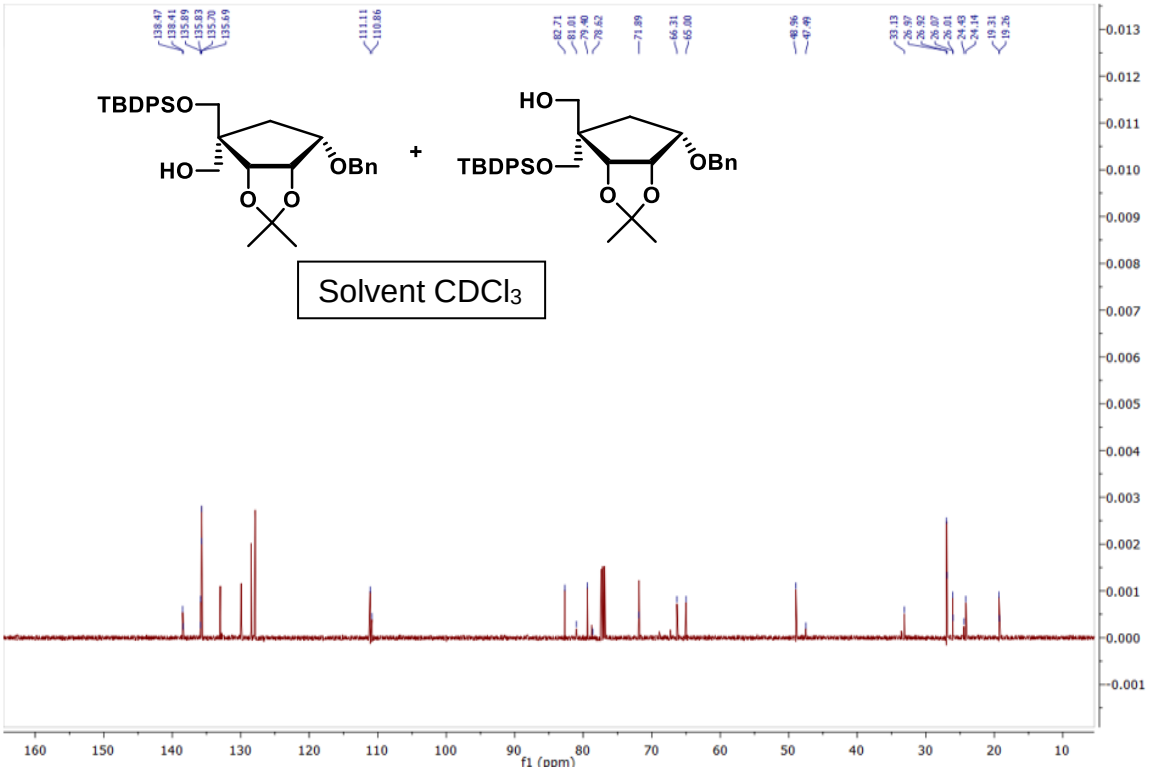

Figure 2.18 ^{13}C NMR of compounds 8a and 8b.

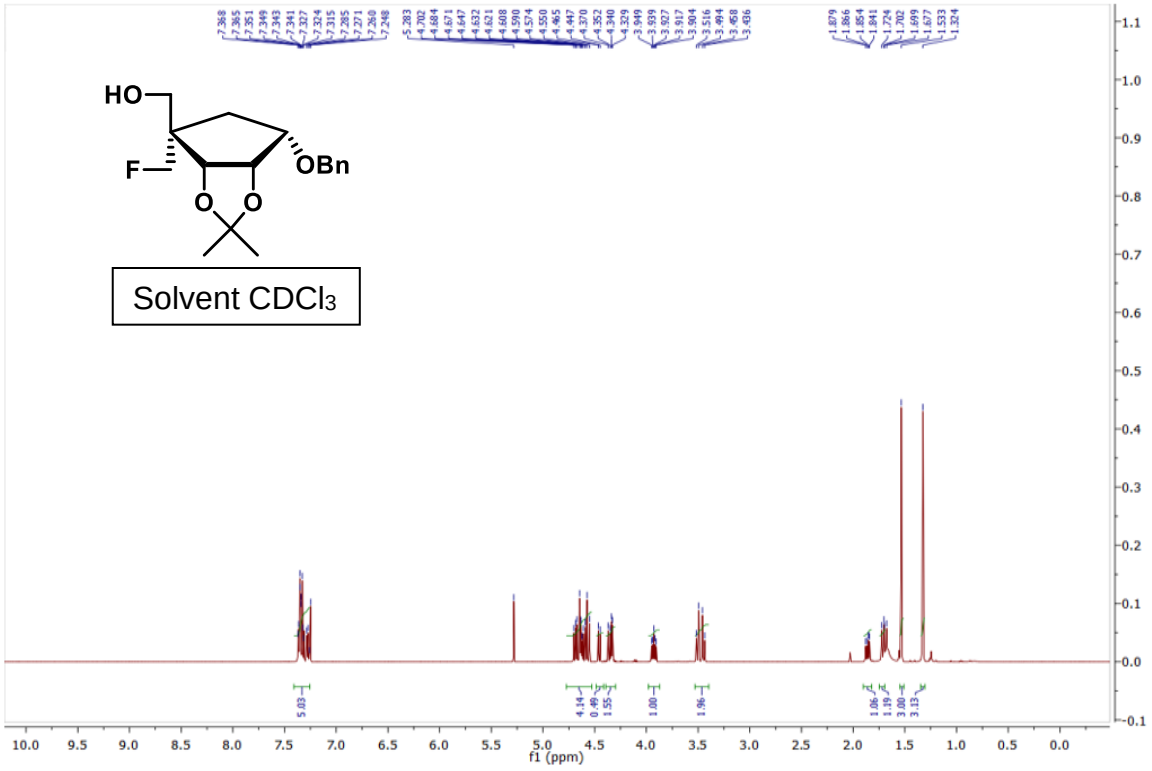

Figure 2.19 ^{1}H NMR of compound 10a. Desired *α*-fluoro compound.

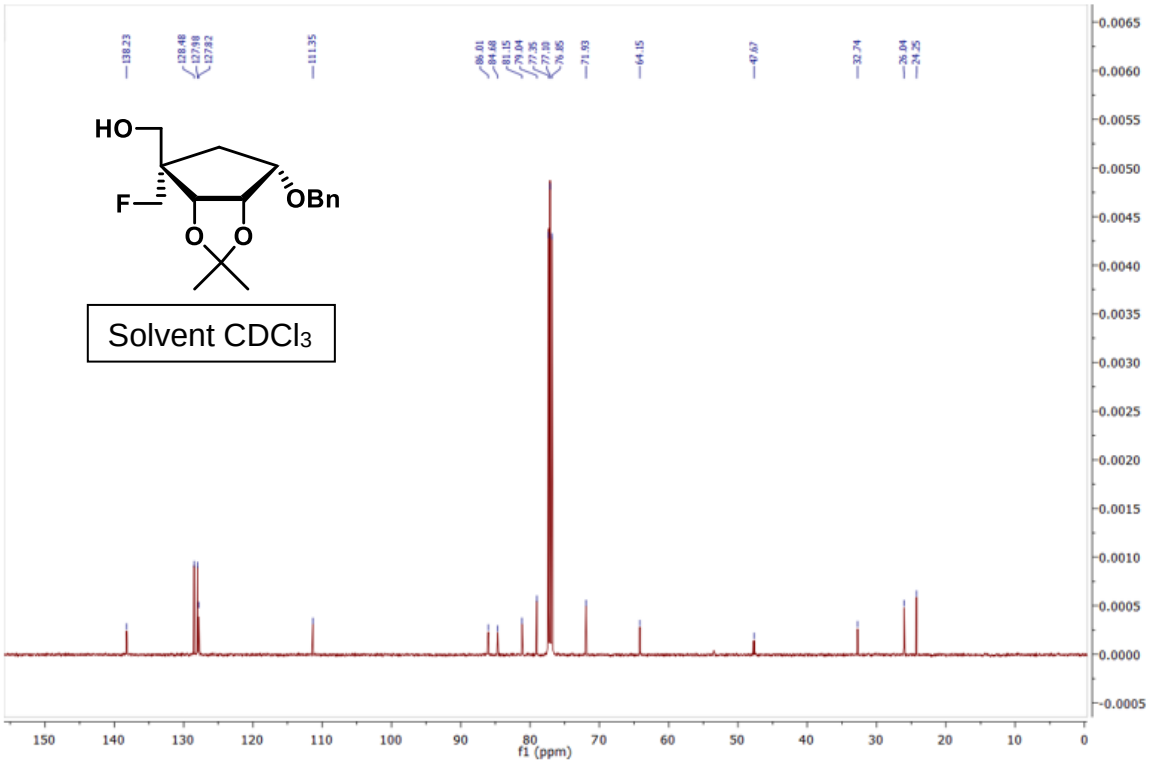

Figure 2.20 ^{13}C NMR of compound 10a. Desired *α*-fluoro compound.

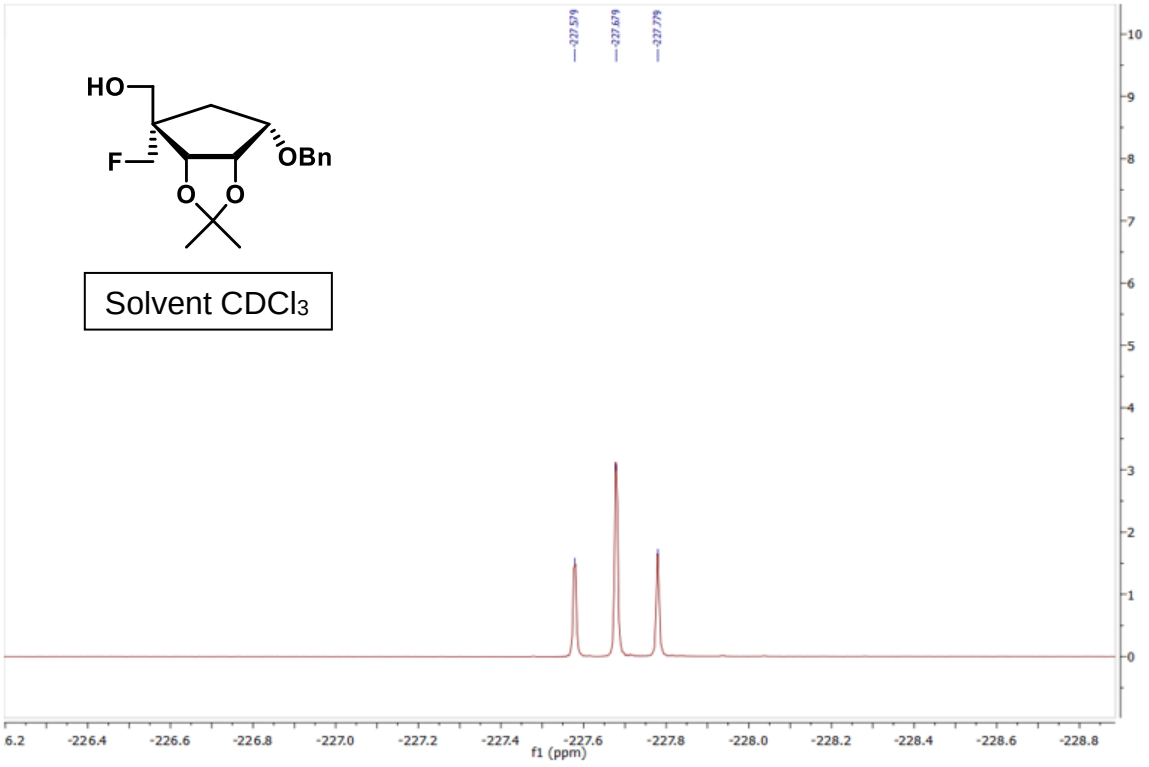

Figure 2.21 **^{19}F NMR of compound 10a.** Desired *α*-fluoro compound.

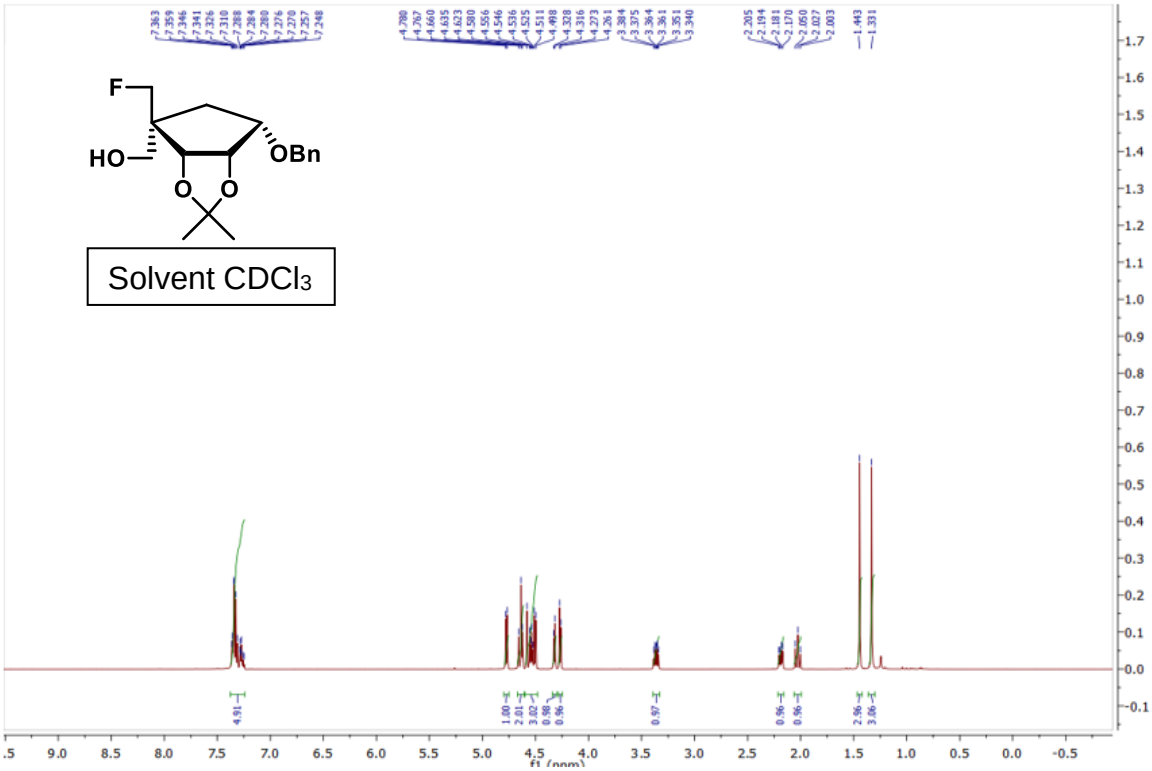

Figure 2.22 **^{1}H NMR of compound 10b.** Undesired *β*-fluoro compound.

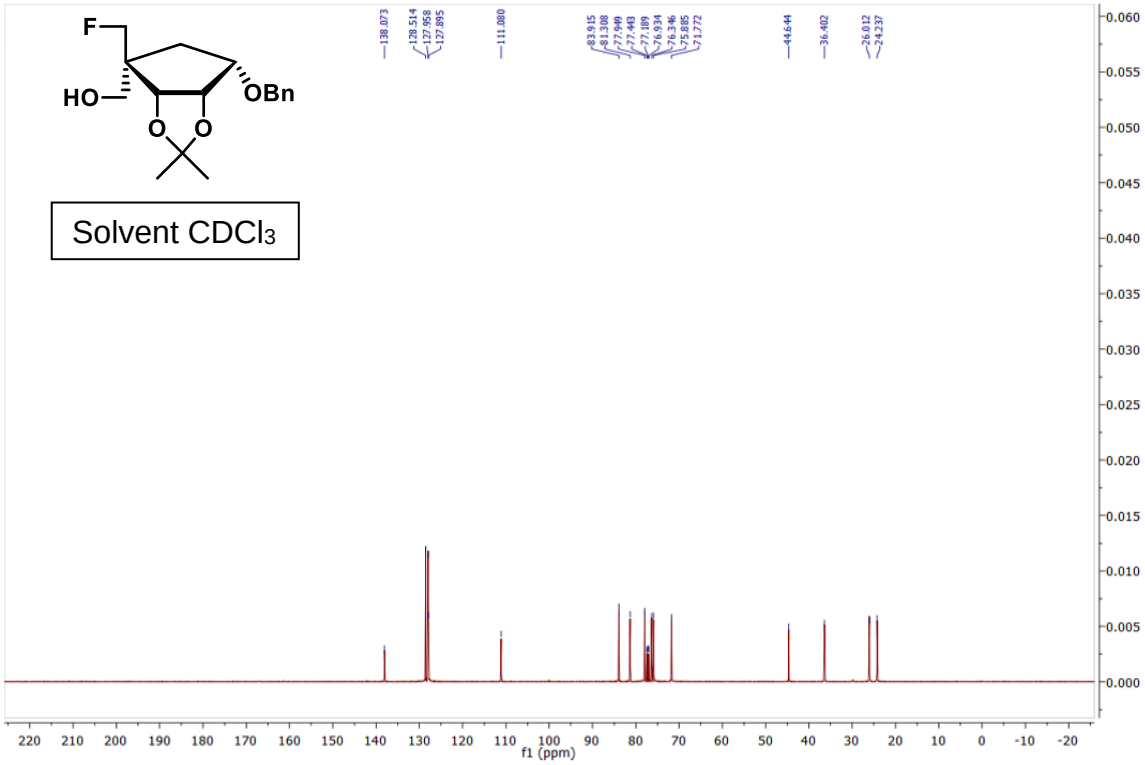

Figure 2.23 **^{13}C NMR of compound 10b**. Undesired *β*-fluoro compound.

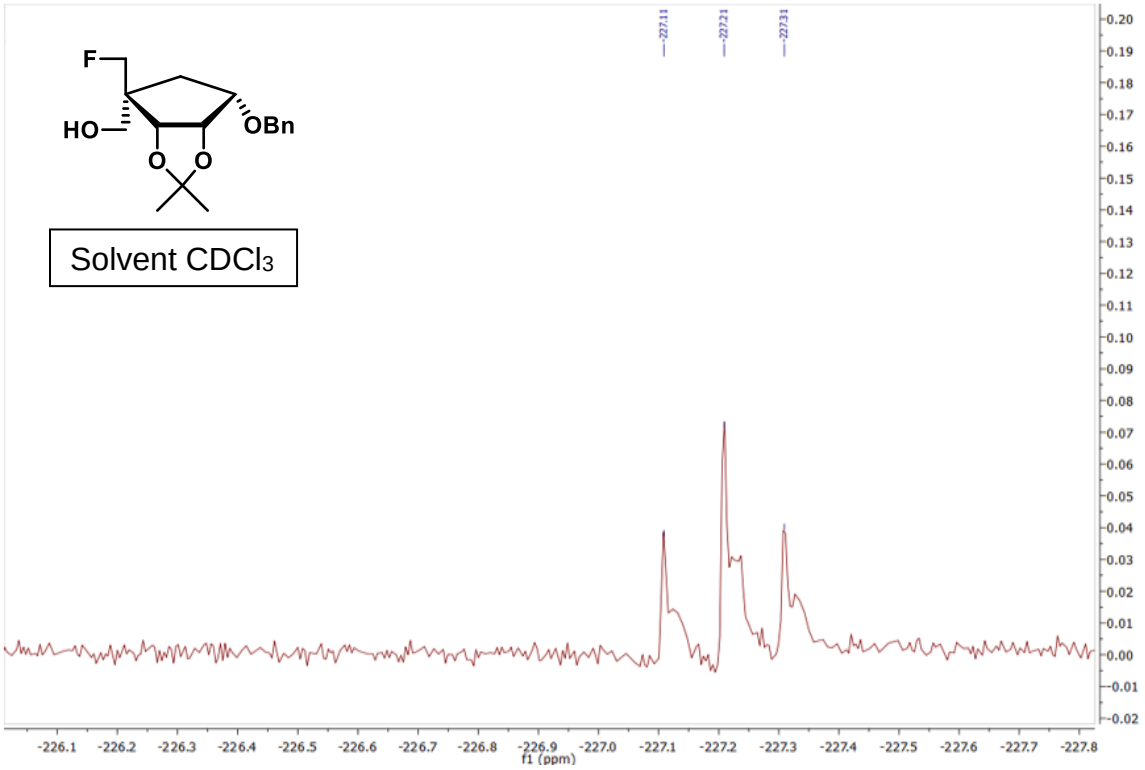

Figure 2.24 **^{19}F NMR of compound 10b**. Undesired *β*-fluoro compound.

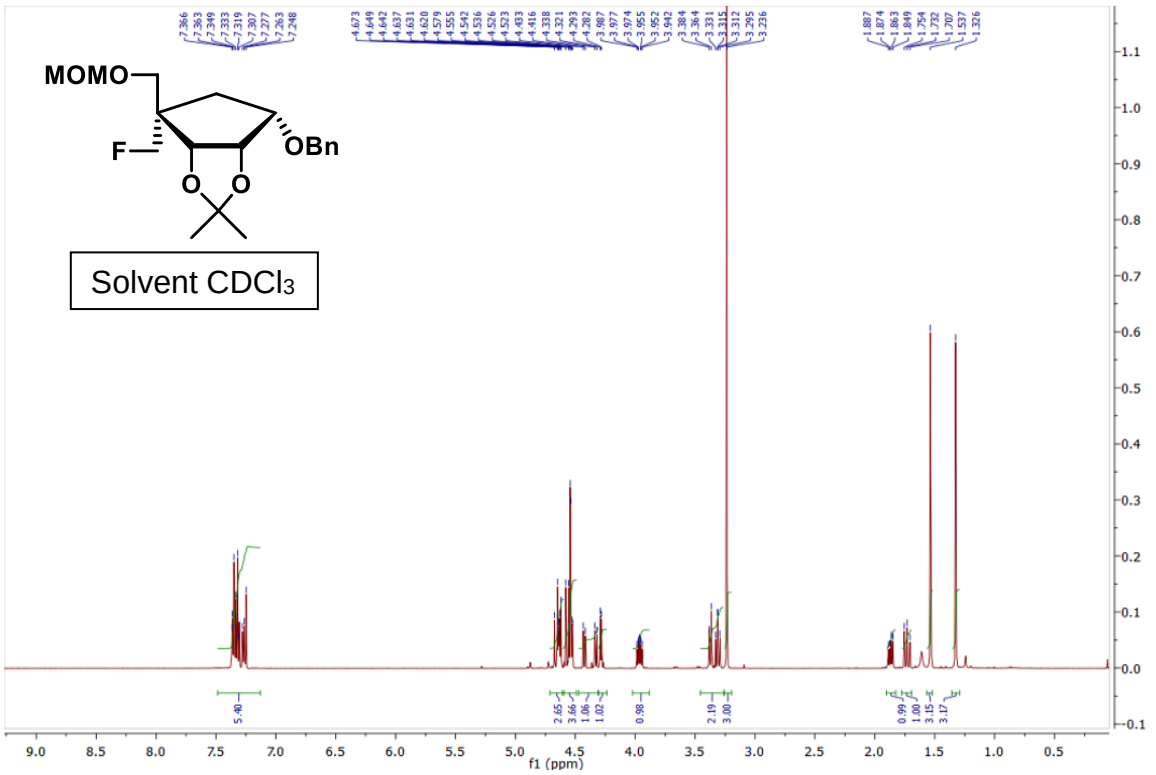

Figure 2.25 ^{1}H NMR of compound 11.

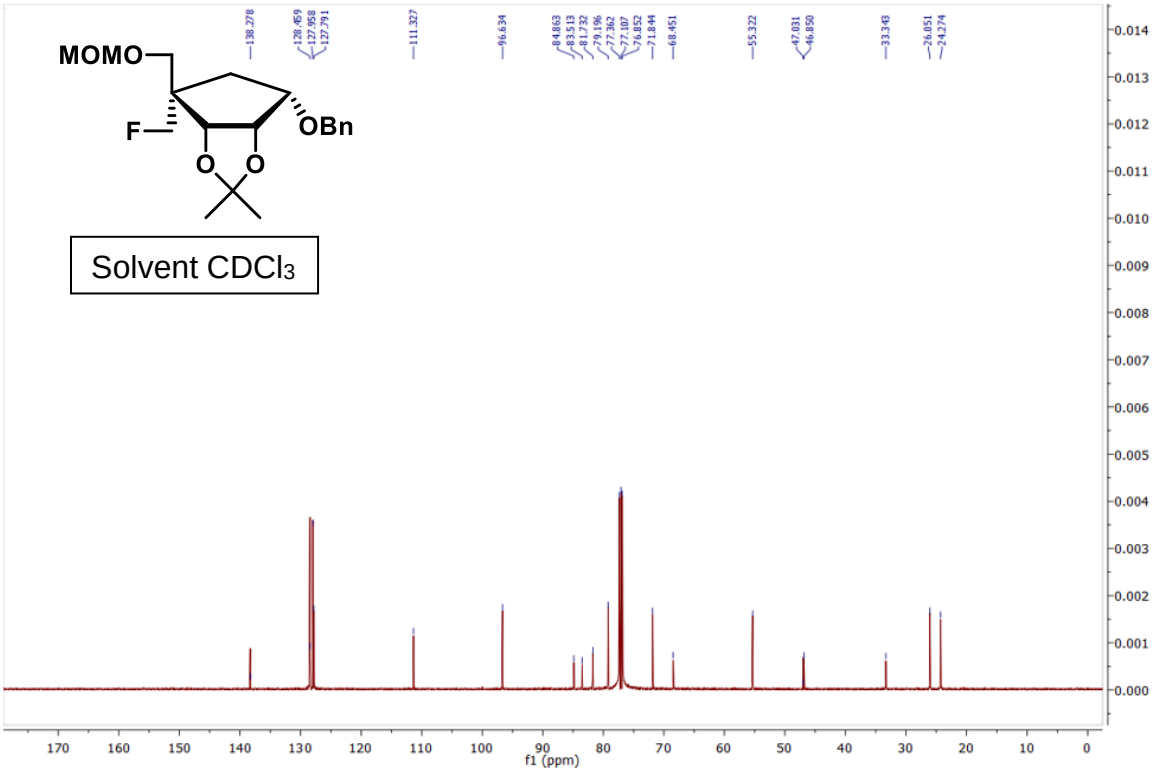

Figure 2.26 ^{13}C NMR of compound 11.

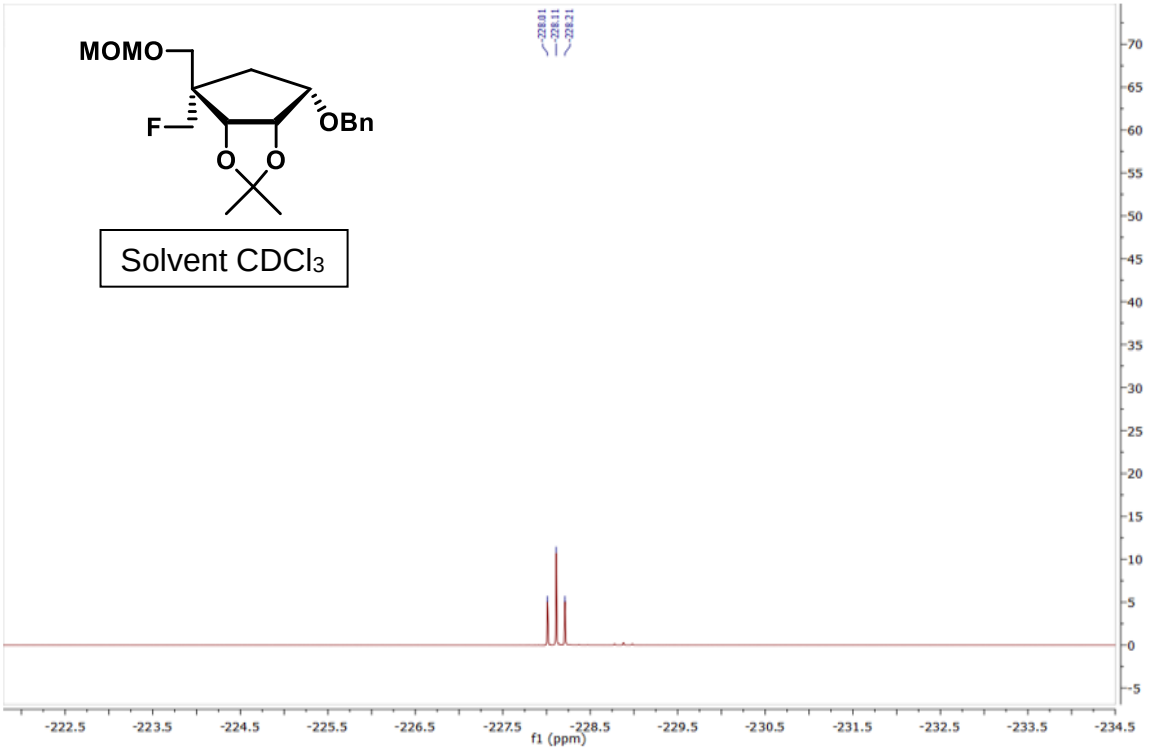

Figure 2.27 ^{19}F NMR of compound 11.

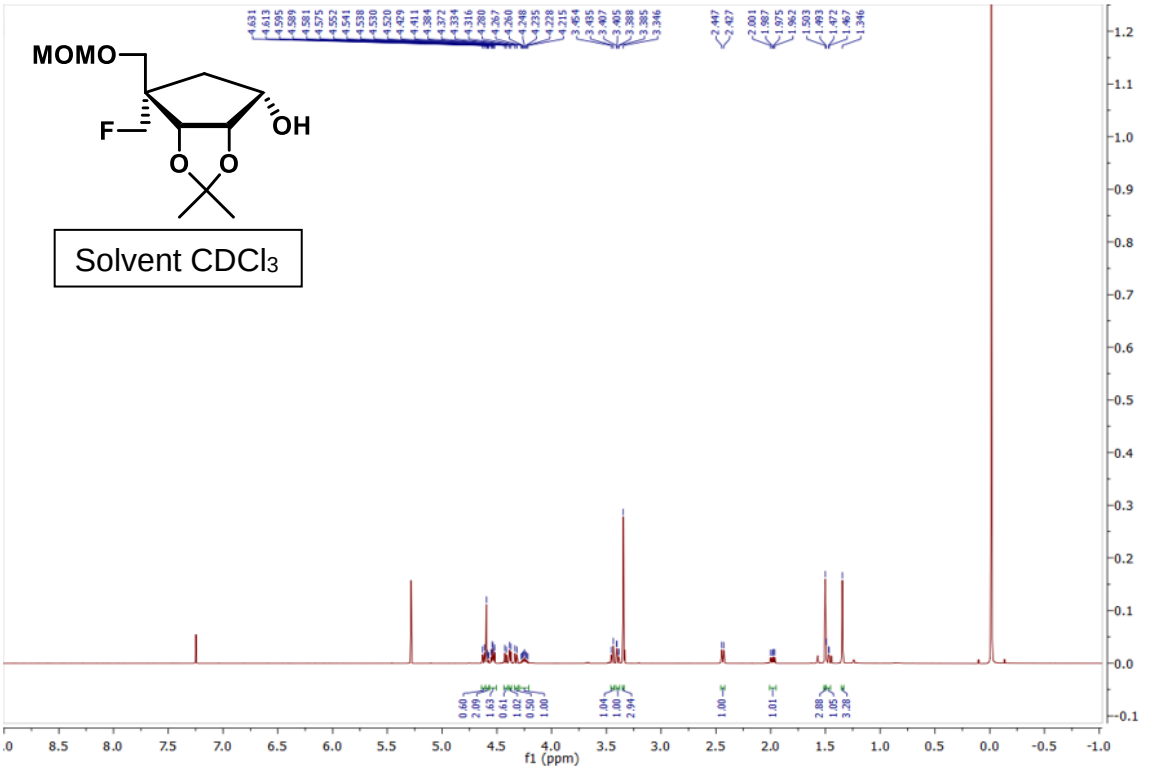

Figure 2.28 ^{1}H NMR of compound 12.

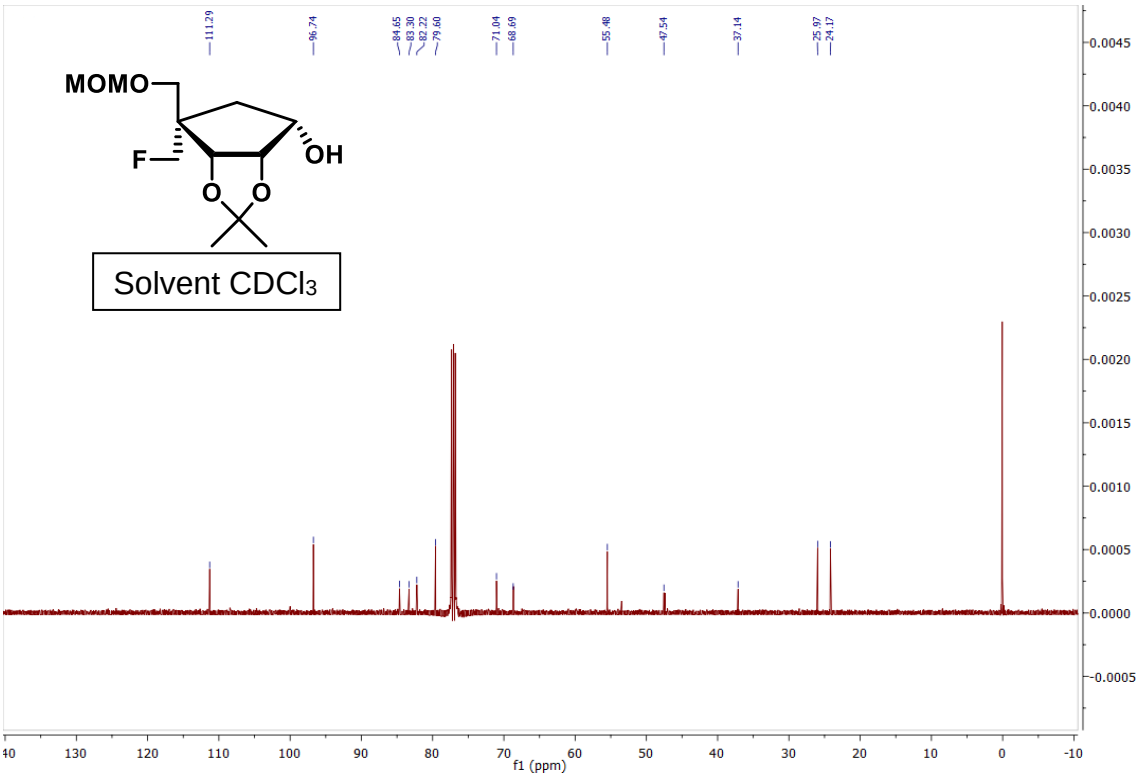

Figure 2.29 ^{13}C NMR of compound 12.

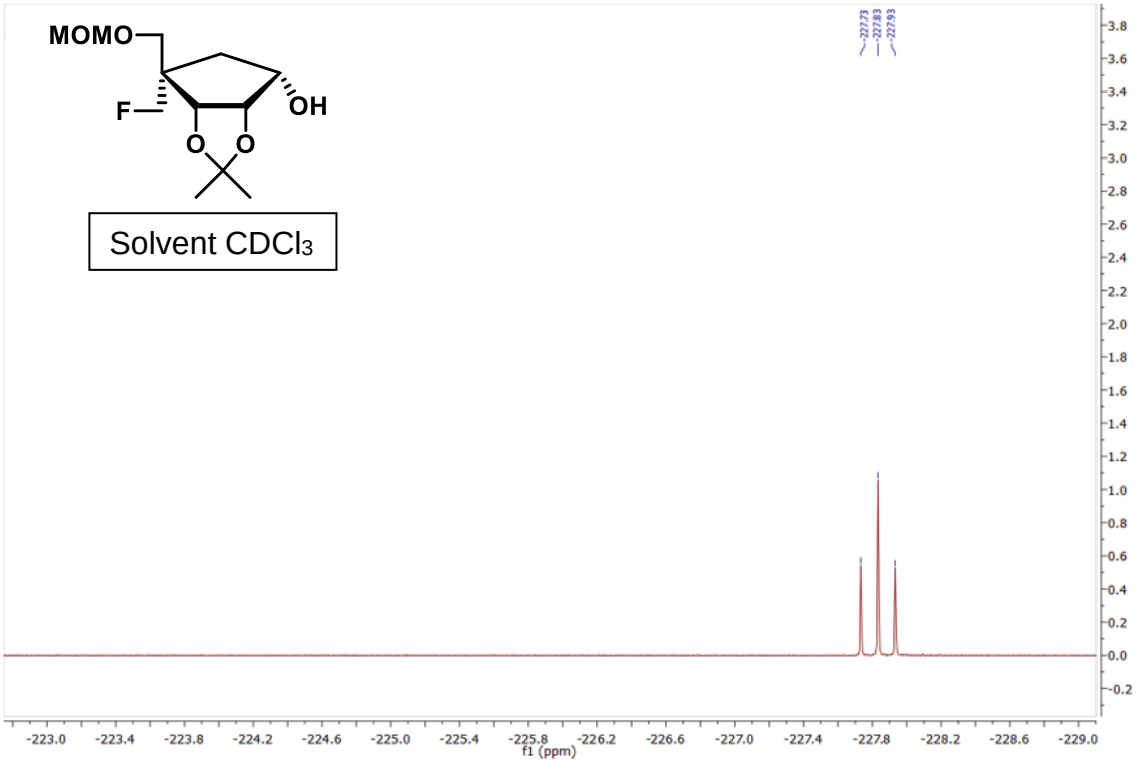

Figure 2.30 ^{19}F NMR of compound 12.

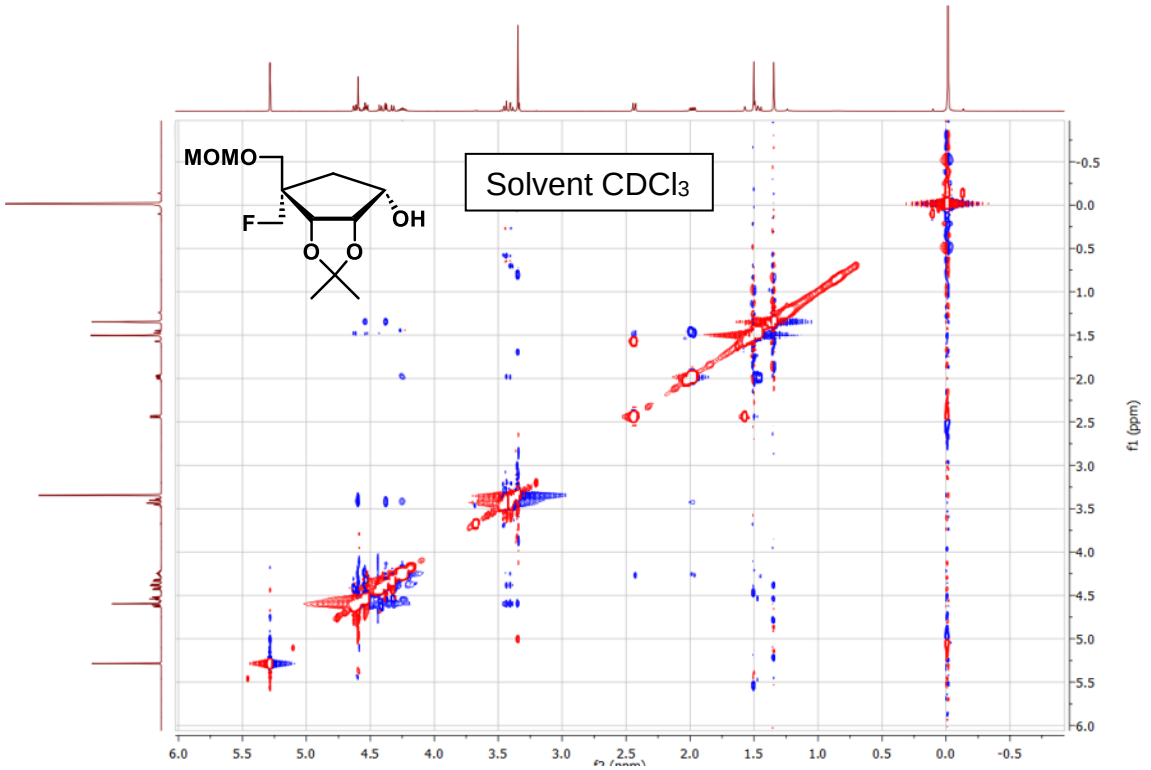

Figure 2.31 ^{1}H-^{1}H ROESY NMR of compound 12.

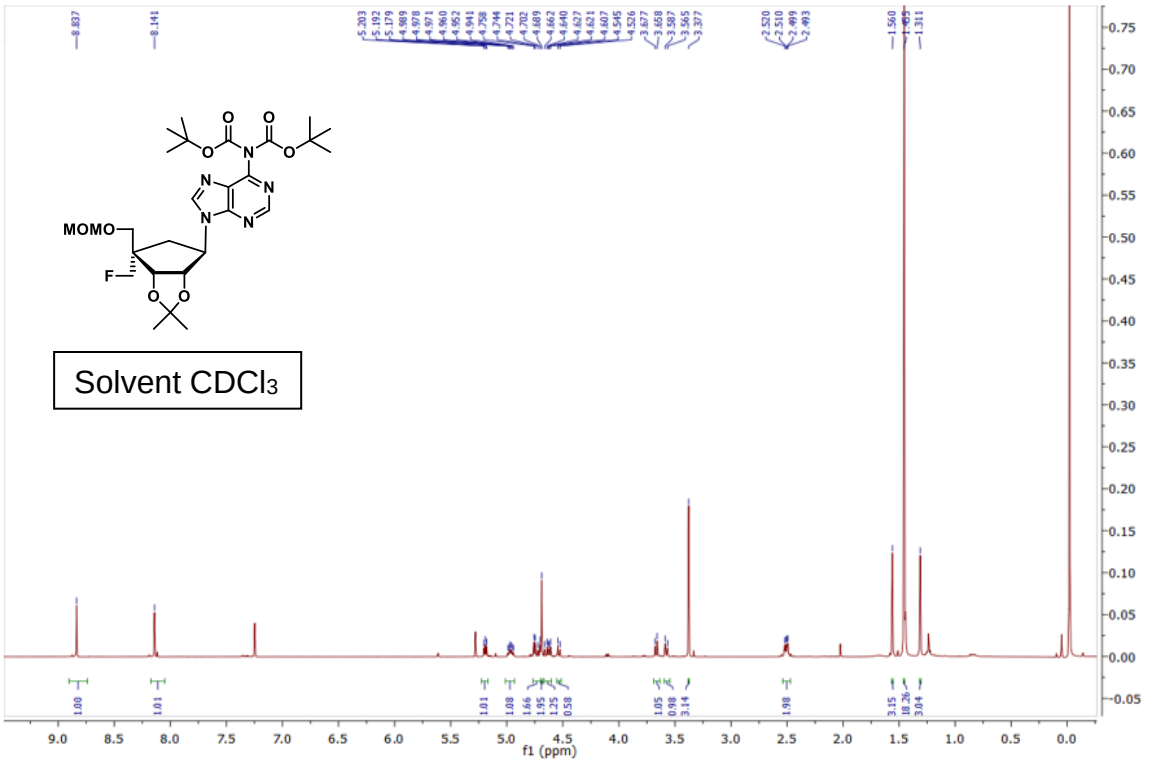

Figure 2.32 ^{1}H NMR of compound 14.

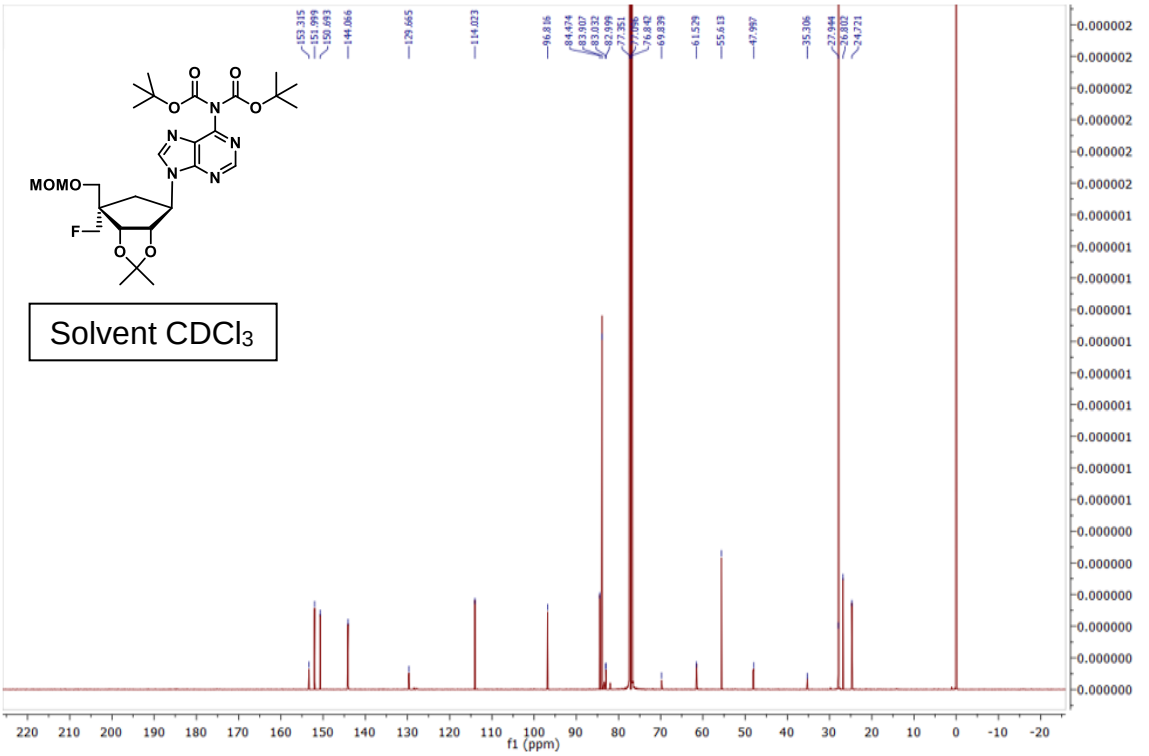

Figure 2.33 ^{13}C NMR of compound 14.

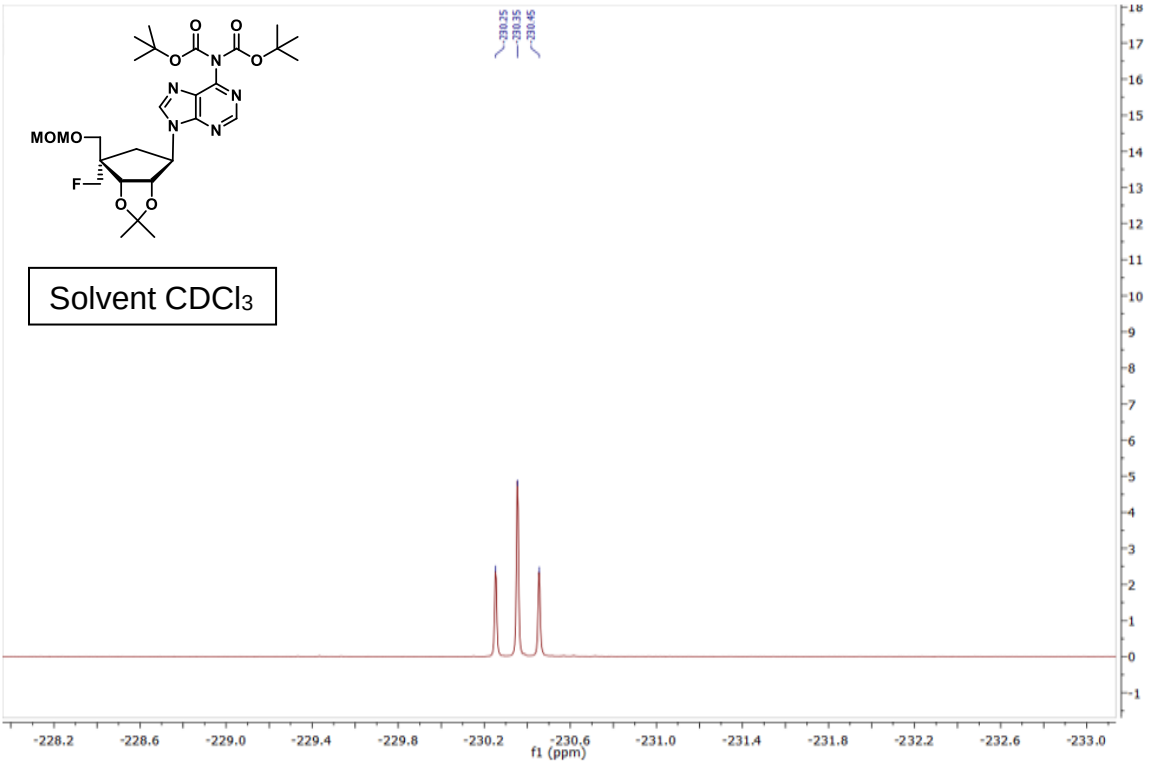

Figure 2.34 ^{19}F NMR of compound 14.

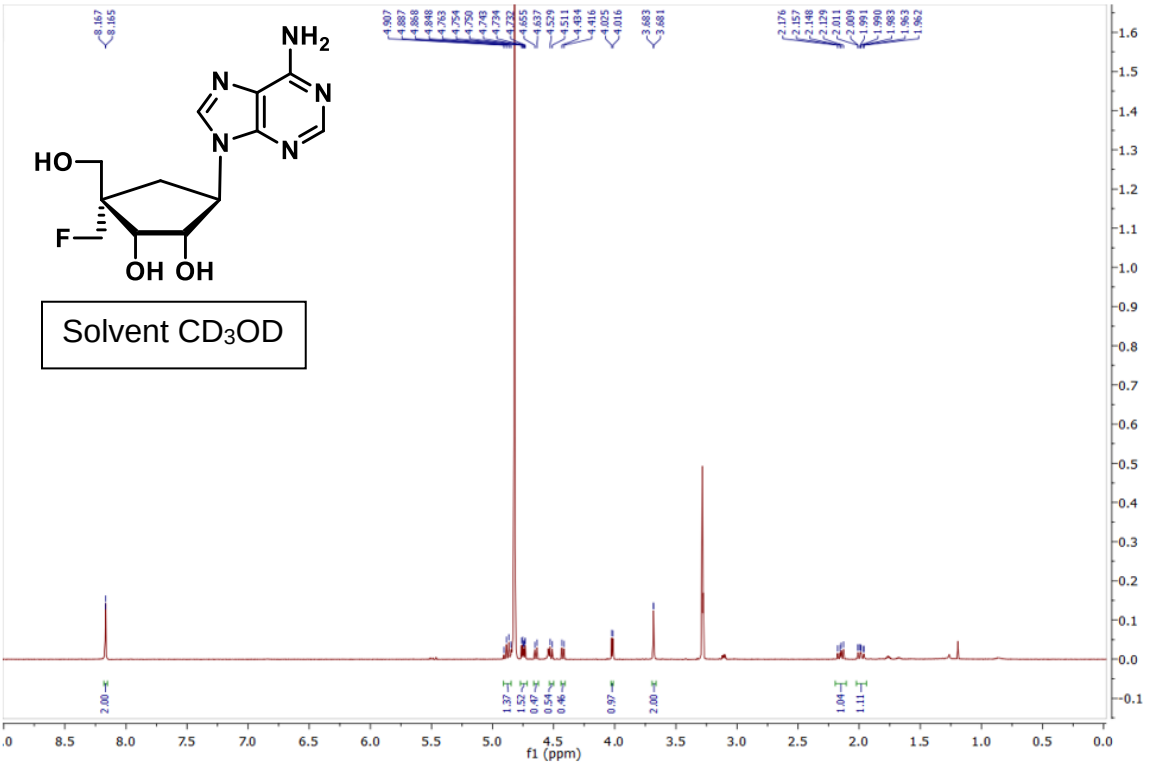

Figure 2.35 ^{1}H NMR of compound 15.

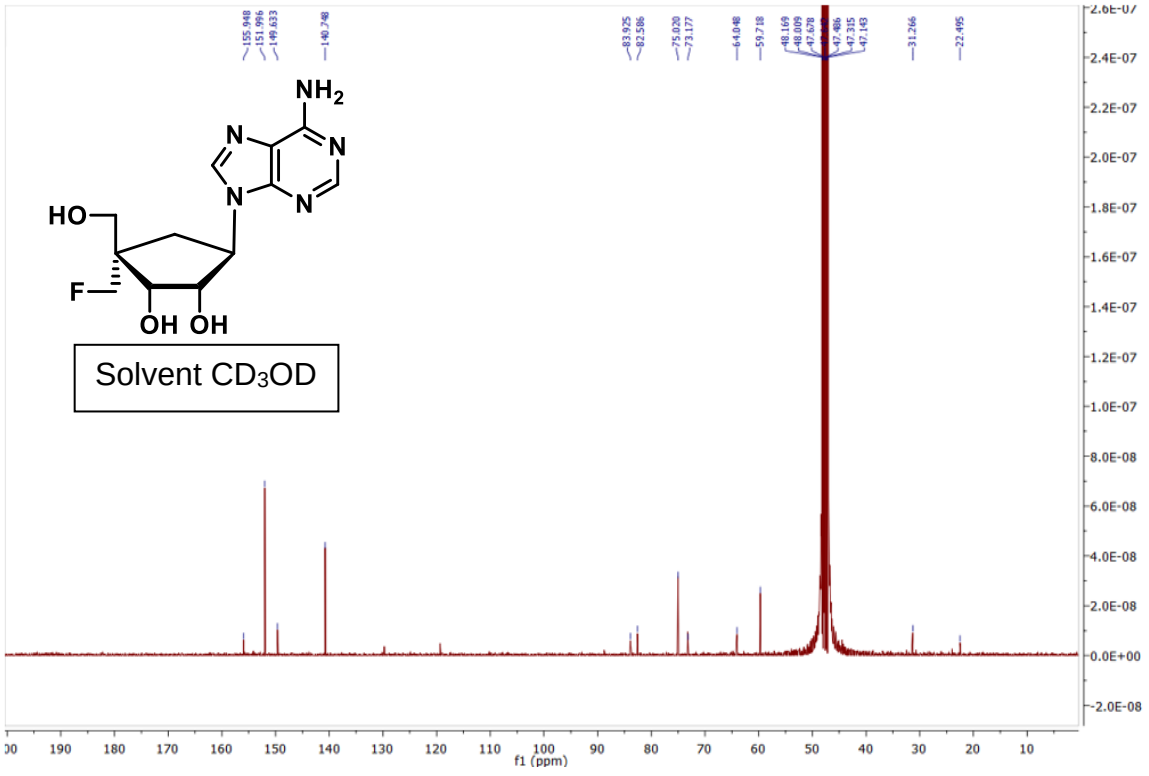

Figure 2.36 ^{13}C NMR of compound 15.

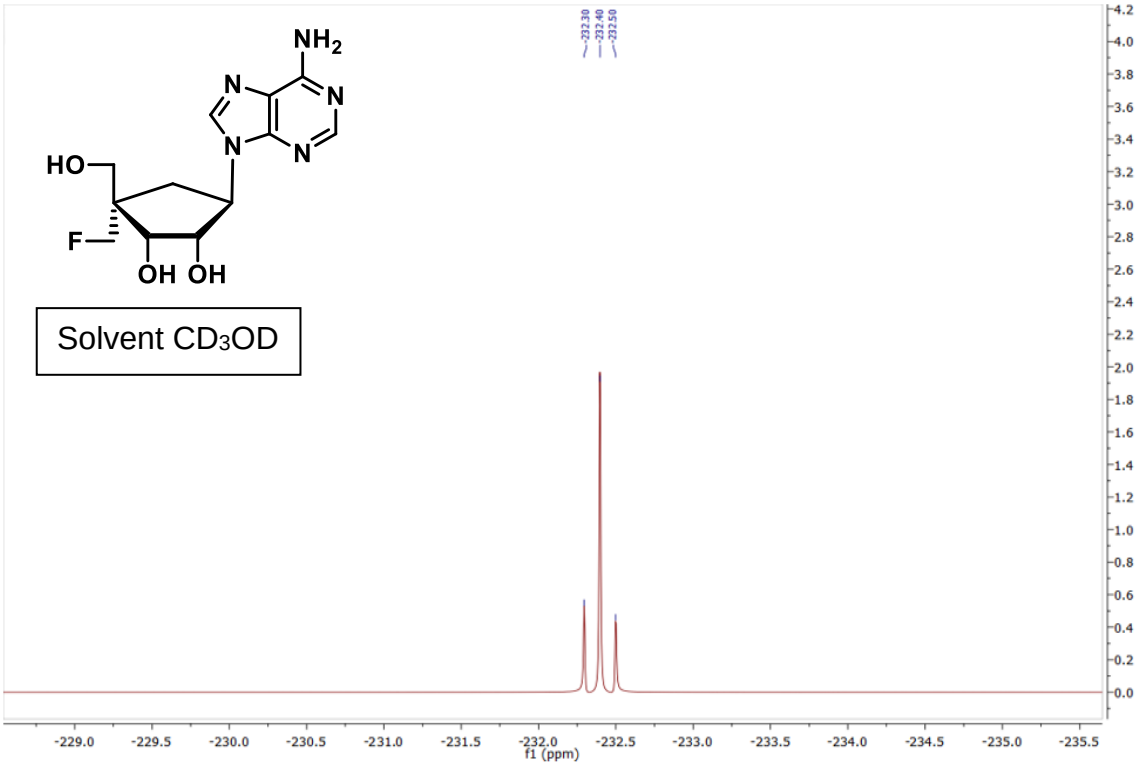

Figure 2.37 ^{19}F NMR of compound 15.

CHAPTER 3

Synthesis of Dioxolane Derived 7-Deazapurine Nucleoside Analogs Against Poxviruses and Herpesviruses

3.1 INTRODUCTION

Dioxolanes, heterocyclic acetal cyclopentyl rings, offer a potential replacement sugar scaffold which lacks the crucial 3' OH necessary to propagate DNA/RNA elongation. By replacing a ribose with a dioxolane ring in nucleosides, specificity and selectivity for DNA viruses without causing toxicity to humans can be generated. The incorporation of a dioxolane derived nucleotide into an elongating viral DNA chain would end up with chain termination which ultimately inhibits viral growth. In the past, dioxolane nucleos(t)ides have shown potent antiviral and anticancer activity. Troxacitabine, a dioxolane pyrimidine analog, has shown promising anticancer activities across numerous cancers, and has exhibited anti-HIV and anti-HBV activity.[40, 55] Our group, the antiviral drug discovery group in the College of Pharmacy at the University of Georgia, has previously synthesized numerous dioxolane analogs, out of them, some analogs have shown promising antiviral activity. L-BHDU, a vinyl bromide, and L-HDVD, a vinyl uracil, dioxolane nucleosides, have shown activity against herpesviruses.[56] L-BHDU showed activity mainly against VZV, while L-HDVD expressed broad antiviral activity against EBV, KSHV, and HSV-1. DAPD, another diaminopurine dioxolane nucleoside, was a potent HIV replication inhibitor. [57] DOT, a dioxolane

thymidine nucleoside, and its prodrugs have exhibited potent anti-HIV activity.[58] Based on these structures, oxathiolane sugars, similar to dioxolane though with a 3′ sulfur in-lieu of an oxygen, have been shown to have potent antiviral activity.[33] Lamivudine and emtricitabine derived from oxathiolane sugars have been approved for the treatment of HBV and HIV infections respectively.[33]

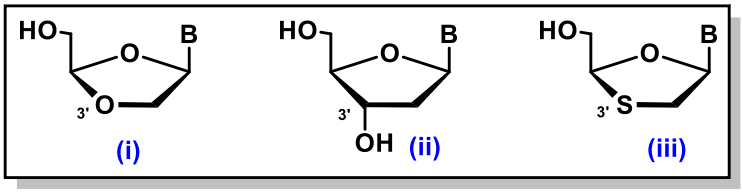

Figure 3.1 Dioxolane (i), deoxyribose (ii), and oxathiolane (iii) rings. Representation of the absence of the 3′ OH on the dioxolane/oxathiolane ring as compared to a deoxyribose ring. *B represents base A, G, C, U & T*

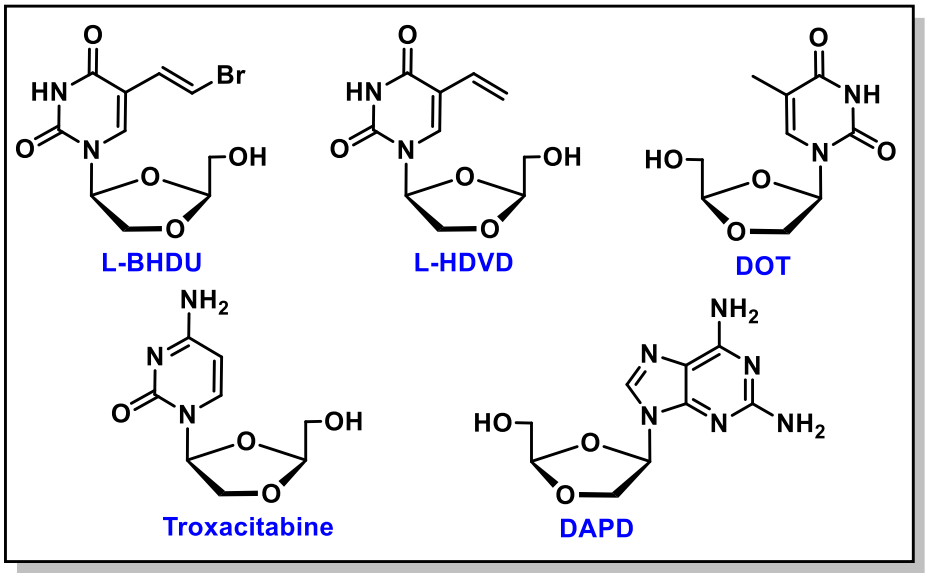

Figure 3.2 Structures of potent dioxolane nucleoside analogs

There is still need to generate efficacious and selective dioxolane nucleosides for antiviral use, for which additional alterations either on the dioxolane ring or nucleobase are required. As mentioned in chapter 2, increased complexity is associated with an increase in viral specificity and selectivity. Nitrogen substitutions on the nucleobase result in potent effects on activity with the removal of a potential hydrogen bond acceptor/donator, which may greatly affect the properties of the molecule. This has been shown before with multiple nucleos(t)ide analogs and based on similar substitutions, 7-Deazapurines have gained much attention as antiviral agents. These are modified base analogs of adenine wherein the N7 nitrogen is replaced by a carbon atom, which makes the five-membered ring more flexible and provides a possibility of replacing additional substituents at the C7 position. Additionally, substitution at the 7-position of the 7-deazapurine base dramatically changes the antiviral activity of this class of compounds. Tubercidin, a 7-deazaadenosine analog, and its derivatives have shown nanomolar potency against HCV, and anti-cancer activity.[59] 3-deaza-deoxyguanosine, another deazapurine analog, has shown antiviral activity across both RNA and DNA viruses.[40] Taking the lead from the above-described molecule, in this project, numerous analogs of modified 7-deazapurines with a dioxolane have been synthesized and their antiviral potency is being evaluated against various infectious DNA viruses. The synthesis of the targeted 7-deazapurine dioxolane was commenced with the previously reported dioxolane ketone (**16**).[60] In this effect, as a starting point, five nucleoside analogs have been reported, and

based on the antiviral results of the synthesized analogs, in the future, further SAR studies will be performed.

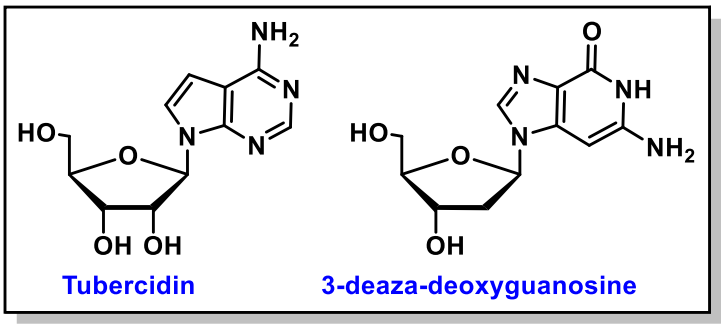

Figure 3.3 Structures of deazapurine nucleosides with potent antiviral activity.

3.2 RESULTS AND DISCUSSION

Chemistry

To initiate the synthesis of the desired dioxolane nucleoside analogs, dioxolane ketone **16** (starting material) was synthesized according to the literature reported method.[60] Reduction of the ketone was performed via lithium tri-tert-butoxyaluminum hydride (LTBA) solution in THF (1M) to afford the racemic alcohol **17**. However, during the purification of **17** via silica gel chromatography, a degradation of **17** was observed which concluded **17** is unstable for purification. Thus, it was thought to move with an *in-situ* acetylation of **17** which may provide the stable acetylated compound **18**. **17** was treated with DMAP and acetic anhydride to give a diastereomeric (*α* & *β*) mixture of **18** in 39% yield. The *α*/*β*

diastereomers of **18** were inseparable via column chromatography and were utilized as a mixture for the next step coupling reaction.

Coupling with the deazapurines proved to be a tedious and extensive challenge. Previous reported procedures had shown coupling of purines with dioxolane sugars via purine silylation.[61, 62] Following the reported protocol in literature, 6-chloro-7-deazapurine was refluxed in hexamethyldisilazane with catalytic ammonium sulfate to produce the silylated 7-deazapurine, which was used immediately in the next step. Compound **18** was treated with iodotrimethylsilane (TMSI) to produce the intermediate **19**, followed by immediate addition of the silylated 7-deazapurine. However, multiple attempts had been tried for the coupling of **19** with silylated 7-deazaadenine but in each case a complex mixture was obtained. Thus, it is concluded that the 7th position nitrogen on the purine ring may be essential for silylation, and the absence of the 7th position nitrogen may inhibit this process and resulted in the multiple spot formation.

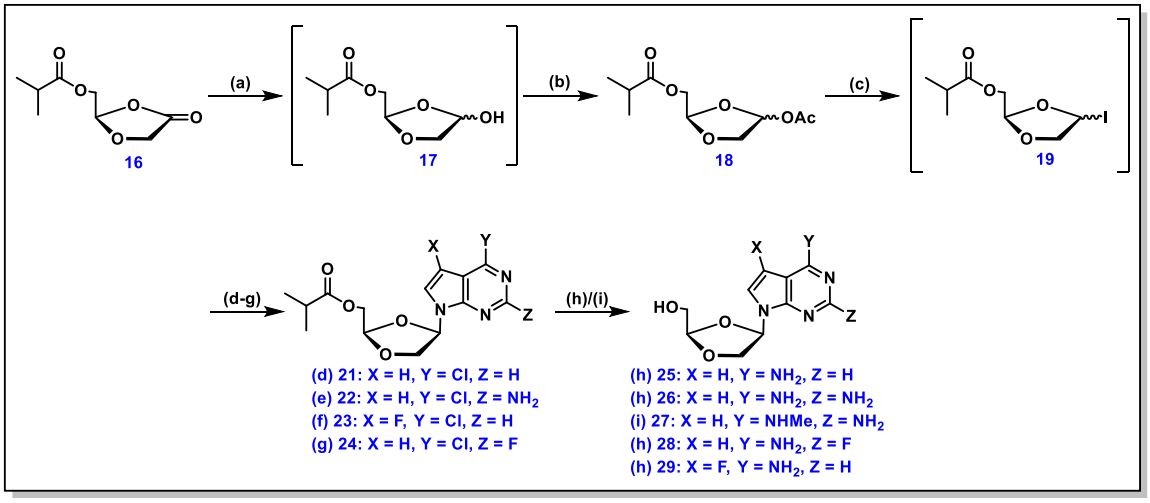

Scheme 3.1 Synthetic pathway to form compounds 25-29.

Reagents and Conditions: (a) LTBA, THF (1M); (b) DMAP, Ac_2O, THF; (c) TMSI, $CHCl_3$; (d) KOH, ACN, TDA-1, 6-chloro-7-deazapurine; (e) KOH, ACN, TDA-1, 2-amino-6-chloro-7-deazapurine; (f) KOH, ACN, TDA-1, 4-chloro-5-fluoro-7H-pyrrolo[2,3-d]pyrimidine; (g) KOH, ACN, TDA-1, compound **20**; (h) NH_4OH, Dioxane; (i) Methylamine, EtOH;

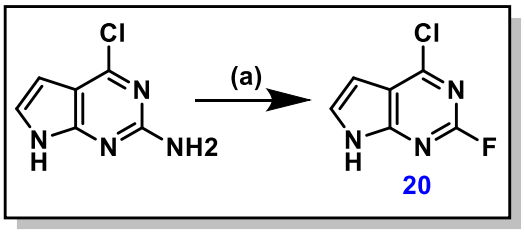

Scheme 3.2 Synthetic pathway to form compound 20.

Reagents and Conditions: (a) t-butyl nitrite, HF/pyridine (70%)

Next, an S_N2 approach was adopted for the coupling of 6-chloro-7-deazapurine with intermediate **19**. In this effort, 6-chloro-7-deazapurine was treated with NaH (60% dispersion in mineral oil) in acetonitrile and to this solution, freshly prepared **19** was added, and the mixture was allowed to stir for 3 hours. After purification, it was determined that the desired (**21**) coupled nucleoside had formed. However, in these coupling conditions, surprisingly four major products were formed rather than the expected two 1′ *α*/*β* products. It was speculated that the additional products may be a result of epimerization, due to higher basic anhydrous condition of NaH Therefore, it was thought that an aqueous salt may provide more specific coupling conditions, resulting in solely two expected *α* and *β* coupled nucleosides.

It was decided that potassium hydroxide with a phase-transfer catalyst may provide the major *β*-coupled nucleoside product.[63] Potassium hydroxide was treated with tris[2-(2-methoxyethoxy)ethyl]amine (TDA-1) in ACN, followed by 6-chloro-7-deazapurine. To this, freshly prepared **19** was added to afford **21** in 14% yield. This procedure produced the two diastereomeric major 1′ *α* and *β* coupled products which was readily separated via silica gel column chromatography. This method was found to be efficient and repeatable and was utilized for coupling of all other analogs (**22-24)** in a range of 14% to 30% yield. 6-chloro-7-deaza-2-fluoropurine (**20**) is not commercially available, and a synthetic procedure was needed. Fluorination *via* Sandmeyer reaction was performed on 2-amino-6-chloro-7-deazapurine with HF/pyridine and tert-butylnitrite to produce **20** in 81% yield.

The structure and *β*-conformation of the coupled nucleosides were elucidated *via* reported NMR data of dioxolane purine nucleosides. ^{1}H-NMR data showed significant differences in shifting for the 4′ proton based on either 1′ *α* or *β* conformation of the coupled product.[61] This relationship was also observed in 7-deazapurine dioxolane nucleosides. Interestingly, it was observed that the *β* conformation nucleosides crystallized readily at room temperature, while the *α* coupled product remained a viscous oil.

To afford the desired targeted nucleosides, deprotection along with 6-position amination was required. In a steel bomb under higher pressure, compound **21** was treated with a 28% aqueous solution of NH_4OH in dioxane to render **25** in 38% yield. In this step both amination and ester deprotection were simultaneously performed to produce the final compound. Following the described procedure

compounds **26**, **28** & **29** were furnished in a yield range of 14-79%. Compound **27** was produced in a similar fashion, though using methylamine in ethanol (33% wt). In the effort of synthesis of the 7-deazaguanosine dioxolane analog - after coupling of the dioxolane ring with 2-amino-6-chloro purine conversion of 6-chloro to hydroxy was necessary. In this attempt both TFA and formic acid were utilized to produce the 6^{th} position hydroxyl. However, in each attempt degradation of the coupled product was observed, and only minor product formation was visible on TLC which was tough to purify. Hence, it was thought that the dioxolane acetal ring is unstable under highly acidic heating conditions, and thus this molecule was dropped for this report. However, there are several other approaches in progress to construct the desired 7-deazaguanosine dioxolane nucleoside which are not in the interest of this thesis.

Antiviral Activity

One of the synthesized analogs (**29**) has demonstrated an EC_{50} of 0.4 µM with a CC_{50} of > 100 µM against EBV, and when compared to acyclovir (EC_{50} = 3.8 µM) this analog is 9.5 times more active than the FDA approved drug. To increase cellular uptake and bioavailability, synthesis of prodrug is progress. A repeated evaluation of active compounds is progress and will be published soon.

3.3 EXPERIMENTAL PROTOCOL

Materials

All solvents and reagents were purchased from Sigma-Aldrich, Fisher Scientific, AK Scientific, and Ambeed and were used without any further purification. Reactions were monitored via thin-layer chromatography plates (TLC, silica gel GF 250 microns) and were visualized with a UV lamp at 254 nm or developed with either a solution of 15% sulfuric acid in methanol or iodine. Melting point data were taken *via* a Laboratory Devices Mel-Temp II apparatus and are uncorrected. High resolution mass spectra were recorded on a Bruker Impact II. Nuclear Magnetic Resonance spectra were recorded on a Varian Inova 500 spectrometer at 500, 125, and 470 MHz for ^{1}H, ^{13}C, ^{19}F NMR respectively with tetramethylsilane as the internal standard. $CFCl_3$ (trichloro-fluoro methane) was used as the internal standard reference for ^{19}F NMR. Chemical shifts (δ) are represented as s (singlet), bs (broad singlet), d (doublet), dd (double doublet), t (triplet), q (quartet), and m (multiplet). Optical Rotations were recorded on a JASCO DIP-370 digital polarimeter.

Synthetic Protocol and Analytical Data

((2R)-4-acetoxy-1,3-dioxolan-2-yl)methyl isobutyrate (18). To a stirred solution of **16** (11.0 g, 58.45 mmol) in THF (50 mL) under N_2 cooled to -78°C, lithium tri-tert-butoxyaluminum hydride (LTBA) (72mL, 1M in THF) was added dropwise over 1 hour at -10°C. After that, the mixture was stirred for an additional 2 hours at -10°C to afford intermediate **17**. DMAP (9.0 g, 73.07 mmol) was added and the

mixture stirred for 30 minutes, after that acetic anhydride (28 mL, 292.27 mmol) was added dropwise. The mixture stirred for 16 hours at room temperature and was quenched with 20 mL NH_4Cl saturated aqueous solution. A murky suspension was obtained which was filtered through a celite bed to yield a clear biphasic mixture. The organic layer was separated and concentrated under reduced pressure to give a brown residue, which was dissolved in EtOAc (500mL). The organic layer was washed with water (30 mL x 2), brine (30 mL x 2), and finally with a saturated aqueous solution of $NaHCO_3$ (aq. 30 mL), and then concentrated under reduced pressure. The crude was purified via column chromatography (6% EtOAc/Hexanes) to give diastereomers **18a/18b** as an inseparable yellow oil. Yield: (5.2 g, 39%); ^{1}H NMR (500 MHz, $CDCl_3$) (mix of diastereomers) δ 6.34-6.28 (m, 1H), 5.35, 5.25 (t, *J* = 4.0Hz, 1H), 4.33-3.90 (m, 4H), 2.58-2.51 (m, 1H), 2.04-2.02 (m, 3H), 1.13-1.11 (m, 6H); ^{13}C NMR (125 MHz, $CDCl_3$) δ 176.5, 176.5, 170.2, 170.1, 103.6, 102.6, 102.3, 94.5, 94.0, 71.3, 70.8, 64.1, 63.5, 63.4, 63.2, 33.8, 21.1, 21.0, 18.9, 18.8; HRMS (ESI-TOF) m/z: $[M + Na]^+$ Calcd for $C_{10}H_{16}O_6Na$ 255.0839; found 255.0836.

4-chloro-2-fluoro-7H-pyrrolo[2,3-d]pyrimidine (20). 2-amino-6-chloro-7-deazapurine (1.0 g, 7.12 mmol), was cooled to -60°C under N_2, and HF in pyridine (70%) (9 mL) was added dropwise. The mixture was stirred for 5 minutes, and after that tert-butylnitrite (1.4 mL, 10.68 mmol) were added dropwise. The mixture was allowed to stir for two hours, and was slowly diluted with 40 mL of EtOAc, to avoid extensive effervescence. The reaction was quenched with $CaCO_3$ (aq.) and a slow

addition of $NaHCO_3$ (aq.) until a slightly basic pH with no bubbling. The organic layer was washed with brine (50 mL x 2) and water (50 mL x 2), dried over Na_2SO_4, concentrated under reduced pressure, and purified via silica plug to give **20** as a yellow flaky solid. Yield: (820 mg, 81%); MP (161-165°C); ^{1}H NMR (500 MHz, CD_3OD) δ 7.36 (d, *J* = 3.5 Hz, 1H), 6.49 (d, *J* = 3.5Hz, 1H); ^{13}C NMR (125 MHz, CD_3OD) δ 158.1, 156.4, 152.2, 127.5, 115.5, 99.5; ^{19}F NMR (470 MHz, CD_3OD) δ -56.30 (s, 1F); HRMS (ESI-TOF) m/z: [M + Na]+ Calcd for $C_6H_3ClFN_3Na$ 193.9892; found 192.9893.

((2R,4R)-4-(4-chloro-7H-pyrrolo[2,3-d]pyrimidin-7-yl)-1,3-dioxolan-2-yl)methylisobutyrate (21). To a stirred solution of **18** (1.0 g, 4.31 mmol) in anhydrous $CHCl_3$ (36 mL) under N_2 cooled to -20°C, iodotrimethylsilane (TMSI, 0.75 mL, 5.17 mmol) was added. The mixture was stirred at -20°C for 3 hours to afford intermediate **19**. In a separate R. B. flask, 725 mg KOH powder (12.93 mmol) was taken under N_2 in anhydrous ACN (25 mL) and stirred for 30 minutes. After that, 0.1 mL of tris[2-(2-methoxyethoxy)ethyl]amine (TDA-1) was added, and the mixture was stirred vigorously for 30 minutes, until the clumps of KOH disappeared. To this mixture, 660 mg (4.31 mmol) of 6-Chloro-7-deazapurine was added, and the mixture was vigorously stirred for an additional 20 minutes. The mixture was cooled to 0°C, and the crude **19** was added slowly over 5 minutes and stirred for 1 hour. The murky suspension was passed through a medium frit, quenched with $Na_2S_2O_3$ (aq. 25 mL), washed with water (50 mL x 2), dried over Na_2SO_4, and concentrated under reduced pressure. The crude residue was

purified *via* column chromatography (11% EtOAc/Hexanes) to give **21** as a white crystalline powder. Yield: (200 mg, 14%); ^{1}H NMR (500 MHz, $CDCl_3$) δ 8.63 (s, 1H), 7.58 (d, *J* = 3.5Hz, 1H), 6.80 (d, *J* = 5.5Hz, 1H), 6.67 (d, *J* = 4.0Hz, 1H), 5.29 (t, *J* = 3.5Hz, 1H), 4.45-4.28 (m, 4H), 2.62-2.54 (m, 1H), 1.16 (dd, *J* = 7.0Hz & 19.5Hz, 6H); ^{13}C NMR (125 MHz, $CDCl_3$) δ 176.6, 152.4, 151.4, 151.2, 125.9, 117.9, 103.1, 101.5, 79.6, 71.3, 63.0, 33.9, 19.0, 19.0; HRMS (ESI-TOF) m/z: $[M + Na]^+$ Calcd for $C_{14}H_{16}ClN_3O_4Na$ 348.0722; found 348.0722.

((2R,4R)-4-(2-amino-4-chloro-7H-pyrrolo[2,3-d]pyrimidin-7-yl)-1,3-dioxolan-2-yl)methylisobutyrate (22). Compound **22** was synthesized according to the above procedure described for the synthesis of **21**. Yield: (200 mg, white solid, 14%); ^{1}H NMR (500MHz, $CDCl_3$) δ 7.12 (d, *J* = 4.0Hz, 1H), 6.54-6.53 (m, 1H), 6.40 (d, *J* = 3.5Hz, 1H), 5.30 (bs, 2H), 5.22 (t, *J* = 4.0Hz, 1H), 4.37-4.28 (m, 2H), 4.25-4.17 (m, 2H), 2.58-2.52 (m, 1H), 1.13 (dd, *J* = 7.0Hz & 18.0Hz, 6H); ^{13}C NMR (125MHz, $CDCl_3$) δ 176.6, 159.0, 154.0, 152.8, 122.1, 110.6, 102.8, 79.2, 70.7, 63.2, 33.8, 19.0, 18.9; HRMS (ESI-TOF) m/z: $[M + Na]^+$ Calcd for $C_{14}H_{17}ClN_4O_4Na$ 363.0831; found 363.0826.

((2R,4R)-4-(4-chloro-5-fluoro-7H-pyrrolo[2,3-d]pyrimidin-7-yl)-1,3-dioxolan-2-yl)methylisobutyrate (23). Compound **23** was synthesized according to the above procedure described for the synthesis of **21**. Yield: (210 mg, pale yellow soild, 14%); MP (37-40°C); ^{1}H NMR (500 MHz, CDCl3) δ 8.60 (s, 1H), 7.35 (d, J = 3.0Hz, 1H), 6.84 (d, J = 6.5Hz, 1H), 5.24 (t, J = 3.5Hz, 1H), 4.38 (dd, J = 1.5Hz &

10.0Hz, 1H), 4.35-4.28 (m, 2H), 4.26 (dd, J = 4.5Hz & 10.0Hz, 1H), 2.62-2.54 (m, 1H), 1.16 (dd, J = 7.0 Hz & 21.5Hz, 6H); ^{13}C NMR (125 MHz, $CDCl_3$) δ 176.6, 151.9, 150.9, 147.2, 143.1, 141.1, 108.7, 107.4, 103.1, 79.2, 71.2, 62.7, 33.9, 18.9; ^{19}F NMR (470 MHz, $CDCl_3$) δ -166.17 (t, *J* = 2.35Hz, 1F); HRMS (ESI-TOF) m/z: $[M + H]^+$ Calcd for $C_{14}H_{16}ClFN_3O_4$ 344.0808; found 344.0805.

((2R,4R)-4-(4-chloro-2-fluoro-7H-pyrrolo[2,3-d]pyrimidin-7-yl)-1,3-dioxolan-2-yl)methylisobutyrate (24). Compound **24** was synthesized according to the above procedure described for the synthesis of **21**. Yield: (200 mg, white powder, 14%); MP (74-76°C); ^{1}H NMR (500 MHz, $CDCl_3$) δ 7.52 (d, *J* = 4.0Hz, 1H), 6.66 (s, 1H), 6.65 (s, 1H), 5.27 (t, *J* = 3.5Hz, 1H), 4.42-4.26 (m, 4H), 2.60-2.55 (m, 1H), 1.16 (dd, *J* = 7.0Hz & 17.5Hz, 6H); ^{13}C NMR (125 MHz, CDCl3) δ 176.6, 158.6, 156.8, 126.3, 116.3, 103.2, 102.0, 101.2, 79.7, 71.3, 62.9, 33.9, 18.9; ^{19}F NMR (470 MHz, CDCl3) δ -51.65 (s, 1F); HRMS (ESI-TOF) m/z: [M + Na]+ Calcd for $C_{14}H_{15}ClFN_3O_4Na$ 366.0627; found 366.0617.

((2R,4R)-4-(4-amino-7H-pyrrolo[2,3-d]pyrimidin-7-yl)-1,3-dioxolan-2-yl)methanol (25). In a sealed tube **21** (180 mg, 0.55 mmol) was taken in dioxane (2 mL) and NH_4OH (4 mL) were added. The solution was allowed to stir under higher pressure for 24 hours at 100°C. After that, the solution was allowed to cool to room temperature, and the solvent was evaporated *in vacuo*. The residue was purified *via* column chromatography (5% MeOH/DCM) and triturated with ether/hexane to give **25** as an off-white fluffy solid. Yield: (50 mg, 38%); MP 138-148 °C; $[\alpha]^{26}_D$ = -47.03 (c 0.5, MeOH); ^{1}H NMR (500 MHz, CD_3OD) δ 8.06 (s, 1H),

7.38 (d, *J* = 3.5Hz, 1H), 6.59-6.57 (m, 2H), 5.08 (t, *J* = 3.0Hz, 1H), 4.36-4.33 (m, 1H), 4.25-4.22 (m, 1H), 3.72 (d, *J* = 6.0Hz, 2H); ^{13}C NMR (125 MHz, CD_3OD) δ 157.6, 151.0, 149.6, 121.5, 105.2, 103.0, 100.2, 79.7, 70.8, 61.8; HRMS (ESI-TOF) m/z: $[M + Na]^+$ Calcd for $C_{10}H_{12}N_4O_3Na$ 259.0802; found 259.0801.

((2R,4R)-4-(2,4-diamino-7H-pyrrolo[2,3-d]pyrimidin-7-yl)-1,3-dioxolan-2-yl)methanol (26). In a sealed tube **22** (200 mg, 0.59 mmol) was taken in dioxane (2 mL) and NH_4OH (4 mL) were added. The solution was allowed to stir under higher pressure for 72 hours at 135°C. After that, the solution was allowed to cool to room temperature, and the solvent was evaporated *in vacuo*. A trituration with EtOAc/MeOH was attempted but failed. A crude NMR in DMSO-d6 was performed, which required the material to be lyophilized for two days to remove the solvent. After lyophilization, purification with a preparatory TLC (10% MeOH/DCM) gave **26** as a yellow powder. Yield: (20mg, 14%); MP (140-145°C); $[\alpha]^{25}_D$ = -73.61 (c 0.5, MeOH); ^{1}H NMR (500 MHz, CD_3OD) δ 6.98 (d, *J* = 4.0 Hz, 1H), 6.40-6.39 (m, 2H), 5.05 (t, *J* = 3.5 Hz, 1H), 4.29 (d, *J* = 2.0 Hz & 9.5 Hz, 1H), 4.19-4.16 (m, 1H), 3.70 (d, *J* = 3.5 Hz, 2H); ^{13}C NMR (125 MHz, CD_3OD) δ 159.5, 158.1, 152.2, 118.1, 104.9, 100.5, 96.5, 79.6, 70.4, 62.1; HRMS (ESI-TOF) m/z: $[M + H]^+$ Calcd for $C_{10}H_{14}N_5O_3$ 252.1091; found 252.1091.

((2R,4R)-4-(2-amino-4-(methylamino)-7H-pyrrolo[2,3-d]pyrimidin-7-yl)-1,3-dioxolan-2-yl)methanol (27). In a sealed tube **22** (100 mg, 0.29 mmol) was taken in methylamine in ethanol (33%/wt, 8 mL). The solution was allowed to stir under

higher pressure for 24 hours at 160°C. After that, the solution was allowed to cool to room temperature, and the solvent was evaporated *in vacuo*. The crude residue was purified via preparatory TLC (7.5% MeOH/DCM) to afford **27** as an off-white powder. Yield: (20mg, 26%); MP (145-155°C); $[\alpha]^{25}_{D}$ = -91.64 (c 0.5, MeOH); ^{1}H NMR (500 MHz, CD_3OD) δ 6.93 (d, *J* = 4.0 Hz, 1H), 6.39-6.37 (m, 1H), 6.35 (d, *J* = 3.5 Hz, 1H), 5.05 (t, *J* = 3.5 Hz, 1H), 4.28 (dd, *J* = 2.0 Hz & 9.5 Hz, 1H), 4.18-4.15 (m, 1H), 3.69 (d, *J* = 3.0 Hz, 2H), 2.96 (s, 3H); ^{13}C NMR (125 MHz, CD_3OD) δ 160.1, 158.1, 117.3, 104.9, 100.1, 100.0, 96.9, 79.6, 70.4, 62.2, 26.5; HRMS (ESI-TOF) m/z: $[M + H]^+$ Calcd for $C_{11}H_{16}N_5O_3$ 266.1248; found 266.1243.

((2R,4R)-4-(4-amino-2-fluoro-7H-pyrrolo[2,3-d]pyrimidin-7-yl)-1,3-dioxolan-2-yl)methanol (28). In a sealed tube **24** (100 mg, 0.29 mmol) was taken in dioxane (2 mL) and NH_4OH (4 mL) were added. The solution was allowed to stir under higher pressure for 24 hours at 100°C. After that, the solution was allowed to cool to room temperature, and the solvent was evaporated *in vacuo* to give a crude yellow solid. The solid was dissolved in 80°C isopropanol (3 mL), and stirred until full dissolution was observed. Purification via antisolvent recrystallization with hexane afforded **28** as a white powder. Yield: (35 mg, 47%); MP (160-165°C); $[\alpha]^{27}_{D}$ = -63.10 (c 0.5, MeOH); ^{1}H NMR (500 MHz, MeOH) δ 7.14 (d, *J* = 3.5 Hz, 1H), 6.52 (d, *J* = 3.5 Hz, 1H), 6.42 (d, *J* = 5.5 Hz, 1H), 5.05 (s, 1H), 4.32-4.18 (m, 2H), 3.72 (d, *J* = 3.0 Hz, 2H); ^{13}C NMR (125 MHz, CD_3OD) δ 183.2, 153.8, 120.3, 105.2, 101.2, 100.0, 95.2, 79.8, 70.6, 61.6; ^{19}F NMR (470 MHz, CD_3OD) δ -129.05

(s, 1F); HRMS (ESI-TOF) m/z: $[M - H]^-$ Calcd for $C_{10}H_{10}FN_4O_3$ 253.0742; found 253.0746.

((2R,4R)-4-(4-amino-5-fluoro-7H-pyrrolo[2,3-d]pyrimidin-7-yl)-1,3-dioxolan-2-yl)methanol (29). In a sealed tube **23** (200 mg, 0.58 mmol) was taken in dioxane (2 mL) and NH_4OH (4 mL) were added. The solution was allowed to stir under higher pressure for 24 hours at 100°C. After that, the solution was allowed to cool to room temperature, and the solvent was evaporated *in vacuo* to give a crude yellow solid. The solid was dissolved in 80°C water (3 mL) and stirred until full dissolution was observed. Purification via cooling recrystallization afforded **29** as an off-white beige powder. Yield: (116mg, 79%); MP (178-180°C); $[\alpha]^{25}_D$ = -77.52 (c 0.5, MeOH); ^{1}H NMR (500 MHz, MeOH) δ 8.06 (s, 1H), 7.21 (d, *J* = 1.5 Hz, 1H), 6.63 (d, *J* = 5.5 Hz, 1H), 5.04 (t, *J* = 2.5 Hz, 1H), 4.31 (d, *J* = 5.5 Hz, 1H), 4.22-4.19 (m, 1H), 3.72 (d, *J* = 2.5 Hz, 2H); ^{13}C NMR (125 MHz, CD_3OD) δ 152.4, 144.9, 142.9, 105.2, 103.9, 103.7, 79.3, 70.7, 61.5; ^{19}F NMR (470 MHz, CD_3OD) δ -169.37 (s, 1F); HRMS (ESI-TOF) m/z: $[M + H]^+$ Calcd for $C_{10}H_{11}FN_4O_3$ 255.0888; found 255.0883.

Protocol for Antiviral Evaluation

In vitro evaluation of the synthesized nucleosides in the replicon (DNA PCR based) and cell-based assay: The synthesized compounds were evaluated by Dr. Robert Schooley and associates at the University of San Diego. BCBL-1 and P3HR-1 cells were seeded in 48-well plates at a density of 3 x 10^5 cells/mL and 1

x 10^6 cells/mL, respectively. EBV replication was induced by adding 20 ng/mL 12-O-tetradecanoylphorbol 13-acetate (TPA; Sigma-Aldrich, Bornem, Belgium) to the growing cells. The next day, cells were washed and resuspended in a fresh medium in the presence or absence of various concentrations of antiviral drugs and proposed nucleosides. At day 5 postinduction, total cellular DNA was extracted (QIAamp DNA kit; Qiagen Benelux B.V, Venlo, Netherlands), and viral DNA was quantified by quantitative PCR (qPCR) using an ABI Prism 7500 Sequence Detection System (Applied Biosystems, Foster City, CA). Thermocycling conditions for all qPCRs were done following the manufacturer's instructions. Forward and reverse primers, as well as TaqMan probe sequences allowing the detection of the target ORF73 of KSHV and BNRF1 of EBV, have been described elsewhere.[64] The concentrations required to effectively reduce EBV DNA synthesis in TPA-stimulated cells by 50% and 90% (EC_{50} and EC_{90}), respectively, were extrapolated from the standard curve using linear regression analysis, and the results were obtained as the means from at least three independent experiments.

Cytotoxicity Assays

The cytostatic effect of the synthesized nucleosides was based on the inhibition of cell growth for each cell line. HEL cells were seeded at a density of 5 x10^3 cells/well into 96-well microtiter plates. NIH 3T3, OMK, and RF cells were seeded at a density of 3 x 10^3 cells/well, and uninduced BCBL-1 and P3HR-1 cells were seeded at a density of 3 x10^5 cells/mL and 1 x 10^6 cells/mL, respectively.

After 24 h of cell growth, a medium containing different concentrations of the test compounds was added. After a period of 3 days of incubation at 37°C, cell counts were determined using a Coulter counter (Analis, Namur, Belgium). The cytostatic concentration, or the concentration of the compound required to reduce cell growth by 50% (CC_{50}) relative to the number of cells in the untreated controls, was calculated. Alternatively, cytotoxicity was expressed as the minimum cytotoxic concentration (MCC), that is, the compound concentration that causes a microscopically detectable alteration of cell morphology.

3.4 CONCLUSION

Overall, 5 modified 7-deazapurine dioxolane nucleoside analogs have been synthesized and their activity has been evaluated against EBV. The synthesis commenced with ketone (**16**) and via acetylation furnished key intermediate **18**. Iodination of **18** followed by S_N2 coupling were performed to afford the coupled *β*-nucleosides **21-24** which on amination and deprotection yielded target nucleoside analogs **25-29**. One of the synthesized analogs (**29**) demonstrated potent anti-EBV activity in comparison to the standard drugs ganciclovir and acyclovir. Moving forward, elaborated in-vitro antiviral screenings against numerous DNA viruses are on-going. Preliminary results of ongoing in-vitro testing will be the basis for further SAR studies.

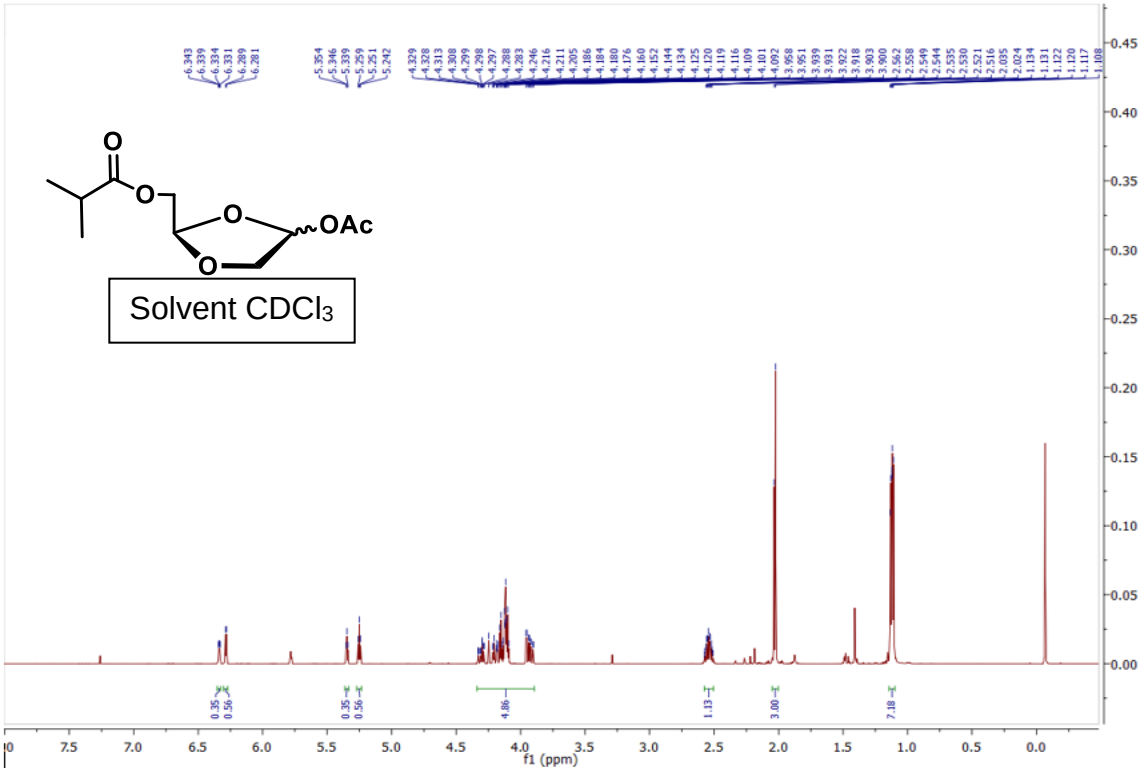

Figure 3.4 ^{1}H NMR of compound 18.

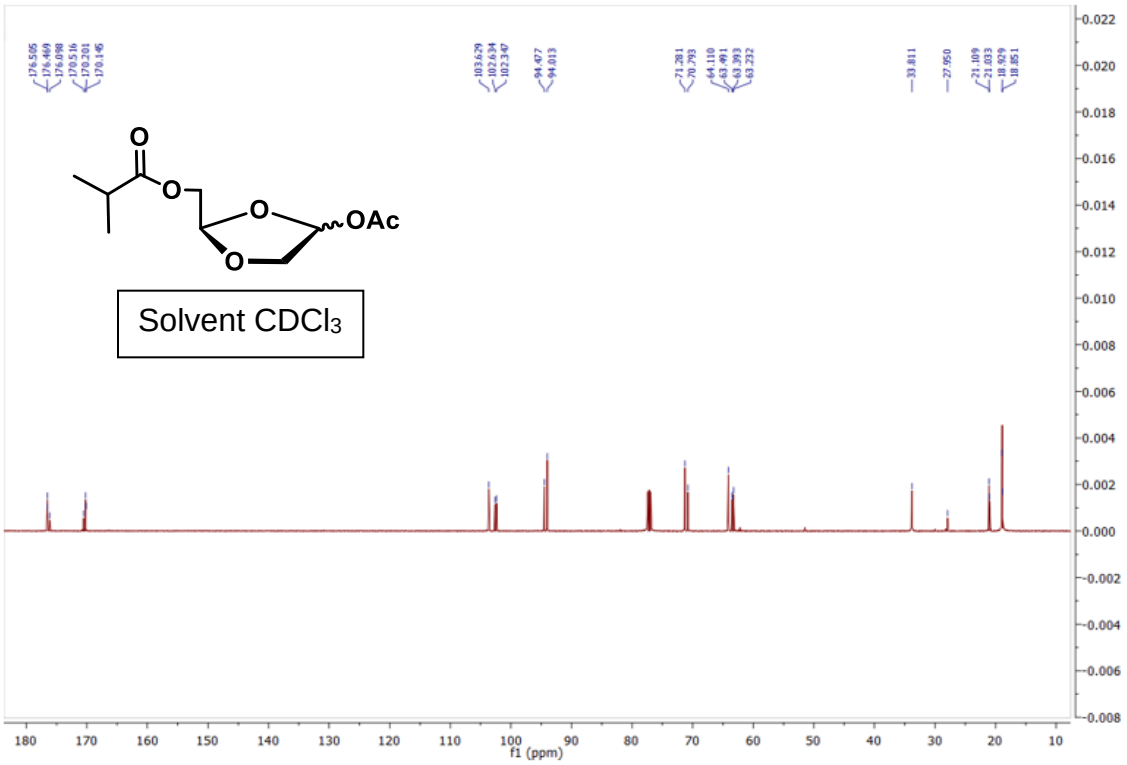

Figure 3.5 ^{13}C NMR of compound 18.

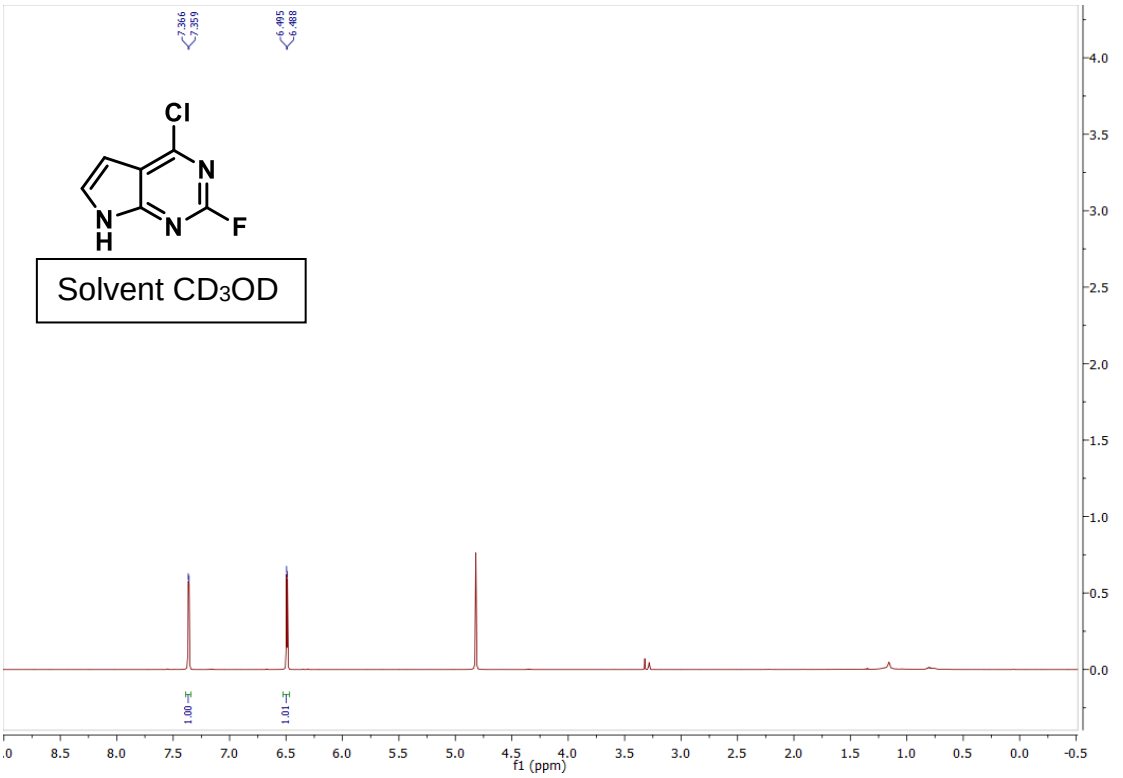

Figure 3.6 ^{1}H NMR of compound 20.

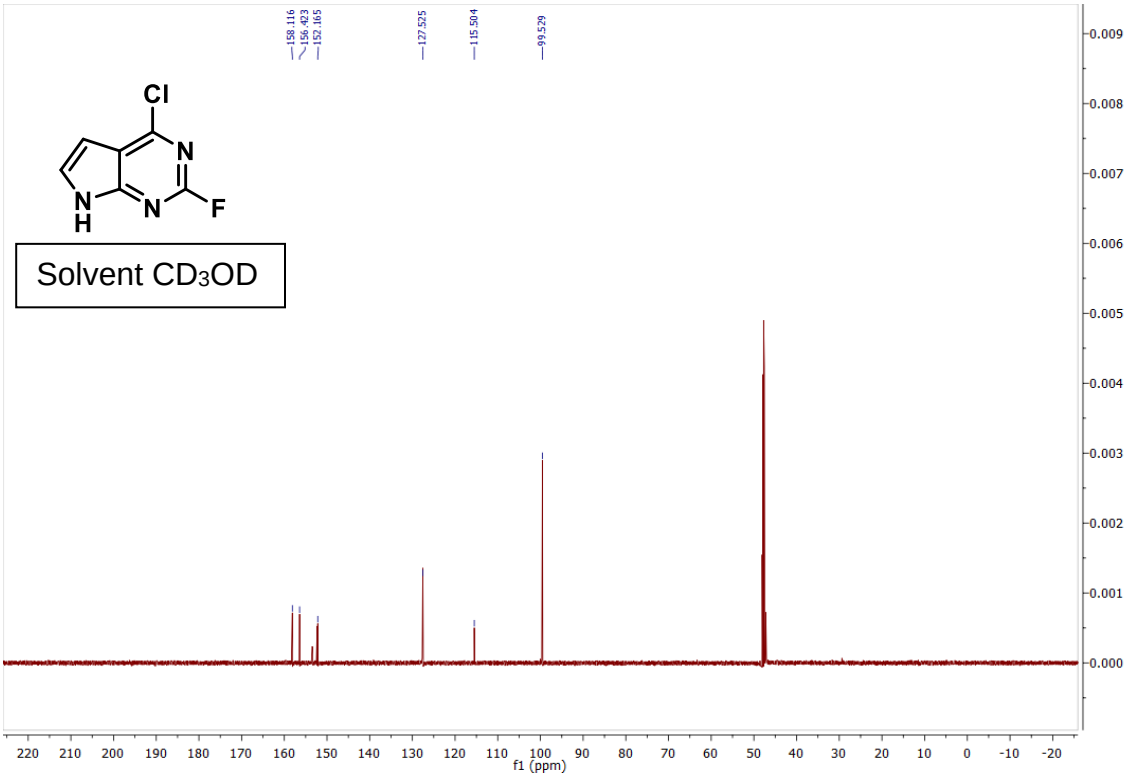

Figure 3.7 ^{13}C NMR of compound 20.

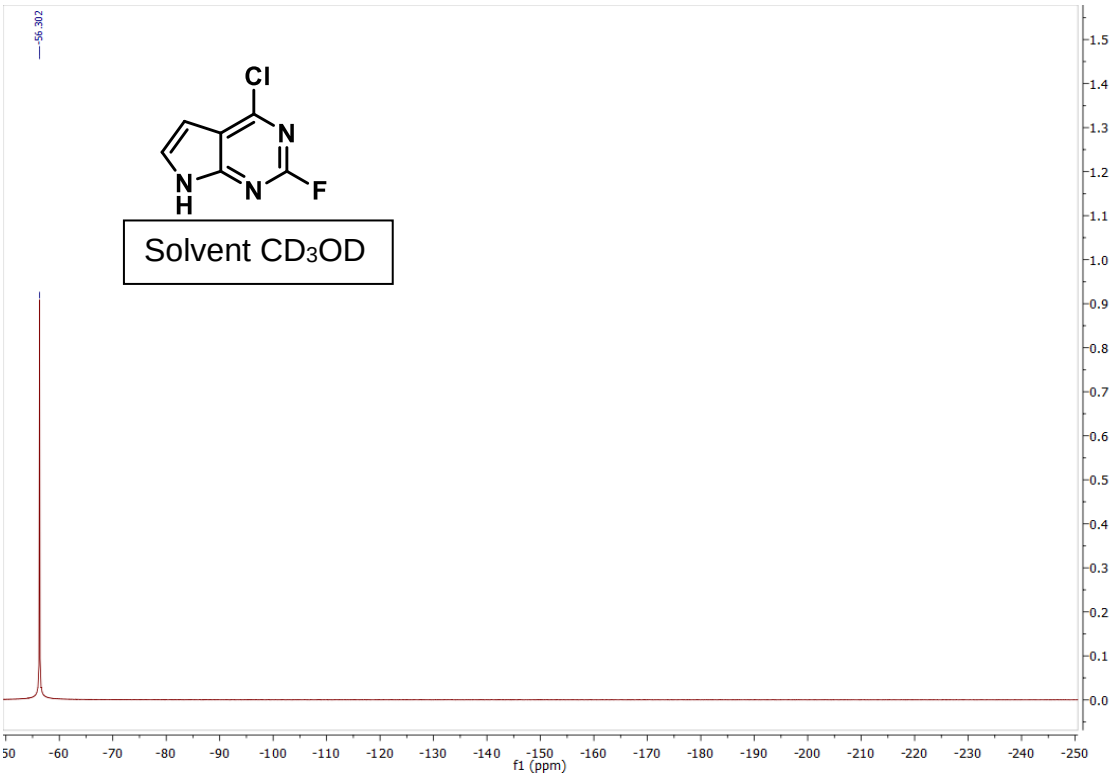

Figure 3.8 **^{19}F NMR of compound 20.**

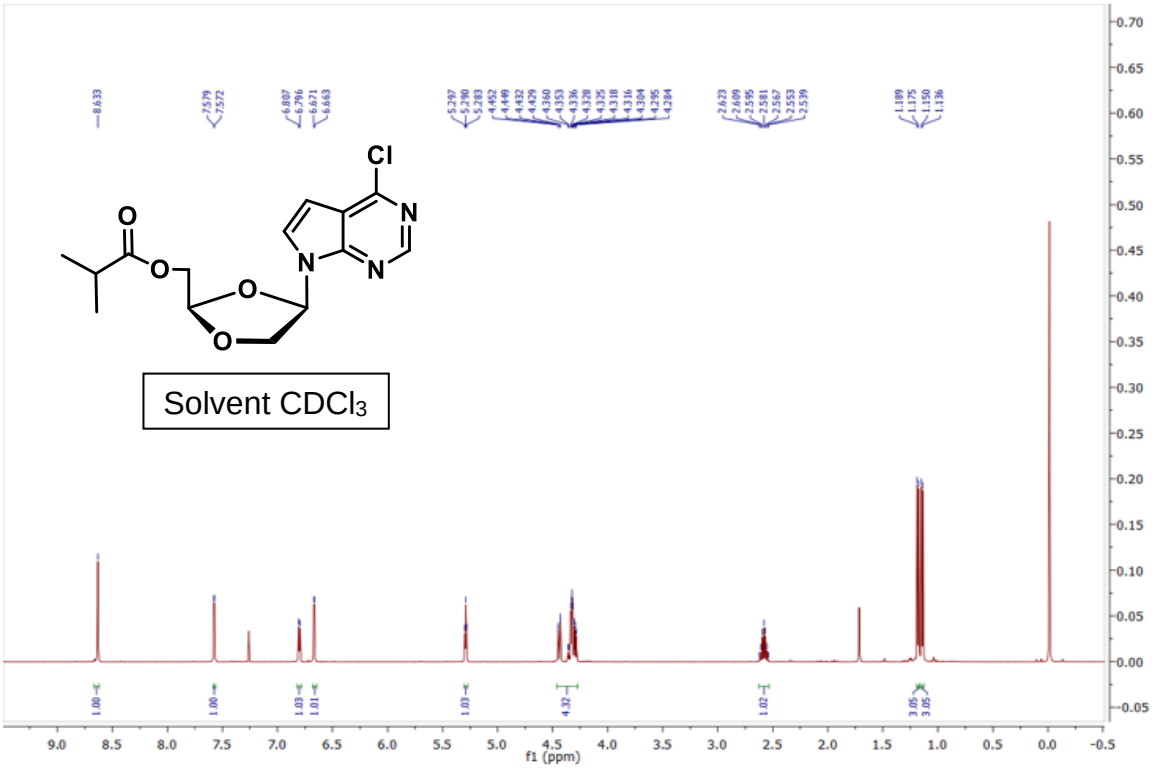

Figure 3.9 **^{1}H NMR of compound 21.** Desired *β*-purine

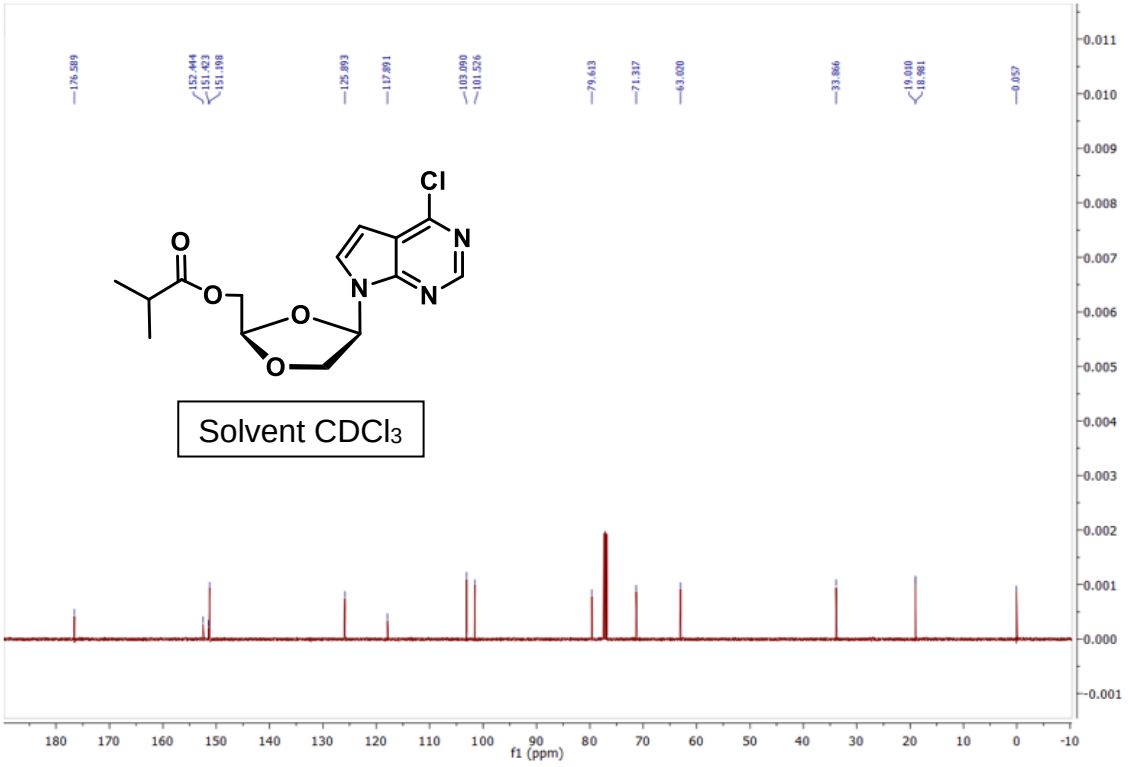

Figure 3.10 ^{13}C NMR of compound 21. Desired *β*-purine

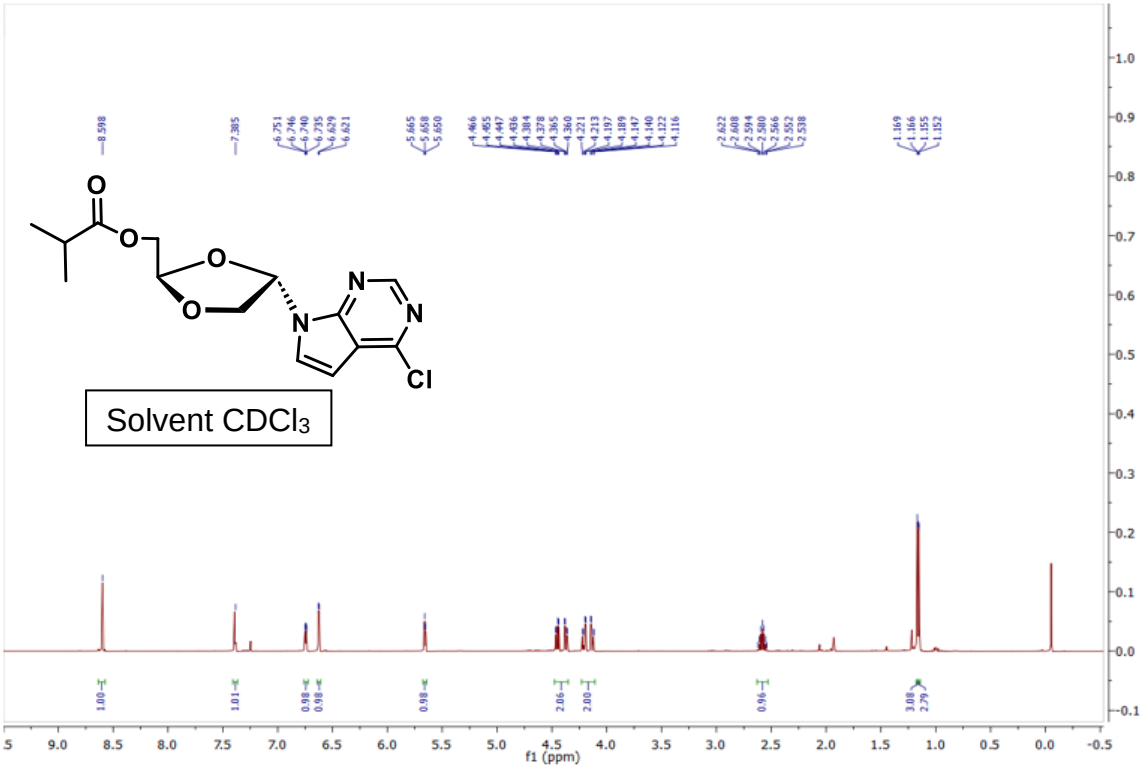

Figure 3.11 ^{1}H NMR of the α-isomer of compound 21. Undesired *α* purine.

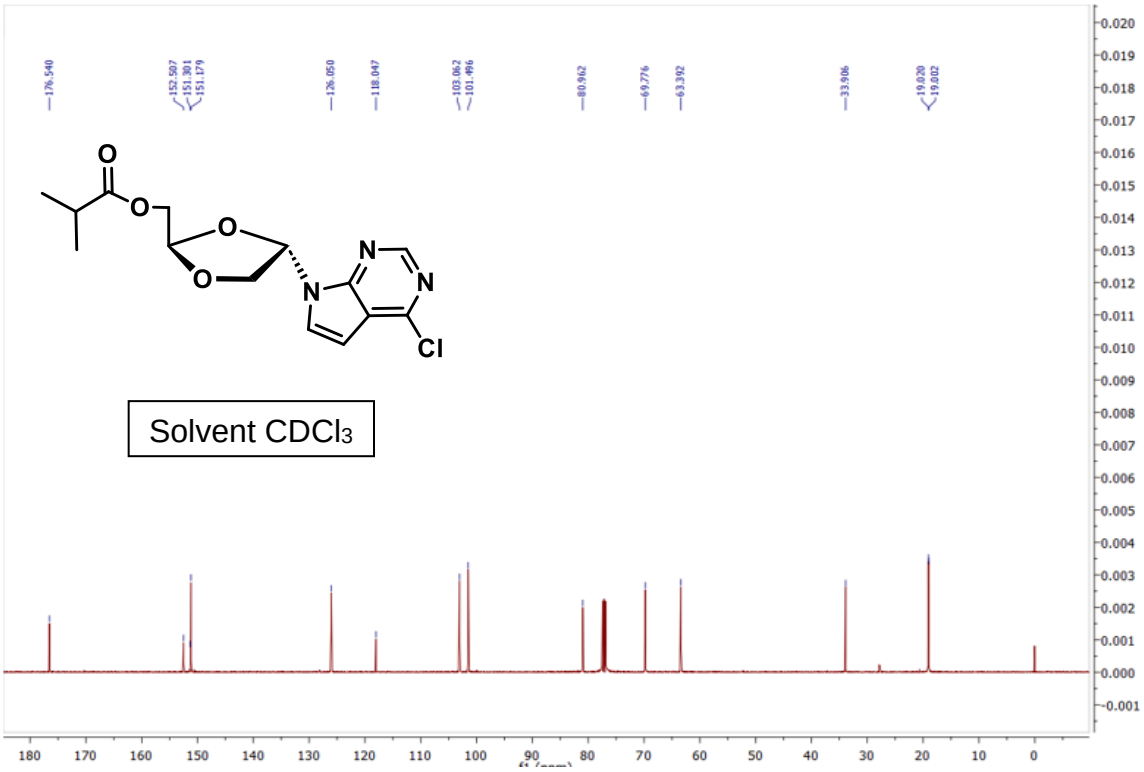

Figure 3.12 ^{13}C NMR of the α-isomer of compound 21. Undesired *α* purine.

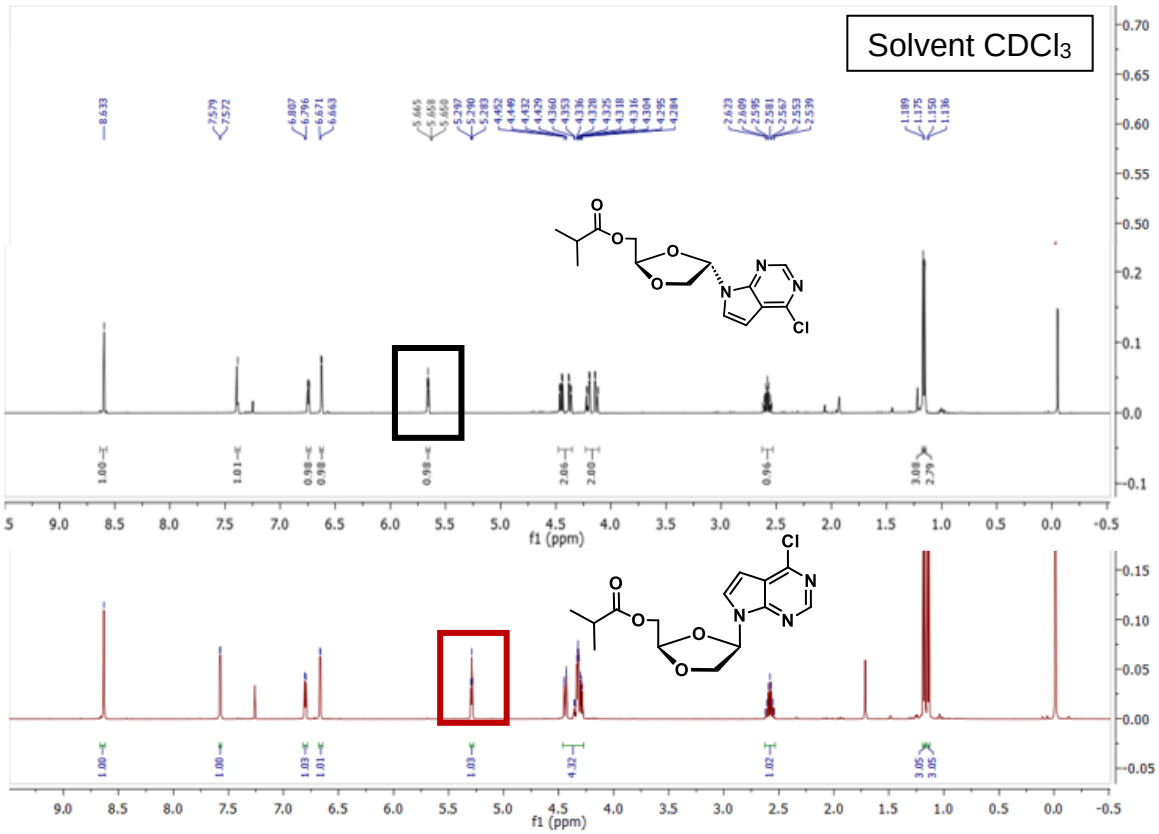

Figure 3.13 Overlayed ^{1}H NMRs of compound 21 *β* and *α*. The H4′ proton δ value changes significantly in correspondence with the configuration (either *α* or *β*) of the respective purine base.

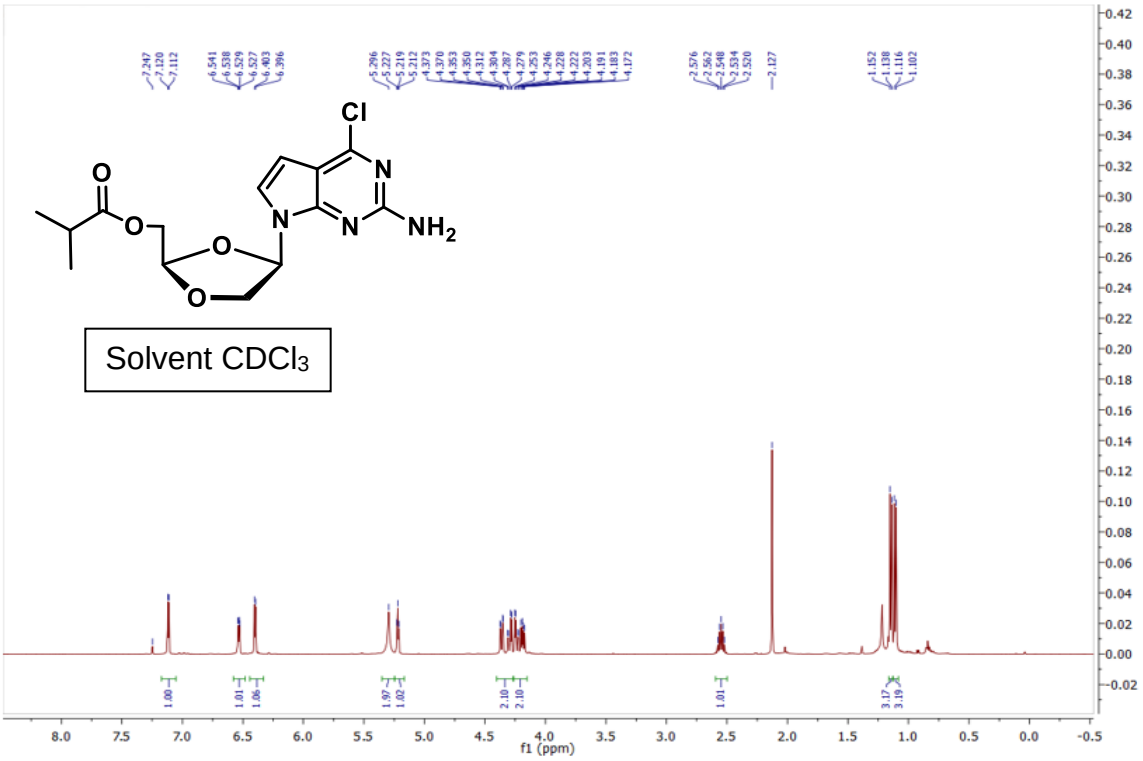

Figure 3.14 ^{1}H NMR of compound 22.

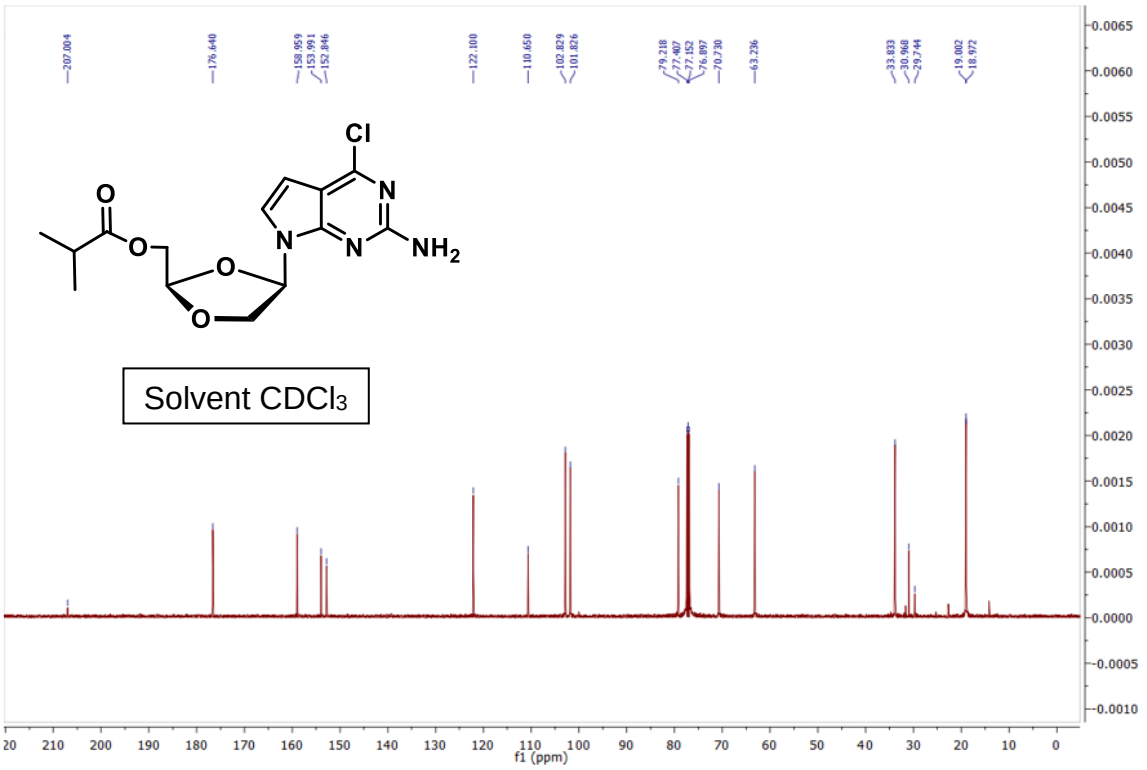

Figure 3.15 ^{13}C NMR of compound 22.

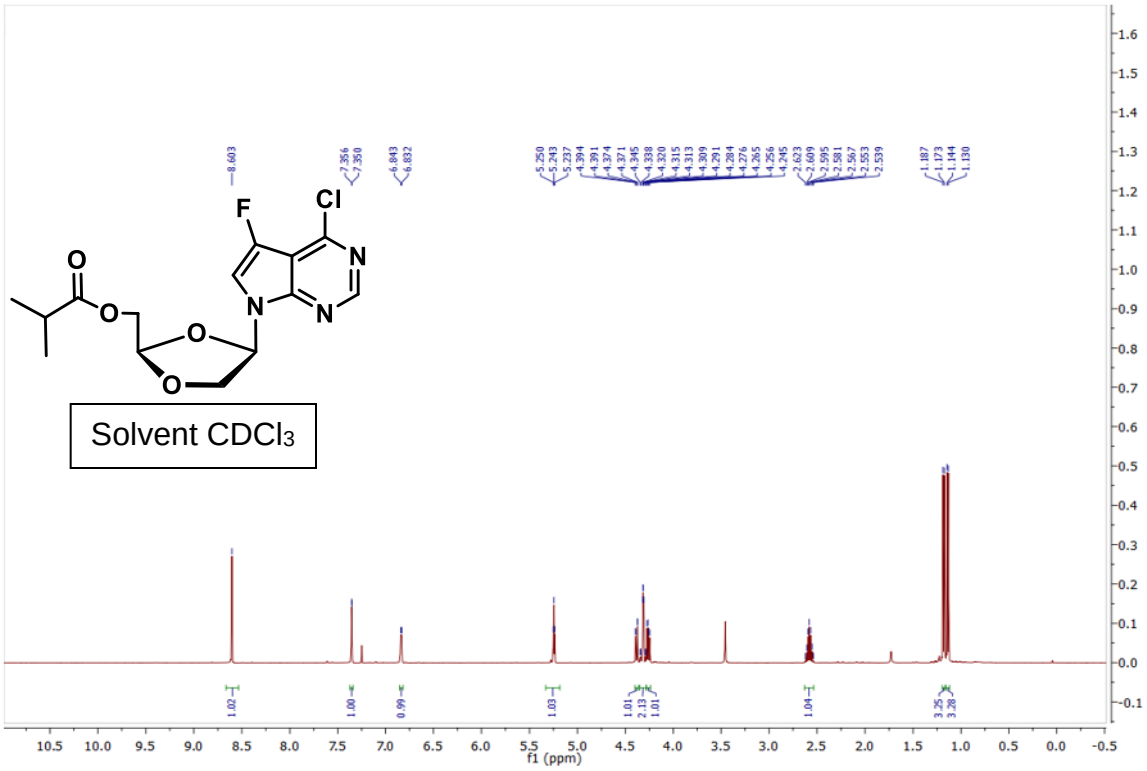

Figure 3.16 ^{1}H NMR of compound 23.

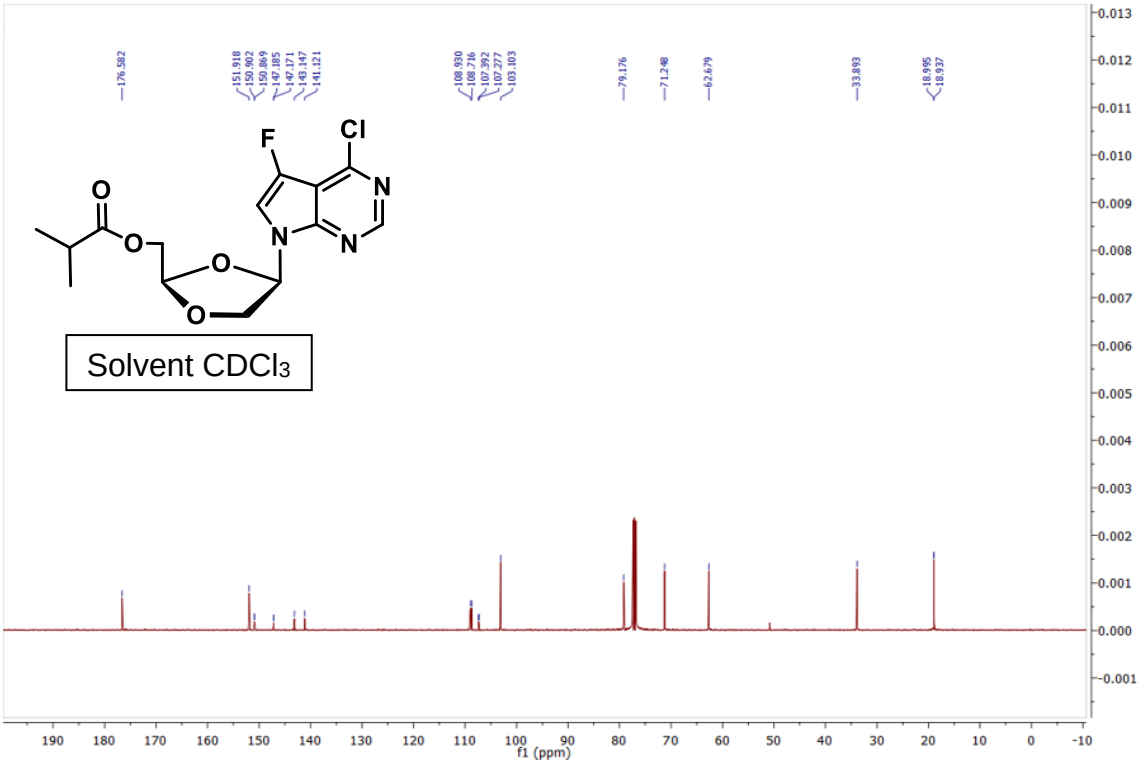

Figure 3.17 ^{13}C NMR of compound 23.

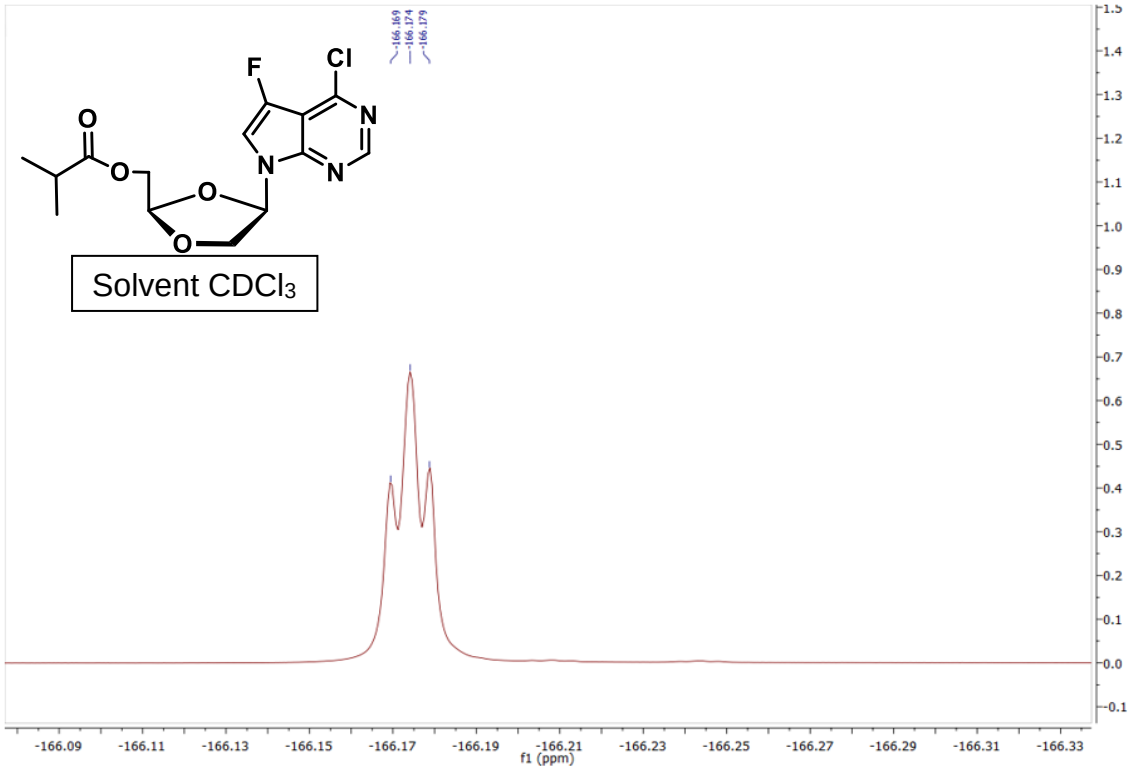

Figure 3.18 ^{19}F NMR of compound 23.

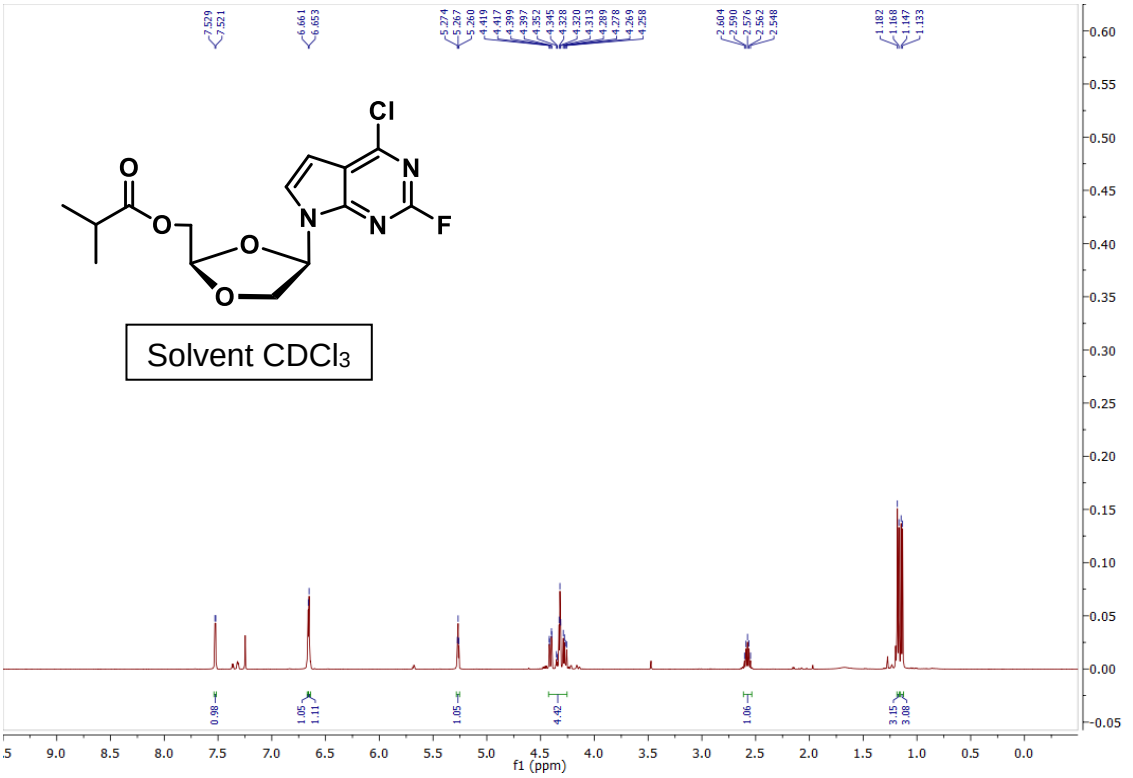

Figure 3.19 ^{1}H NMR of compound 24.

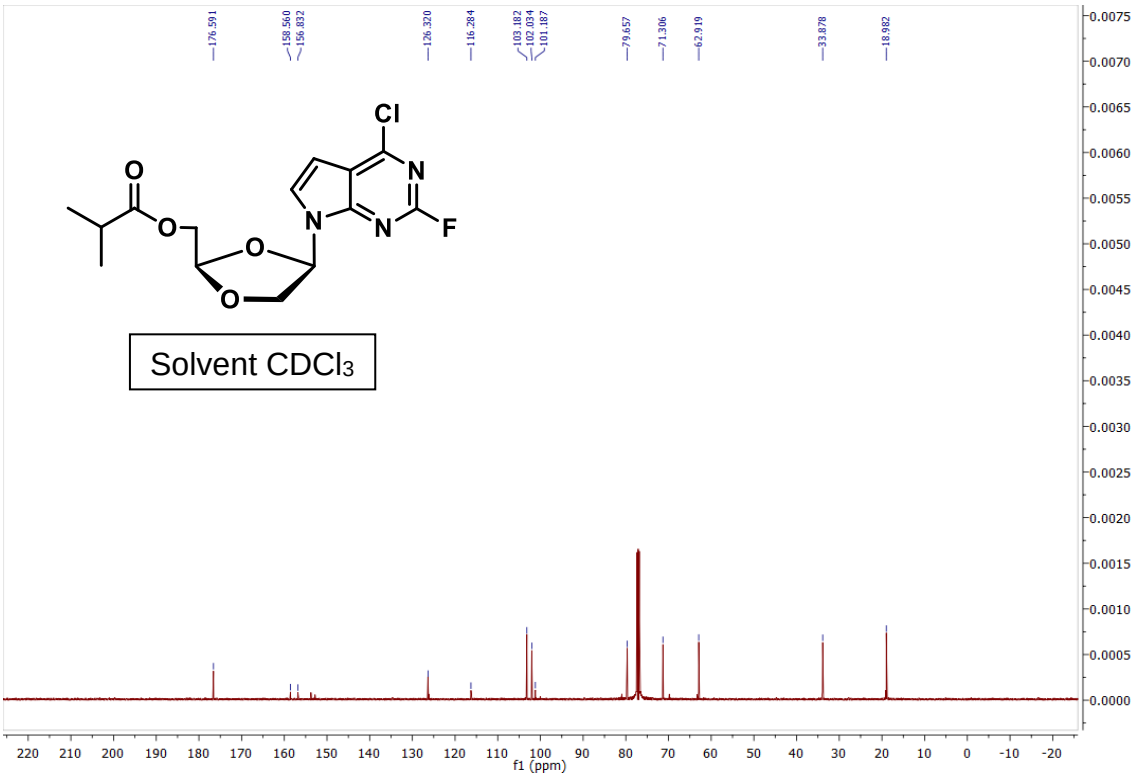

Figure 3.20 ^{13}C NMR of compound 24.

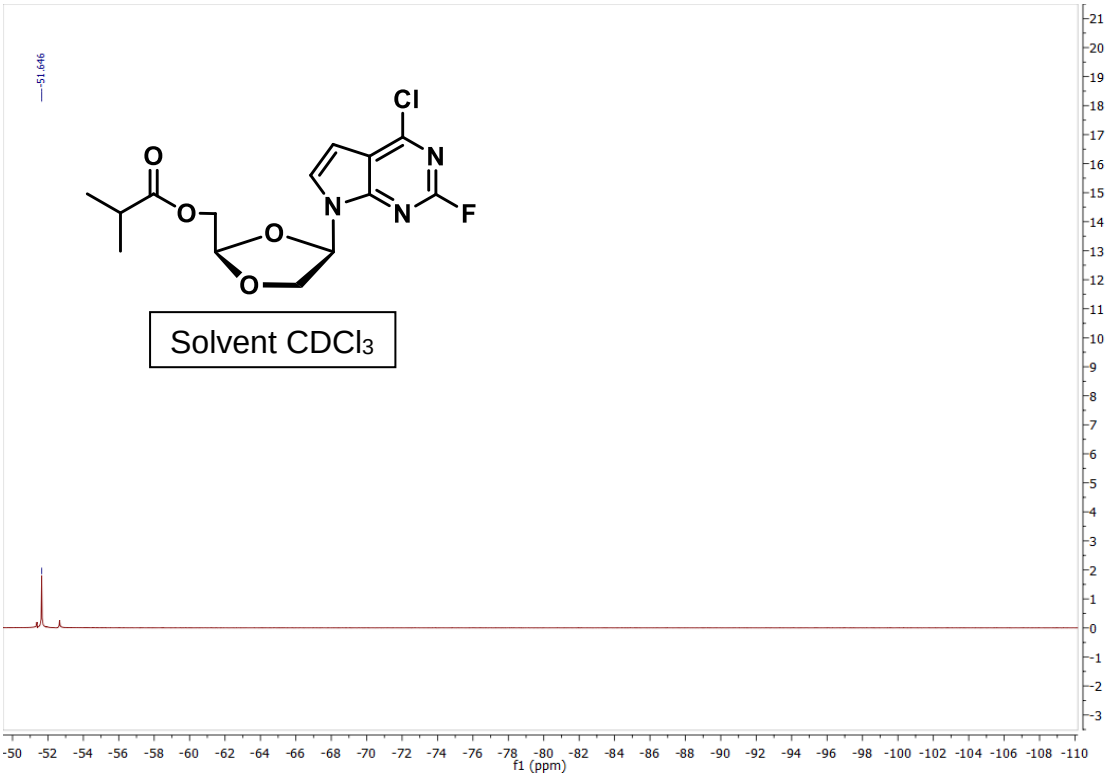

Figure 3.21 ^{19}F NMR of compound 24

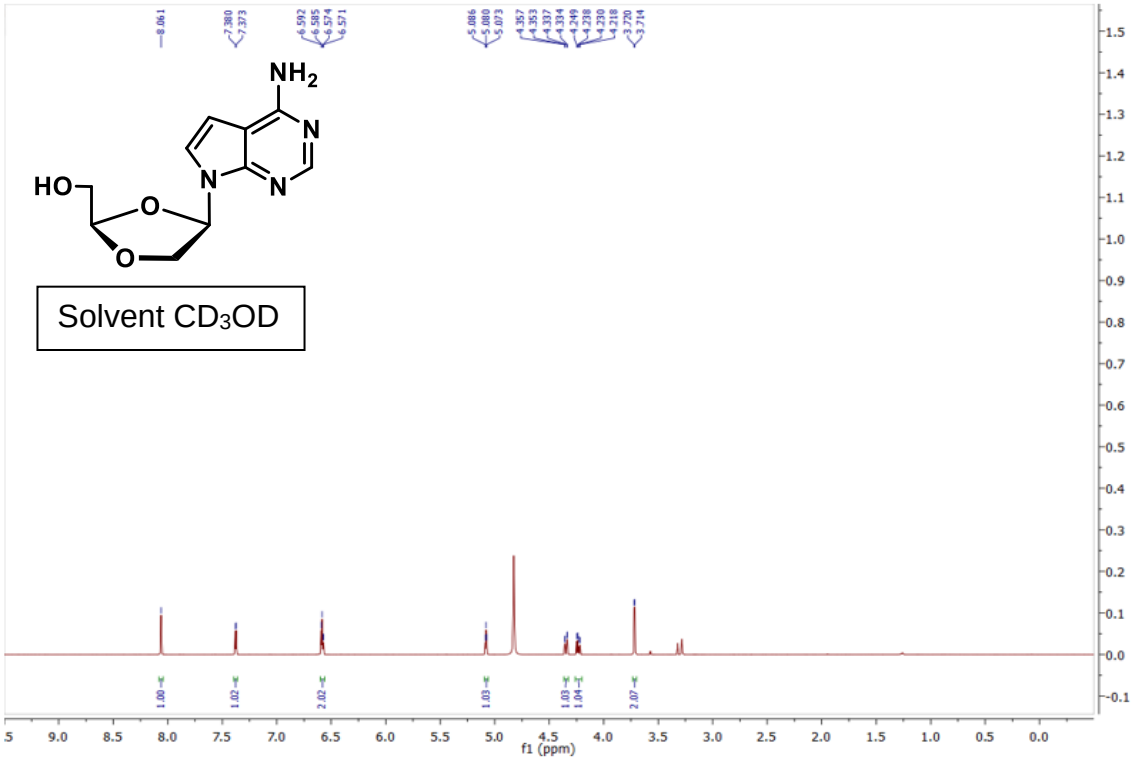

Figure 3.22 ^{1}H NMR of compound 25.

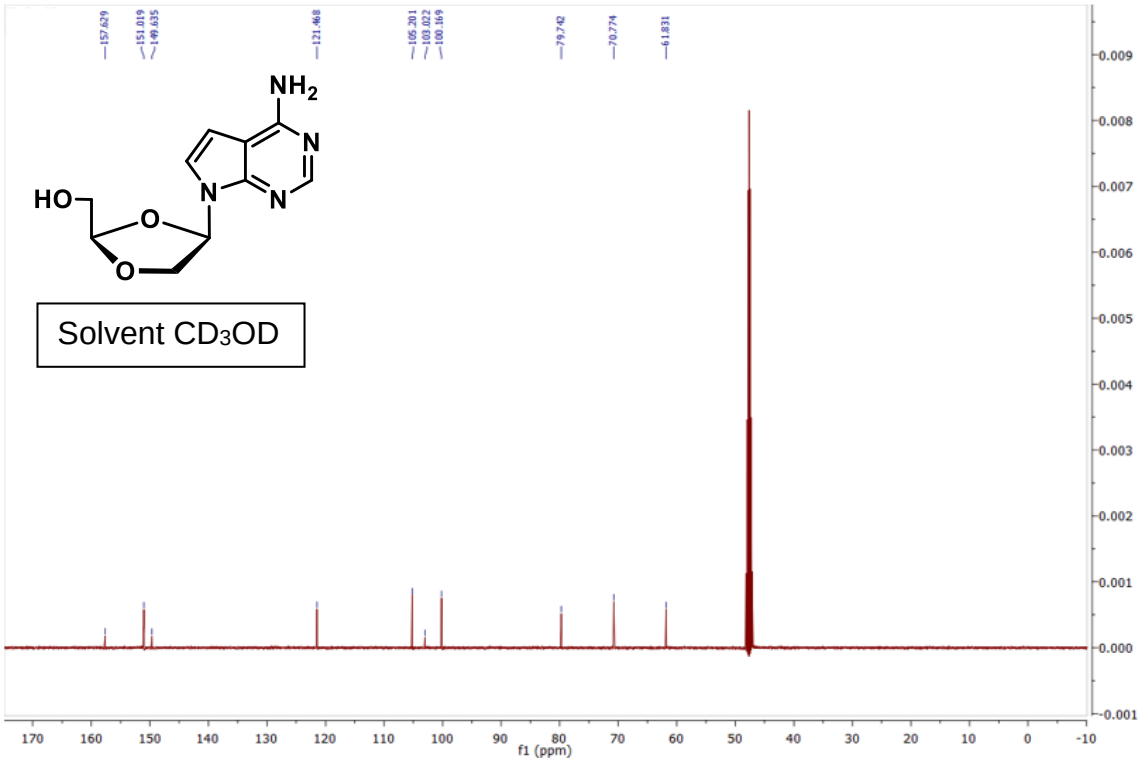

Figure 3.23 ^{13}C NMR of compound 25.

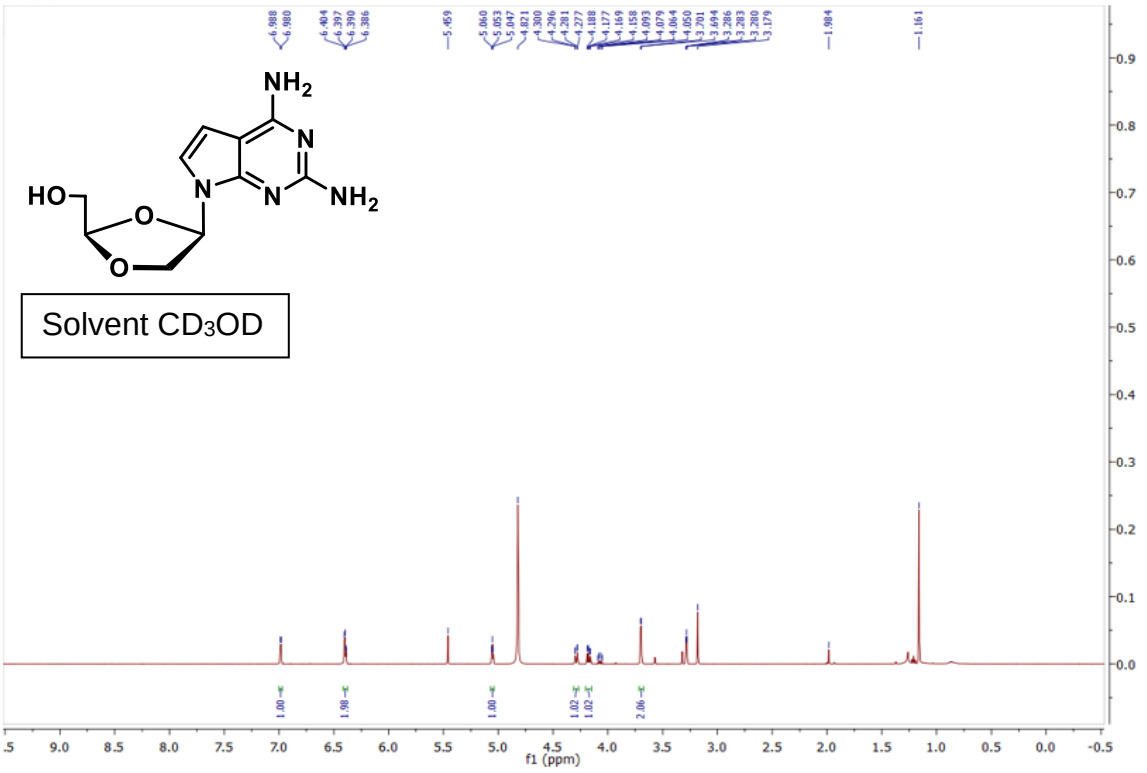

Figure 3.24 ^{1}H NMR of compound 26.

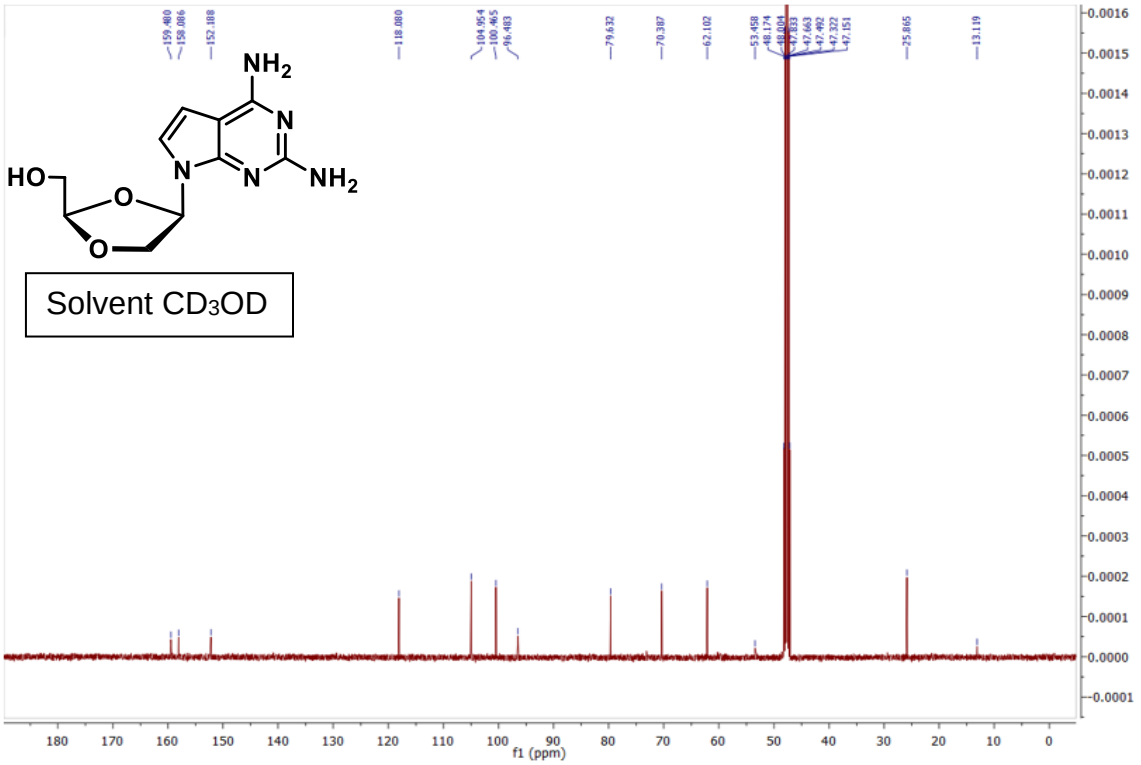

Figure 3.25 ^{13}C NMR of compound 26.

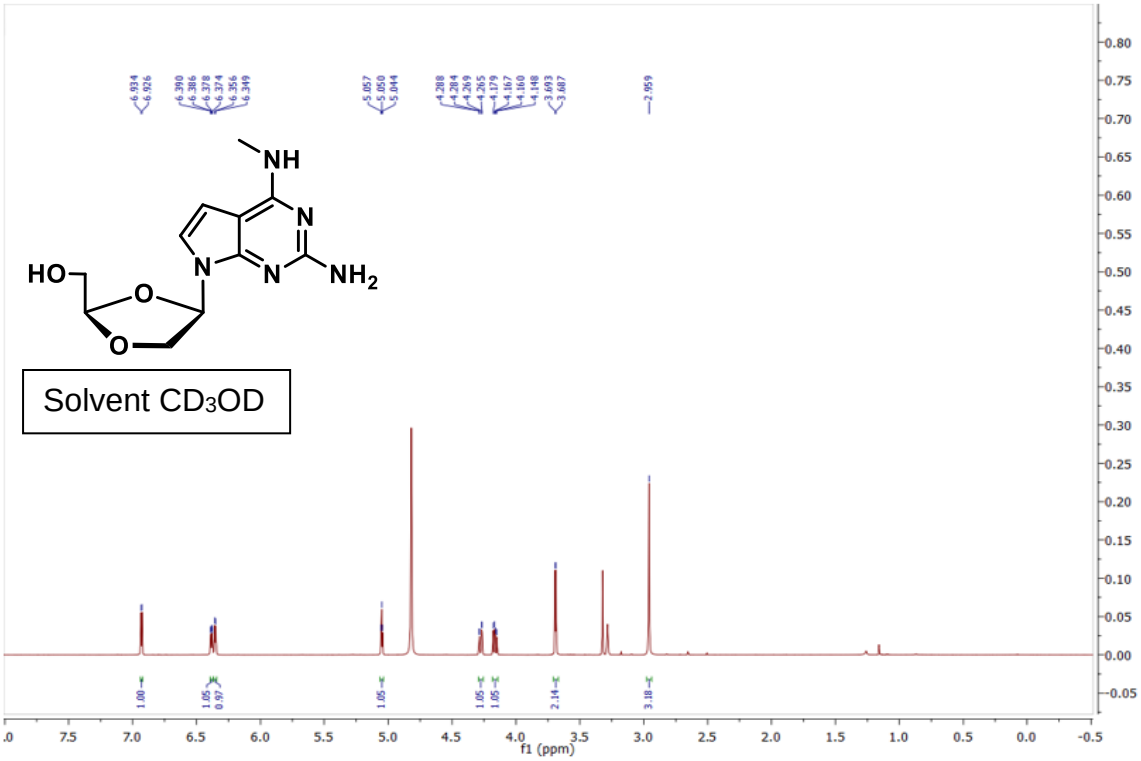

Figure 3.26 ^{1}H NMR of compound 27.

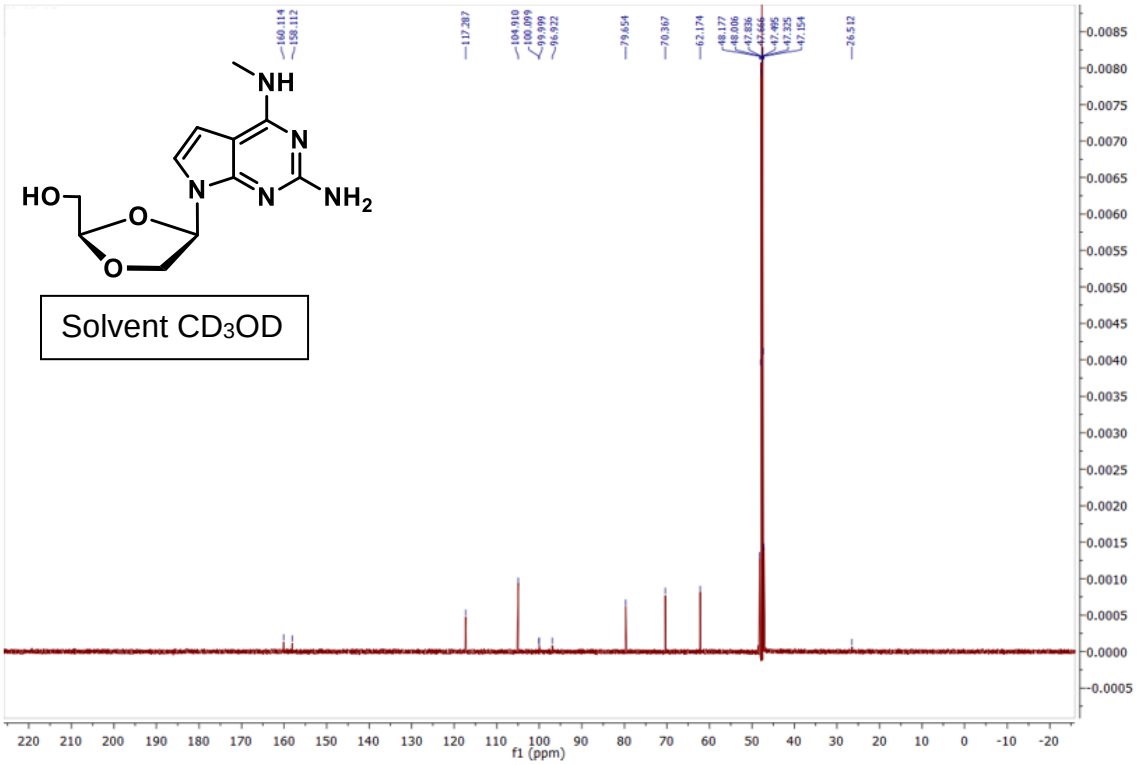

Figure 3.27 ^{13}C NMR of compound 27.

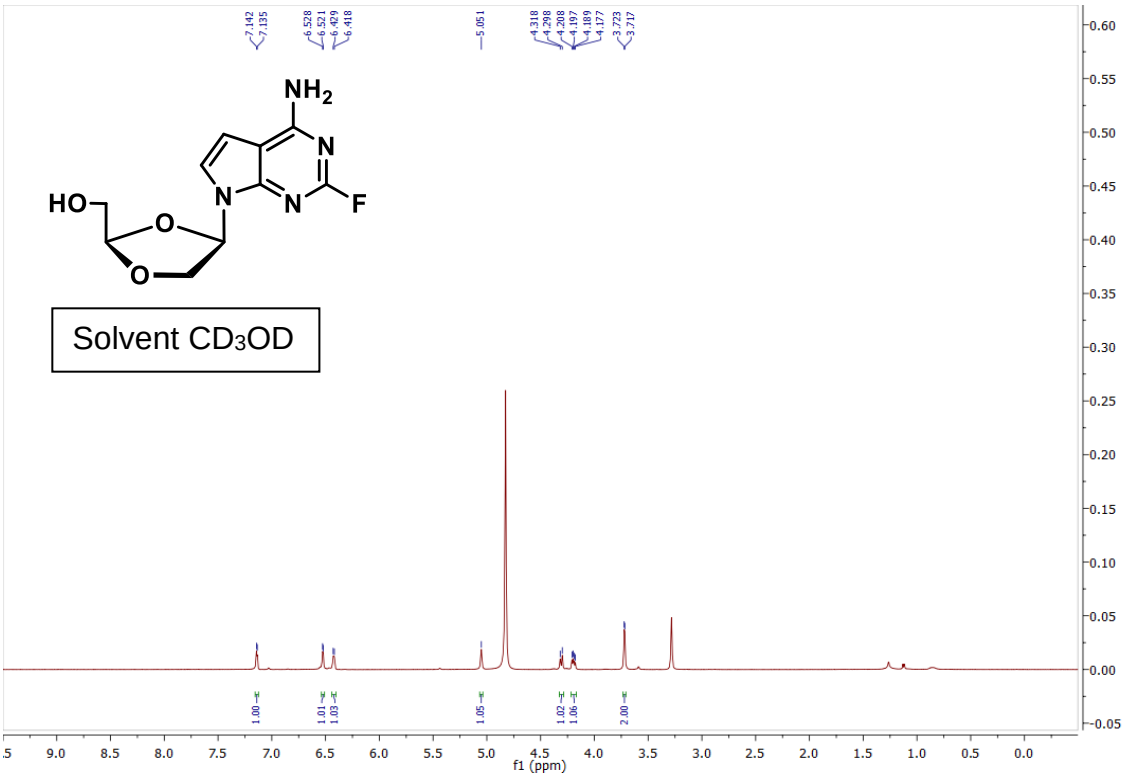

Figure 3.28 ^{1}H NMR of compound 28.

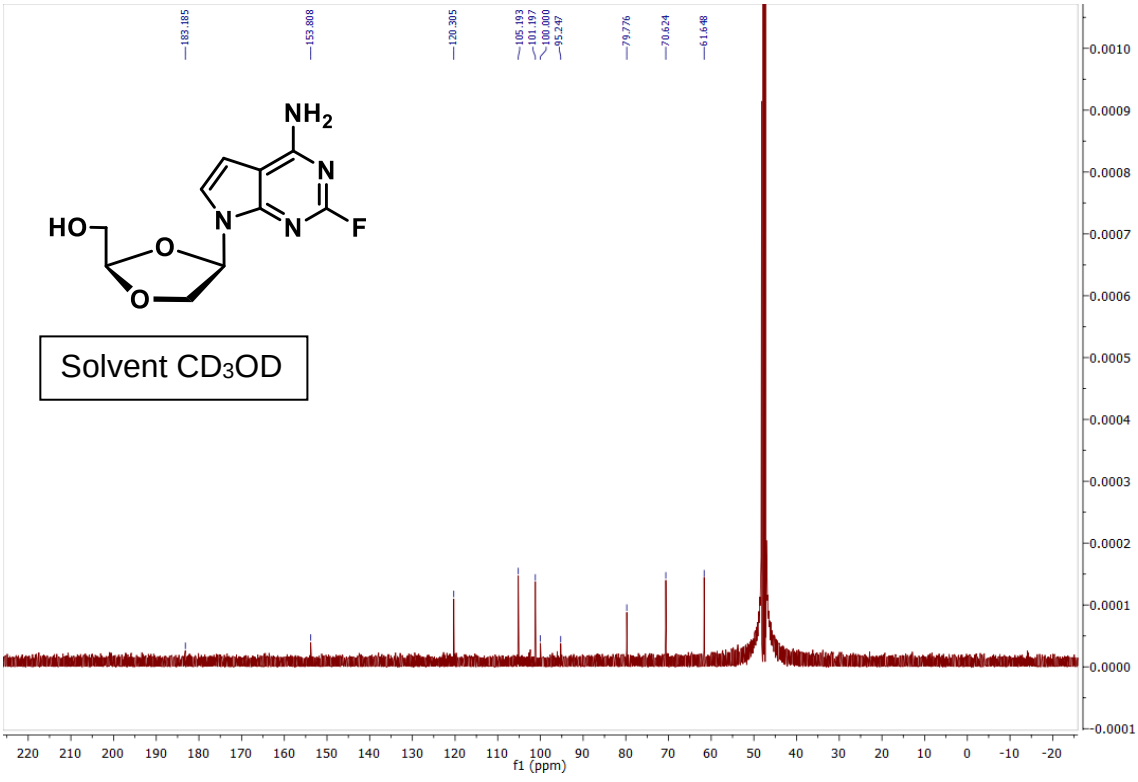

Figure 3.29 ^{13}C NMR of compound 28.

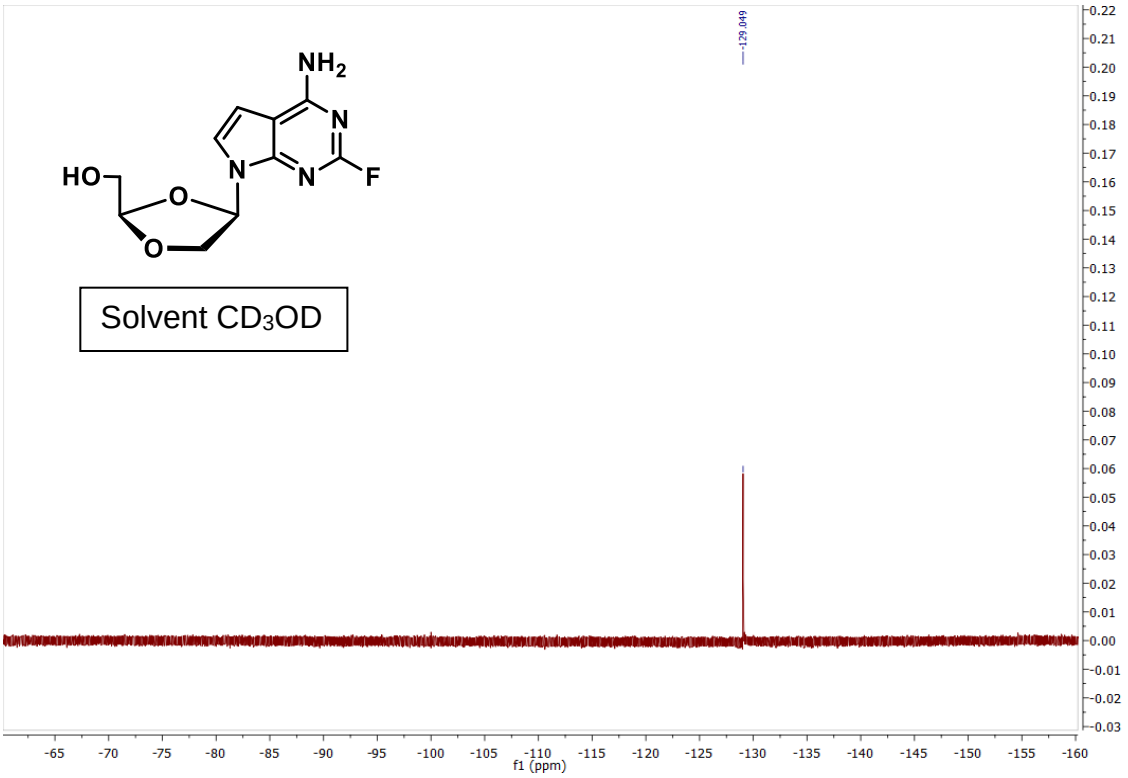

Figure 3.30 ^{19}F NMR of compound 28.

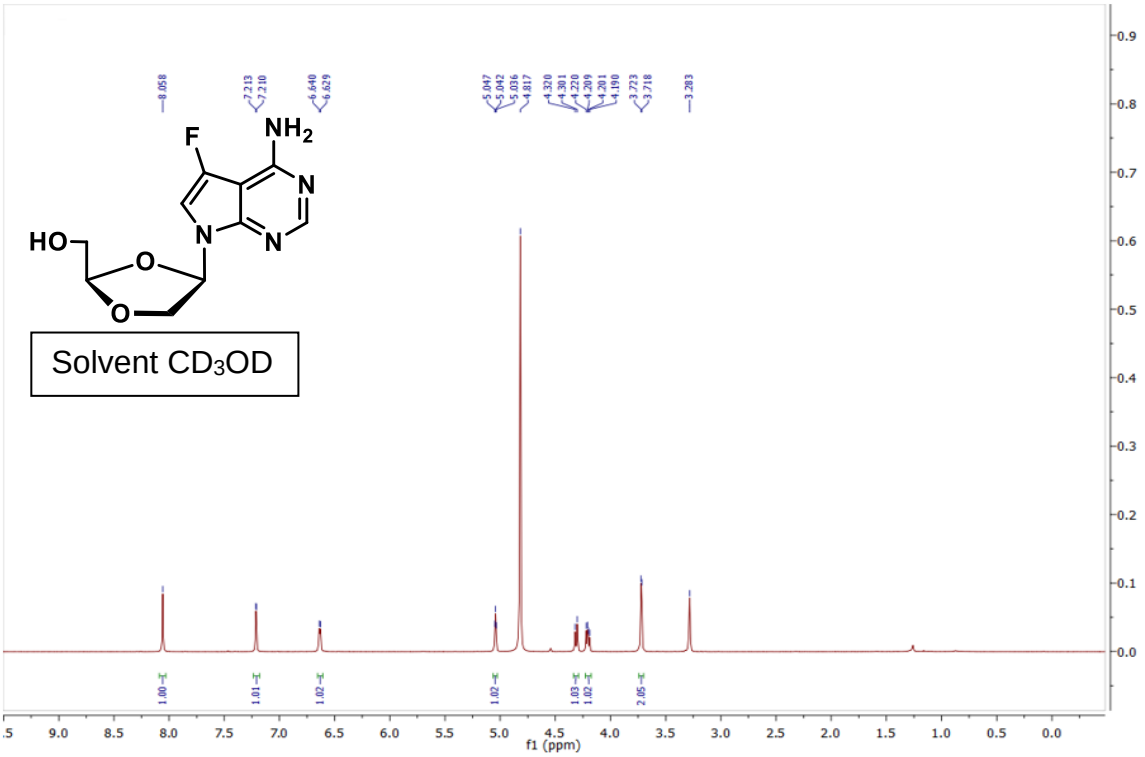

Figure 3.31 ^{1}H NMR of compound 29.

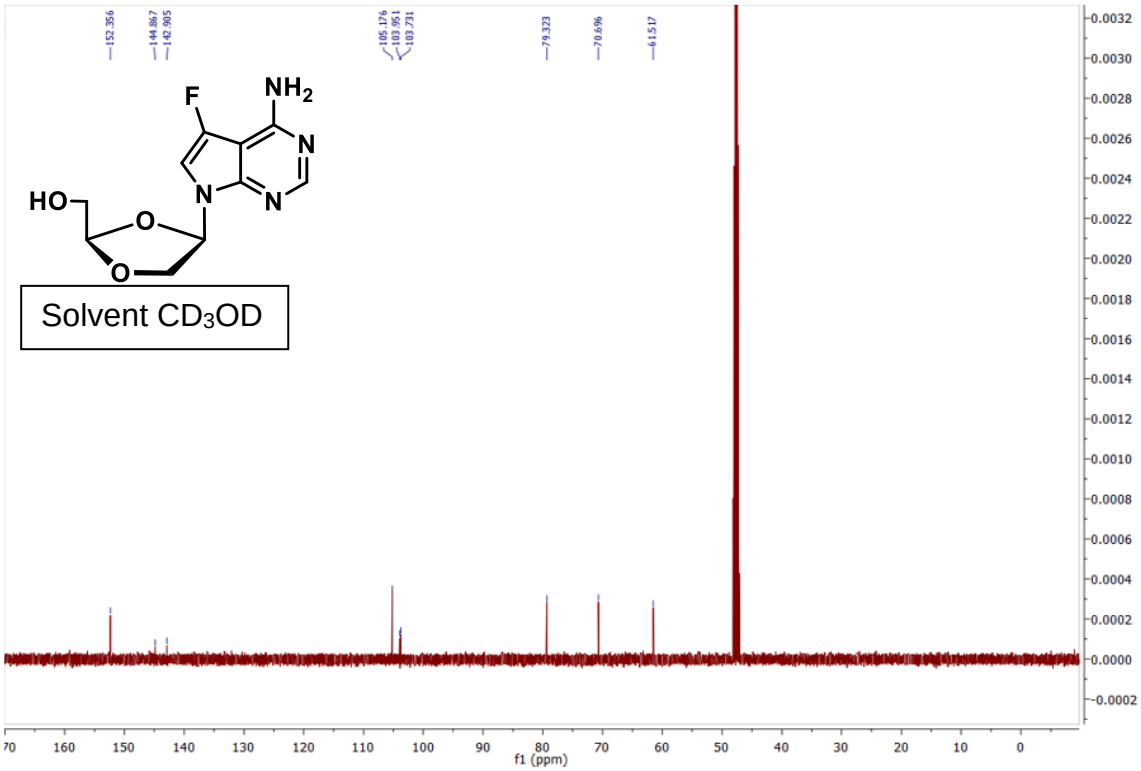

Figure 3.32 ^{13}C NMR of compound 29.

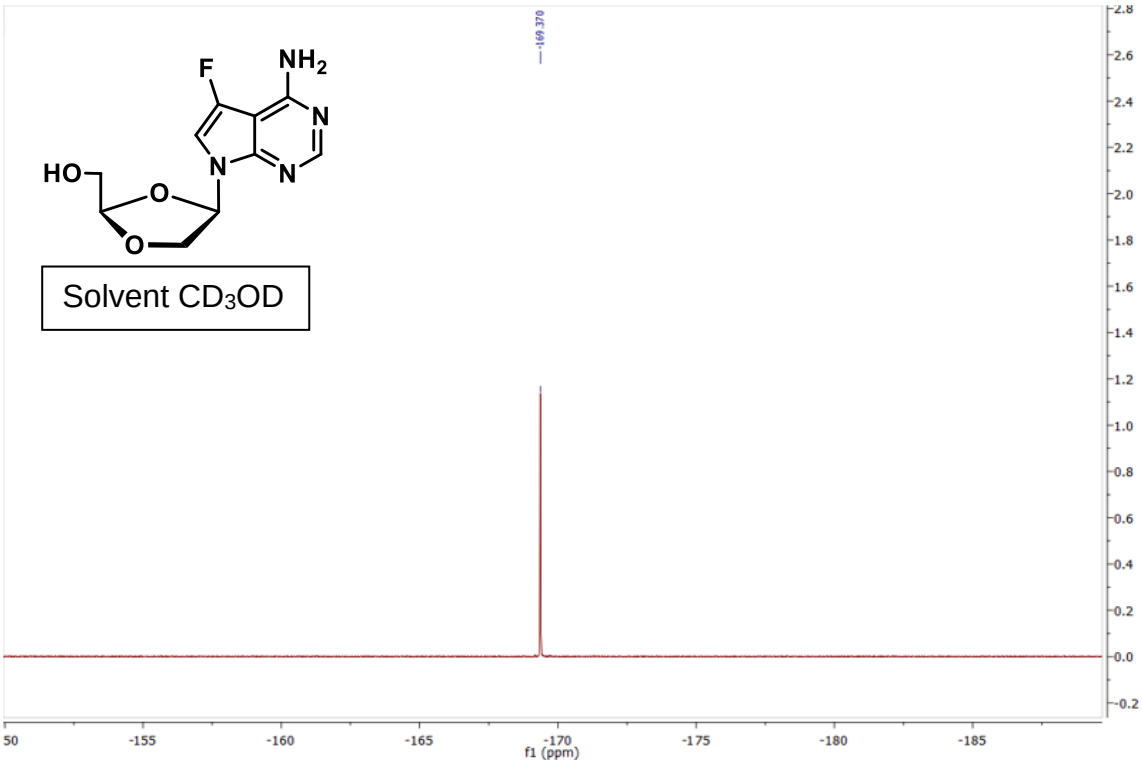

Figure 3.33 ^{19}F NMR of compound 29.

REFERENCES

(1) Piret, J.; Boivin, G. Pandemics Throughout History. *Frontiers in Microbiology* **2021**, *11*, Review.

(2) Meyer, R. R. P.; Adler, R. P. Acquired immunodeficiency syndrome (AIDS). In Salem Press, 2022.

(3) Singer, S. S. Polio. In Salem Press, 2022.

(4) Scott, R. L. P. P. A. C. Herpes. In Salem Press, 2022.

(5) Bjornevik, K.; Cortese, M.; Healy, B. C.; Kuhle, J.; Mina, M. J.; Leng, Y.; Elledge, S. J.; Niebuhr, D. W.; Scher, A. I.; Munger, K. L.; et al. Longitudinal analysis reveals high prevalence of Epstein-Barr virus associated with multiple sclerosis. *Science* **2022**, *375* (6578), 296-301. DOI: 10.1126/science.abj8222 From NLM.

(6) Saghazadeh, A.; Rezaei, N. Poxviruses and the immune system: Implications for monkeypox virus. *Int Immunopharmacol* **2022**, *113* (Pt A), 109364. DOI: 10.1016/j.intimp.2022.109364 From NLM Medline.

(7) Becerra, X. Biden-Harris Administration Bolsters Monkeypox Response; HHS Secretary Becerra Declares Public Health Emergency. HHS.gov: 2022.

(8) Chaitanya, K. V. Structure and Organization of Virus Genomes. From 2019 Nov 18.

(9) Fenner, F.; Bachmann, P. A.; Gibbs, E. P. J.; Murphy, F. A.; Studdert, M. J.; White, D. O. Structure and Composition of Viruses. **1987**. From 1987.

(10) Gelderblom, H. *Structure and Classification of Viruses*; The University of Texas Medical Branch at Galveston, 1996.

(11) Zephyr, J.; Kurt Yilmaz, N.; Schiffer, C. A. Viral proteases: Structure, mechanism and inhibition. *Enzymes* **2021**, *50*, 301-333. DOI: 10.1016/bs.enz.2021.09.004 From NLM Medline.

(12) Mazeaud, C.; Freppel, W.; Chatel-Chaix, L. The Multiples Fates of the Flavivirus RNA Genome During Pathogenesis. *Front Genet* **2018**, *9*, 595. DOI: 10.3389/fgene.2018.00595 From NLM PubMed-not-MEDLINE. Poltronieri, P.; Sun, B.; Mallardo, M. RNA Viruses: RNA Roles in Pathogenesis, Coreplication and Viral Load. *Curr Genomics* **2015**, *16* (5), 327-335. DOI: 10.2174/1389202916666150707160613 From NLM PubMed-not-MEDLINE.

(13) Pierno, K. M. S. Poxviridae. In Salem Press, 2020.

(14) Duffy, S.; Shackelton, L. A.; Holmes, E. C. Rates of evolutionary change in viruses: patterns and determinants. *Nature Reviews. Genetics* **2008**, *9* (4), 267-276. DOI: https://doi.org/10.1038/nrg2323 ProQuest Central; SciTech Premium Collection.

(15) WHO. *WHO Coronavirus (COVID-19) Dashboard*. https://covid19.who.int/, (accessed.

(16) Grabowski, F.; Preibisch, G.; Gizinski, S.; Kochanczyk, M.; Lipniacki, T. SARS-CoV-2 Variant of Concern 202012/01 Has about Twofold Replicative Advantage and Acquires Concerning Mutations. *Viruses* **2021**, *13* (3). DOI: 10.3390/v13030392 From NLM Medline. Shiehzadegan, S.; Alaghemand, N.; Fox, M.; Venketaraman, V. Analysis of the Delta Variant B.1.617.2 COVID-19. *Clin Pract* **2021**, *11* (4), 778-784. DOI: 10.3390/clinpract11040093 From NLM PubMed-not-MEDLINE. Kannan, S.; Shaik Syed Ali, P.; Sheeza, A. Omicron (B.1.1.529) - variant of concern - molecular profile and epidemiology: a mini review. *Eur Rev Med Pharmacol Sci* **2021**, *25* (24), 8019-8022. DOI: 10.26355/eurrev_202112_27653 From NLM Medline.

(17) FDA Approves First Treatment for COVID-19. U.S. Food and Drug Administration: U.S. Food and Drug Administration, 2020. *COVID-19 Treatments and Medications*. Centers for Disease Control and Prevention, 2022. https://www.cdc.gov/coronavirus/2019-ncov/your-health/treatments-for-severe-illness.html

(18) Gessain, A.; Nakoune, E.; Yazdanpanah, Y. Monkeypox. *N Engl J Med* **2022**, *387* (19), 1783-1793. DOI: 10.1056/NEJMra2208860 From NLM Medline.

(19) Rizk, J. G.; Lippi, G.; Henry, B. M.; Forthal, D. N.; Rizk, Y. Prevention and Treatment of Monkeypox. *Drugs* **2022**, *82* (9), 957-963. DOI: 10.1007/s40265-022-01742-y From NLM Medline.

(20) Hoover, K.; Higginbotham, K. *Epstein Barr Virus*; StatPearls Publishing, 2022.

(21) Saha, A.; Robertson, E. S. Mechanisms of B-Cell Oncogenesis Induced by Epstein-Barr Virus. *J Virol* **2019**, *93* (13). DOI: 10.1128/JVI.00238-19 From NLM Medline.

(22) Dunmire, S. K.; Hogquist, K. A.; Balfour, H. H. Infectious Mononucleosis. *Curr Top Microbiol Immunol* **2015**, *390* (Pt 1), 211-240. DOI: 10.1007/978-3-319-22822-8_9 From NLM Medline.

(23) Soldan, S. S.; Lieberman, P. M. Epstein-Barr virus and multiple sclerosis. *Nat Rev Microbiol* **2023**, *21* (1), 51-64. DOI: 10.1038/s41579-022-00770-5 From NLM Medline.

(24) Gupta, M.; Shorman, M. *Cytomegalovirus*; StatPearls Publishing LLC, 2022.

(25) Akpan, U.; Pillarisetty, L. *Congenital Cytomegalovirus Infection*; StatPearls Publishing, 2022.

(26) Randhawa, P. S.; Markin, R. S.; Starzl, T. E.; Demetris, A. J. Epstein-Barr virus-associated syndromes in immunosuppressed liver transplant recipients. Clinical profile and recognition on routine allograft biopsy. *Am J Surg Pathol* **1990**, *14* (6), 538-547. DOI: 10.1097/00000478-199006000-00004 From NLM.

(27) Shannon-Lowe, C.; Rickinson, A. The Global Landscape of EBV-Associated Tumors. *Front Oncol* **2019**, *9*, 713. DOI: 10.3389/fonc.2019.00713 From NLM.

(28) Hu, W. S.; Hughes, S. H. HIV-1 reverse transcription. *Cold Spring Harb Perspect Med* **2012**, *2* (10). DOI: 10.1101/cshperspect.a006882 From NLM Medline.

(29) *Summary of the global HIV epidemic*. World Health Organization, 2021. https://www.who.int/data/gho/data/themes/hiv-aids

(30) Meyer, R. R. P.; Alder, R. P. Human immunodeficiency virus (HIV). In Salem Press, 2022.

(31) Kassel, K. S. M. S. R. D. M. E.; Horn, D. L. M. D. F. Hepatitis B. In Salem Press, 2020.

(32) Tsukuda, S.; Watashi, K. Hepatitis B virus biology and life cycle. *Antiviral Research* **2020**, *182*, 104925. DOI: https://doi.org/10.1016/j.antiviral.2020.104925.

(33) De Clercq, E.; Li, G. Approved Antiviral Drugs over the Past 50 Years. *Clin Microbiol Rev* **2016**, *29* (3), 695-747. DOI: 10.1128/CMR.00102-15 From NLM Medline.

(34) Gorbalenya, A. E.; Baker, S. C.; Baric, R. S.; de Groot, R. J.; Drosten, C.; Gulyaeva, A. A.; Haagmans, B. L.; Lauber, C.; Leontovich, A. M.; Neuman, B. W.; et al. The species Severe acute respiratory syndrome-related coronavirus: classifying 2019-nCoV and naming it SARS-CoV-2. *Nature Microbiology* **2020**, *5* (4), 536-544. DOI: 10.1038/s41564-020-0695-z.

(35) Efridi, W.; Lappin, S. L. Poxviruses. In *StatPearls*, 2023.
(36) Whitley, R. J. Herpesviruses. In *Medical Microbiology*, 4th ed.; Baron, S. Ed.; 1996.

(37) Cloyd, M. W. Human Retroviruses. In *Medical Microbiology*, 4th ed.; Baron, S. Ed.; 1996.

(38) Family - Hepadnaviridae. In *Virus Taxonomy*, King, A. M. Q., Adams, M. J., Carstens, E. B., Lefkowitz, E. J. Eds.; Elsevier, 2012; pp 445-455.

(39) Vardanyan, R.; Hruby, V. Antiviral Drugs. **2016**. From 2016.

(40) Seley-Radtke, K. L.; Yates, M. K. The evolution of nucleoside analogue antivirals: A review for chemists and non-chemists. Part 1: Early structural modifications to the nucleoside scaffold. *Antiviral Res* **2018**, *154*, 66-86. DOI: 10.1016/j.antiviral.2018.04.004 From NLM Medline.

(41) Safrin, S. Antiviral Agents. In *Basic & Clinical Pharmacology, 15e*, Katzung, B. G., Vanderah, T. W. Eds.; McGraw-Hill, 2021.

(42) Warren, T.; Jordan, R.; Lo, M.; Soloveva, V.; Ray, A.; Bannister, R.; Mackman, R.; Perron, M.; Stray, K.; Feng, J.; et al. Nucleotide Prodrug GS-5734 Is a Broad-Spectrum Filovirus Inhibitor That Provides Complete Therapeutic Protection Against the Development of Ebola Virus Disease (EVD) in Infected Non-human Primates. *Open Forum Infectious Diseases* **2015**, *2* (suppl_1). DOI: 10.1093/ofid/ofv130.02 (acccessed 1/30/2023). *A Trial of Remdesivir in Adults With Mild and Moderate COVID-19*. ClinicalTrials.gov identifier: NCT04252664, 2020.

(43) Gordon, C. J.; Tchesnokov, E. P.; Woolner, E.; Perry, J. K.; Feng, J. Y.; Porter, D. P.; Gotte, M. Remdesivir is a direct-acting antiviral that inhibits RNA-dependent RNA polymerase from severe acute respiratory syndrome coronavirus 2 with high potency. *J Biol Chem* **2020**, *295* (20), 6785-6797. DOI: 10.1074/jbc.RA120.013679 From NLM Medline.

(44) Yin, W.; Mao, C.; Luan, X.; Shen, D. D.; Shen, Q.; Su, H.; Wang, X.; Zhou, F.; Zhao, W.; Gao, M.; et al. Structural basis for inhibition of the RNA-dependent RNA polymerase from SARS-CoV-2 by remdesivir. *Science* **2020**, *368* (6498), 1499-1504. DOI: 10.1126/science.abc1560 From NLM Medline.

(45) Rawal, R. K.; Singh, U. S.; Chavre, S. N.; Wang, J.; Sugiyama, M.; Hung, W.; Govindarajan, R.; Korba, B.; Tanaka, Y.; Chu, C. K. 2'-Fluoro-6'-methylene-carbocyclic adenosine phosphoramidate (FMCAP) prodrug: in vitro anti-HBV activity against the lamivudine-entecavir resistant triple mutant and its mechanism of action. *Bioorg Med Chem Lett* **2013**, *23* (2), 503-506. DOI: 10.1016/j.bmcl.2012.11.027 From NLM Medline.

(46) Wang, G.; Deval, J.; Hong, J.; Dyatkina, N.; Prhavc, M.; Taylor, J.; Fung, A.; Jin, Z.; Stevens, S. K.; Serebryany, V.; et al. Discovery of 4'-chloromethyl-2'-deoxy-3',5'-di-O-isobutyryl-2'-fluorocytidine (ALS-8176), a first-in-class RSV polymerase

inhibitor for treatment of human respiratory syncytial virus infection. *J Med Chem* **2015**, *58* (4), 1862-1878. DOI: 10.1021/jm5017279 From NLM Medline.

(47) Sourimant, J.; Lieber, C. M.; Aggarwal, M.; Cox, R. M.; Wolf, J. D.; Yoon, J. J.; Toots, M.; Ye, C.; Sticher, Z.; Kolykhalov, A. A.; et al. 4'-Fluorouridine is an oral antiviral that blocks respiratory syncytial virus and SARS-CoV-2 replication. *Science* **2022**, *375* (6577), 161-167. DOI: 10.1126/science.abj5508 From NLM Medline.

(48) Wójtowicz-Rajchel, H. Synthesis and applications of fluorinated nucleoside analogues. *Journal of Fluorine Chemistry* **2012**, *143*, 11-48. DOI: https://doi.org/10.1016/j.jfluchem.2012.06.026.

(49) Rawal, R. K.; Singh, U. S.; Chavre, S. N.; Wang, J.; Sugiyama, M.; Hung, W.; Govindarajan, R.; Korba, B.; Tanaka, Y.; Chu, C. K. 2′-Fluoro-6′-methylene-carbocyclic adenosine phosphoramidate (FMCAP) prodrug: In vitro anti-HBV activity against the lamivudine–entecavir resistant triple mutant and its mechanism of action. *Bioorganic & Medicinal Chemistry Letters* **2013**, *23* (2), 503-506. DOI: https://doi.org/10.1016/j.bmcl.2012.11.027.

(50) Singh, U. S.; Mulamoottil, V. A.; Chu, C. K. 2′-Fluoro-6′-methylene carbocyclic adenosine and its phosphoramidate prodrug: A novel anti-HBV agent, active against drug-resistant HBV mutants. *Medicinal Research Reviews* **2018**, *38* (3), 977-1002. DOI: https://doi.org/10.1002/med.21490.

(51) Wang, P.; Agrofoglio, L. A.; Gary Newton, M.; Chu, C. K. Asymmetric synthesis of L-cyclopentyl carbocyclic nucleosides. *Tetrahedron Letters* **1997**, *38* (24), 4207-4210. DOI: https://doi.org/10.1016/S0040-4039(97)00898-8.

(52) Wang, P.; Agrofoglio, L. A.; Newton, M. G.; Chu, C. K. Chiral Synthesis of Carbocyclic Analogues of l-ribofuranosides. *The Journal of Organic Chemistry* **1999**, *64* (11), 4173-4178. DOI: 10.1021/jo9812330.

(53) Gemal, A. L.; Luche, J. L. Lanthanoids in organic synthesis. 6. Reduction of .alpha.-enones by sodium borohydride in the presence of lanthanoid chlorides: synthetic and mechanistic aspects. *Journal of the American Chemical Society* **1981**, *103* (18), 5454-5459. DOI: 10.1021/ja00408a029.

(54) Gordon, C. J.; Tchesnokov, E. P.; Woolner, E.; Perry, J. K.; Feng, J. Y.; Porter, D. P.; Götte, M. Remdesivir is a direct-acting antiviral that inhibits RNA-dependent RNA polymerase from severe acute respiratory syndrome coronavirus 2 with high potency. *J Biol Chem* **2020**, *295* (20), 6785-6797. DOI: 10.1074/jbc.RA120.013679 From NLM.

(55) Kim, H. O.; Shanmuganathan, K.; Alves, A. J.; Jeong, L. S.; Warren Beach, J.; Schinazi, R. F.; Chien-Neng, C.; Yung-Chi, C.; Chu, C. K. Potent anti-HIV and

anti-HBV activities of (−)-L-β-dioxolane-C and (+)-L-β-dioxolane-T and their asymmetric syntheses. *Tetrahedron Letters* **1992**, *33* (46), 6899-6902. DOI: https://doi.org/10.1016/S0040-4039(00)60890-0. Kim, H. O.; Ahn, S. K.; Alves, A. J.; Beach, J. W.; Jeong, L. S.; Choi, B. G.; Van Roey, P.; Schinazi, R. F.; Chu, C. K. Asymmetric synthesis of 1,3-dioxolane-pyrimidine nucleosides and their anti-HIV activity. *Journal of Medicinal Chemistry* **1992**, *35* (11), 1987-1995. DOI: 10.1021/jm00089a007.

(56) De, C.; Liu, D.; Zheng, B.; Singh, U. S.; Chavre, S.; White, C.; Arnold, R. D.; Hagen, F. K.; Chu, C. K.; Moffat, J. F. β-l-1-[5-(E-2-bromovinyl)-2-(hydroxymethyl)-1,3-(dioxolan-4-yl)] uracil (l-BHDU) prevents varicella-zoster virus replication in a SCID-Hu mouse model and does not interfere with 5-fluorouracil catabolism. *Antiviral Research* **2014**, *110*, 10-19. DOI: https://doi.org/10.1016/j.antiviral.2014.07.007. Coen, N.; Singh, U.; Vuyyuru, V.; Van den Oord, J. J.; Balzarini, J.; Duraffour, S.; Snoeck, R.; Cheng, Y. C.; Chu, C. K.; Andrei, G. Activity and mechanism of action of HDVD, a novel pyrimidine nucleoside derivative with high levels of selectivity and potency against gammaherpesviruses. *J Virol* **2013**, *87* (7), 3839-3851. DOI: 10.1128/jvi.03338-12 From NLM.

(57) Furman, P. A.; Jeffrey, J.; Kiefer, L. L.; Feng, J. Y.; Anderson, K. S.; Borroto-Esoda, K.; Hill, E.; Copeland, W. C.; Chu, C. K.; Sommadossi, J. P.; et al. Mechanism of action of 1-beta-D-2,6-diaminopurine dioxolane, a prodrug of the human immunodeficiency virus type 1 inhibitor 1-beta-D-dioxolane guanosine. *Antimicrob Agents Chemother* **2001**, *45* (1), 158-165. DOI: 10.1128/aac.45.1.158-165.2001 From NLM.

(58) Liang, Y.; Narayanasamy, J.; Schinazi, R. F.; Chu, C. K. Phosphoramidate and phosphate prodrugs of (−)-β-d-(2R,4R)-dioxolane-thymine: Synthesis, anti-HIV activity and stability studies. *Bioorganic & Medicinal Chemistry* **2006**, *14* (7), 2178-2189. DOI: https://doi.org/10.1016/j.bmc.2005.11.008.

(59) Perlíková, P.; Hocek, M. Pyrrolo[2,3-d]pyrimidine (7-deazapurine) as a privileged scaffold in design of antitumor and antiviral nucleosides. *Medicinal Research Reviews* **2017**, *37* (6), 1429-1460, https://doi.org/10.1002/med.21465. DOI: https://doi.org/10.1002/med.21465 (acccessed 2023/02/10). Olsen, D. B.; Eldrup, A. B.; Bartholomew, L.; Bhat, B.; Bosserman, M. R.; Ceccacci, A.; Colwell, L. F.; Fay, J. F.; Flores, O. A.; Getty, K. L.; et al. A 7-deaza-adenosine analog is a potent and selective inhibitor of hepatitis C virus replication with excellent pharmacokinetic properties. *Antimicrob Agents Chemother* **2004**, *48* (10), 3944-3953. DOI: 10.1128/aac.48.10.3944-3953.2004 From NLM.

(60) Sznaidman, M. L.; Du, J.; Pesyan, A.; Cleary, D. G.; Hurley, K. P.; Waligora, F.; Almond, M. R. Synthesis of (−)-DAPD. *Nucleosides, Nucleotides & Nucleic Acids* **2004**, *23* (12), 1875-1887. DOI: 10.1081/NCN-200040643.

(61) Kim, H. O.; Schinazi, R. F.; Nampalli, S.; Shanmuganathan, K.; Cannon, D. L.; Alves, A. J.; Jeong, L. S.; Beach, J. W.; Chu, C. K. 1,3-Dioxolanylpurine nucleosides (2R,4R) and (2R,4S) with selective anti-HIV-1 activity in human lymphocytes. *Journal of Medicinal Chemistry* **1993**, *36* (1), 30-37. DOI: 10.1021/jm00053a004.

(62) Narayanasamy, J.; Pullagurla, M. R.; Sharon, A.; Wang, J.; Schinazi, R. F.; Chu, C. K. Synthesis and anti-HIV activity of (−)-β-d-(2R,4R)-1,3-dioxolane-2,6-diamino purine (DAPD) (amdoxovir) and (−)-β-d-(2R,4R)-1,3-dioxolane guanosine (DXG) prodrugs. *Antiviral Research* **2007**, *75* (3), 198-209. DOI: https://doi.org/10.1016/j.antiviral.2007.03.005.

(63) Bera, S.; Malik, L.; Bhat, B.; Carroll, S. S.; Hrin, R.; MacCoss, M.; McMasters, D. R.; Miller, M. D.; Moyer, G.; Olsen, D. B.; et al. Synthesis and biological evaluation of 5R- and 5S-methyl substituted d- and l-configuration 1,3-dioxolane nucleoside analogs. *Bioorganic & Medicinal Chemistry* **2004**, *12* (23), 6237-6247. DOI: https://doi.org/10.1016/j.bmc.2004.08.054.

(64) Friedrichs, C.; Neyts, J.; Gaspar, G.; Clercq, E. D.; Wutzler, P. Evaluation of antiviral activity against human herpesvirus 8 (HHV-8) and Epstein–Barr virus (EBV) by a quantitative real-time PCR assay. *Antiviral Research* **2004**, *62* (3), 121-123. DOI: https://doi.org/10.1016/j.antiviral.2003.12.005.